

Spatio-temporal Dynamics of the Wnt/ β -catenin Signaling Pathway: A Computational Systems Biology Approach

Dissertation

zur

Erlangung des akademischen Grades

Doktor-Ingenieur (Dr.-Ing.)

der Fakultät für Informatik und Elektrotechnik

der Universität Rostock

vorgelegt von

M.Sc. Orianne Mazemondet, geb. am 1981/11/02 in Brest (Fr)

aus Rostock

Rostock, 2011/05/06

Principal Advisor: Prof. Dr. rer. nat. habil. Adelinde M. Uhrmacher
University of Rostock, Germany

External Reviewers: Prof. Dr. med. Arndt Rolfs
University of Rostock, Germany

Prof. Dr. James R. Faeder
University of Pittsburg, USA

Date of Defense: 2011/07/01

Abstract

Human neural progenitor cells (hNPCs) are a new prospect for neuron replacement therapy in the context of neurodegenerative diseases, e.g. Parkinson's disease. ReNcell VM cells are hNPCs cultured *in vitro* that allow to investigate and understand the mechanisms of neuron differentiation, before clinical studies can be performed. The Wnt/ β -catenin signaling pathway is involved in ReNcell VM cell differentiation. A first step to understand its role in this biological process is to investigate the spatio-temporal dynamics of its signaling proteins.

This dissertation employs the cyclic workflow of computational systems biology, deploying both wet- and dry-lab experiments, to investigate the spatio-temporal dynamics of Wnt/ β -catenin pathway in ReNcell VM cells. By means of cellular and molecular biology techniques, quantitative kinetic analyses of the pathway's signaling proteins are performed. These show biphasic kinetics during the first three days of physiological differentiation.

A computational model of ReNcell VM cell population is developed to investigate *in silico* the sources of the biphasic kinetics observed *in vitro*. The *in silico* experiments describe the impact of the cell asynchrony w.r.t. the cell cycle on the protein dynamics and give insights about the role of self-induced Wnt signaling in the cell population. A stochastic investigation reveals discrepancies in the deterministic approximation and emphasizes the importance of stochastic approaches for modeling biological systems. We propose additional wet-lab experiments in order to validate the *in silico* predictions, and hence close the loop of computational systems biology.

Computational systems biology, Wnt/ β -catenin signaling pathway, ReNcell VM cells, Stochastic modeling

Zusammenfassung

Humane neurale Progenitorzelle (hNPZs) bilden eine neue Perspektive für Neuronen-Ersatztherapien zur Behandlung neurogenerativer Krankheiten, wie z.B. Parkinson. ReNcell VM-Zellen sind gezüchtete hNPZs, die es ermöglichen, als Grundlage für klinische Studien, die Mechanismen der Neuronendifferenzierung zu untersuchen und zu verstehen. Es ist bekannt, dass der Wnt/ β -catenin Signalweg im Differenzierungsprozess von ReNcell VM-Zellen involviert ist. Ein erster Schritt, um seine genaue Rolle in diesem Zusammenhang zu verstehen, ist die Untersuchung der spatio-temporalen Dynamik seiner Signalproteine.

Diese Dissertation folgt dem zyklischen Arbeitsablauf der Systembiologie, um, basierend auf sowohl Nasslabor- wie auch Computerexperimenten, die spatio-temporalen Dynamik der Signalproteine des Wnt/ β -catenin Signalwegs in ReNcell VM-Zellen zu studieren. Mit Hilfe von zell- und molekularbiologischen Techniken werden quantitative Analysen der zentralen Proteine des Signalwegs durchgeführt. Diese zeigen eine biphasische Kinetik während der ersten drei Tage physiologischer Differenzierung.

Ein Computermodell wird entwickelt, um die Quellen der biphasischen Kinetik zu untersuchen. Experimente mit diesem Modell zeigen den Einfluss von Zellsynchronität hinsichtlich des Zellzyklus auf die Proteindynamik. Sie geben desweiteren Einsicht in die Rolle autoinduzierter Wnt-Signale. Eine Untersuchung der stochastischen Eigenschaften des Modells zeigt Diskrepanzen in der deterministischen Approximation auf und unterstreicht damit die Signifikanz stochastischer Ansätze zur Modellierung biologischer Systeme. Vorschläge für weiterführende Experimente zur Validierung der auf Basis des Modells getätigten Vorhersagen werden unterbreitet. Dadurch wird der Kreis der Systembiologie, vom Labor zum Computer und zurück, geschlossen.

Systembiologie, Wnt/ β -catenin Signalweg, ReNcell VM Zellen, Stochastische modellierung

Contents

1	Introduction	1
1.1	ReNcell VM cells and Wnt/ β -catenin signaling pathway	4
1.2	Contributions	5
1.2.1	Quantitative kinetics of Wnt/ β -catenin pathway signaling proteins	6
1.2.2	Computational model of the Wnt/ β -catenin pathway in ReNcell VM cells	7
1.3	Outline	9
1.4	Bibliography note	10
2	Biological background	11
2.1	Wnt signaling pathway	11
2.1.1	Wnt proteins	11
2.1.2	Wnt/ β -catenin pathway	12
2.2	Human neural progenitor cells	15
2.2.1	ReNcell VM cell line	15
2.2.2	Cell cycle in ReNcell VM cell line	16
2.2.3	Wnt/ β -catenin pathway and neural progenitor cells	18
2.2.4	Wnt3a and neural progenitor cells	19
3	<i>in vitro</i> exploration	21
3.1	Material & Methods	21
3.1.1	Solutions & Material lists	21
3.1.2	Cell culture	24
3.1.3	Cell volume	25
3.1.4	Subcellular fractions	25
3.1.5	Protein determination & Western blot analysis	26
3.1.6	Quantification & statistics	28

3.2	Spatio-temporal dynamics of Wnt signaling proteins	29
3.2.1	Early regulation during the first hours of differentiation	29
3.2.2	Late response during the first days of differentiation	32
3.3	Protein dynamics under Wnt3a stimulation	35
3.3.1	Wnt3a influences during proliferation	35
3.3.2	Wnt3a influences during differentiation	35
3.4	Discussion	43
3.4.1	Protein dynamics during differentiation	43
3.4.2	Pathway dynamics under Wnt3a stimulation	45
3.4.3	Nuclear β -catenin dynamics	46
4	<i>in silico</i> validation	49
4.1	Existing Wnt/ β -catenin pathway models	49
4.1.1	Lee et al. (2003)	49
4.1.2	<i>Lee model</i> extensions	50
4.1.3	Tymchyshyn et al. (2008)	53
4.2	Model	55
4.2.1	The intracellular Wnt/ β -catenin pathway model	55
4.2.2	Assumptions	56
4.3	Parametrization & Methods	58
4.3.1	Spatial parameters	58
4.3.2	Molecule number & Stochastic rate constants	61
4.3.3	Duration and distribution of cell cycle phases	61
4.3.4	Delays	62
4.3.5	Parameter estimation & Simulation	62
4.4	Model Evaluation	63
4.4.1	Against the <i>Lee model</i>	63
4.4.2	Against the <i>in vitro</i> data	64
4.4.3	Sensitivity analysis	65
4.5	Results & Discussion	68
4.5.1	Stochastic effects	68
4.5.2	Impact of the cell cycle on β -catenin dynamics	69
4.5.3	Self-induced Wnt signaling	73
5	Conclusions and Future Work	77

List of Figures

2.1	Wnt intra- and extra-cellular traffic. Adapted from [Coudreuse and Korswagen, 2007].	12
2.2	Overview of the Wnt/ β -catenin signaling pathway.	13
2.3	Schema of β -catenin phosphorylation and degradation cascade. Adapted from [Amit et al., 2002].	14
2.4	Typical cell cycle showing the four phases and their relative duration in mammalian cells.	17
2.5	Cell cycle analyses during differentiation of ReNcell VM cells.	18
3.1	Representative Western-blot for the subcellular fractions.	26
3.2	Analyses of LRP6 protein in the membrane fraction during ReNcell VM cell differentiation	30
3.3	Analyses of Dvl2 protein in the membrane and cytosol fractions during ReNcell VM cell differentiation	31
3.4	Analyses of GSK3 β protein in the cytosol fraction during ReNcell VM cell differentiation	32
3.5	Analyses of phosphorylated GSK3 α/β proteins in the membrane and cytosol fractions during ReNcell VM cell differentiation	33
3.6	Analyses of β -catenin protein in the cytosol and nuclear fractions during ReNcell VM cell differentiation	34
3.7	Protein expression during ReNcell VM cell proliferation with Wnt3a	36
3.8	Analyses of t-LRP6 protein in the membrane fraction during ReNcell VM cell differentiation with Wnt3a	38
3.9	Analyses of p-LRP6 protein in the membrane fraction during ReNcell VM cell differentiation with Wnt3a	39
3.10	Analyses of Dvl2 protein in the membrane and cytosol fractions during ReNcell VM cell differentiation with Wnt3a	40

3.11	Analyses of phosphorylated GSK3 α/β proteins in the membrane and cytosol fractions during ReNcell VM cell differentiation with Wnt3a	41
3.12	Analyses of β -catenin protein in the cytosol and nuclear fractions during ReN-cell VM cell differentiation with Wnt3a	42
3.13	Overview of protein dynamics during physiological differentiation of ReNcell VM cells.	47
3.14	Overview of protein dynamics during differentiation of ReNcell VM cells with Wnt3a.	48
4.1	The reaction steps of the Wnt pathway (reproduced from [Lee et al., 2003], Figure 1).	51
4.2	Model of the intracellular reactions of Wnt/ β -catenin pathway.	56
4.3	Comparison of β -catenin dynamics with the <i>Lee model</i>	64
4.4	Model evaluation in comparison to the experimental data	65
4.5	Effects of <i>AxinP</i> on nuclear β -catenin dynamics according to stochastic simulation	70
4.6	Nuclear β -catenin dynamics with higher number of <i>AxinP</i>	71
4.7	Dynamics of nuclear β -catenin in heterogeneous cell population	72
4.8	Simulation results for the time-course of nuclear β -catenin (<i>β_{nuc}</i>)	75

List of Tables

3.3	Primary antibodies used for protein detection by Western-blot	27
3.4	Secondary antibodies used for fluorescence analysis of Western-blot	27
4.1	Reactions of the intracellular Wnt/ β -catenin pathway model	57
4.2	Parameters from the <i>Lee model</i> [Lee et al., 2003] used in the model and their stochastic conversion	66
4.3	Sensitivity analysis of the model parameters	66
4.4	List of model parameters	67

Acknowledgements

First of all, I would like to thank my supervisor Prof. Adelinde M. Uhrmacher, who believed in me from the beginning, and stayed always on my side. This dissertation is the result of her unconditional trust in me. Thank you.

I would like to thank Prof. James Faeder who agreed to review my dissertation, and I agree with his definition of science: "Dealing with that frustration is a major part of the battle". I won the battle.

I am grateful to Prof. Arndt Rolfs for supporting my independence, and to my colleagues at the AKos-Institute who were patient with my lucubration about modeling. A special thank goes to Dr. Mix who welcomed me so warmly in Rostock, and taught me all his Wnt-related and scientific knowledge. I also want to thank Dr. Jana Frahm, who had to learn her post-doc job with me, not such an easy task! We have been through a lot together, and I hope that looking back she keeps as many good memories as I do.

The work on this thesis was financially supported by the DFG in the research training group dIEM oSiRis and the DiEr MoSiS project.

I am thankful to my dIEM oSiRis and Mosi colleagues. I really enjoyed the scientific environment I had in both groups, and the discussion we had over a coffee, a Frühstück, or a Glühwein. I have learned a lot from each of them and they also made my life in Germany so much better, especially when inviting me for family-week-ends, Christmas celebrations, but also during conference trips, and, of course, during the long days and the dark-winter-week-ends in the office. I am pleased to thank Ramona Kirch, Lea Macioleck, and Anna Norton, who came as students and left as friends. You all have done a tremendous job dealing with my daily stress and were such a great help with the routine lab work.

I show my gratitude to the teachers of the Sprachzentrum and the Hochschulsport at Rostock University for helping me to go through German grammar, and for keeping me physically and mentally healthy.

There are a few people without whom I would not write these words and this dissertation. First of all, Prof. Cino Pertoldi who was the trigger of my scientific carrier as he was already believing in me during my first year of Master. Cino, without you I would have never had the crazy idea to do a PhD thesis, thanks for that.

Joachim Niehren and Celine Kuttler who were, even before we met, the starting point of this PhD story. They have been a constant source of support and help even during the hard times.

More generally, I am really indebted and grateful to the Biocomputing group of Lille and Cedric Lhoussaine, for the support, help, working environment, friendship, and desk provided in the last months of this work. Thank you all, I really enjoyed being part of the group.

Of course, I could have never gone through this dissertation without the love, encouragement, and understanding of my family and friends. First of all my mother, step-father, and father who brought me emotional and financial supports during my long lasting education, and who have never doubted about me. I really value the efforts made by all the family members to let me follow my path far from, them and to never show their disappointment when I was not coming back home for Christmas. I am so lucky to have such understanding people around me. *Merci à tous.*

I am grateful to the families John and Wagner for their concern and care. Lot of thanks goes to Anja, Yvonne, Dagmar, Tareck, and the guys from the French evenings for their friendship that helped me to keep my "head out of the water" and to give me memorable time in Germany. A special thanks goes to my friends in south of France, for their long lasting friendship that does not decrease with time nor distance. *A vous aussi, mille fois merci.*

At last, this dissertation is not the only *price* I won during my time as a PhD student, as I also found a wonderful team-mate, boyfriend, and supportive colleague, Mathias John. Mathias has contributed a lot to this work, both directly and indirectly, although all the knowledge he gave me about the π -calculus is unfortunately not included in this dissertation. It is common to say "*this work would have never been done without you*", but I guess this has never been so true. I hope to have another chance to work with you. This dissertation could not have been written without you.

This dissertation is dedicated to my uncles and grand-father,
they have witnessed the beginning of my PhD,
they would have been so proud to witness its end.

Roger Laurents (02.1929-04.2008)
Franck Laurents (11.1958-01.2007)
Raymond Hampson (08.1941-11.2007)

Abbreviations

APC	Adenomatous polyposis coli
bFGF	Basic fibroblast growth factor
Cdk	Cyclin-dependent kinase
CNS	Central nervous system
DDEs	Delay differential equations
Dkk1	Dickkopf 1
Dvl2	Dishevelled 2
Dsh	Dishevelled
EGF	Epidermal growth factor
ER	Endoplasmic reticulum
FRAP	Fluorescence Recovery After Photobleaching
Fz	Frizzled
GAPDH	Glyceraldehyde-3-phosphate dehydrogenase
GRP78	Glucose-regulated protein 78
GSK3 α	Glycogen synthase kinase 3 alpha
GSK3 β	Glycogen synthase kinase 3 beta
hNPCs	Human neural progenitor cells
kDa	Kilodalton
LRP6	Low-density lipoprotein receptor-related protein 6
NGF	Nerve growth factor
ODEs	Ordinary differential equations
RNA	Ribonucleic acid
SEM	Standard error of the mean
TIM23	Translocase of the Inner Mitochondrial membrane
TCF	T-cell factor
VM	Ventral midbrain

Chapter 1

Introduction

Neurodegenerative diseases, such as Parkinson's or Huntington's diseases, are characterized by a large amount of dysfunctional or lost neural cells and neurons, especially dopaminergic neurons. Among conceivable treatments, e.g. drug treatments, regenerative therapies that consist in neuron transplantation into the patient brain, are a new hope. In this context human neural progenitor cells (hNPCs) are a recent prospect to obtain the required amount of neurons and dopaminergic neurons before transplantation. They are issued from different parts of the brain and are defined by two properties: self-renewal (capability to remain undifferentiated and to stay in proliferation) and multipotentiality (differentiation in different cell types restricted to neural cell line). Nowadays, hNPCs can be isolated, cultured and expanded *in vitro* that allows, before any clinical studies, the investigation of the mechanisms underlying their differentiation and neurogenesis. Especially, understanding in an integrative manner the molecular aspects of these cellular processes will increase our comprehension of such biological processes.

Signaling pathways are responsible for cellular adaptation toward environmental changes, leading to physiological decisions such as cell death, differentiation, cell fate but also to oncogenesis. Signaling molecules are present extracellularly, and constitute intermediates for cell-cell communication: they are the means by which a cell can influence the behavior of neighbor cells, i.e. paracrine signal, or its own behavior, i.e. autocrine signal. Signaling pathways are triggered when signaling molecules bind to cell membrane receptors, followed by a cascade of intracellular reactions, among which are protein phosphorylation and spatial relocation, mediated by signaling proteins. Finally, a target protein transfers the signal into the nucleus where it results in specific gene expression in order to adapt the cell behavior.

It is common that signaling proteins are shared components between pathways. This can lead

to potential cross-talk that can be undesirable as it might result to inappropriate cell changes [Albert and Oltvai, 2007]. A signal specificity is defined as follows: a given stimulus (signal), activates one pathway leading to the desired cell response [Bardwell et al., 2007]. To ensure specificity, mechanisms have evolved among which pathways mutual inhibition or activation, but most importantly, spatial and temporal insulation [Takahashi et al., 2006, Kholodenko, 2006, Albert and Oltvai, 2007].

Spatial insulation is achieved by compartmentalization, protein relocation, and the presence of macromolecular complexes [Albert and Oltvai, 2007]. Temporal insulation is due to the magnitude and duration of the signal, and of protein activation and phosphorylation [Sabbagh et al., 2001]. It is reinforced by the presence of feedback loops, negative ones that downregulate the pathway, and positive ones that amplify it [Kholodenko, 2000, Xiong and Ferrell, 2003, Brandman and Meyer, 2008]. Furthermore, temporal insulation is also involved at the cell level, as the response to a specific signal depends on the cell development stage.

Thus, to fully understand a pathway involvement in a cellular response, time-course analysis and spatial resolution are needed. This underlines the importance of kinetic analyses when studying signaling pathways. Nonetheless, due to the broad time scale involved in signaling pathway, from phosphorylation (milliseconds), diffusion (seconds), to cell responses and gene transcriptions (minutes, hours) [Tyson et al., 2001], [Alon, 2007, pg.6], kinetic analyses are fund and time consuming, not to mention that they are limited by technical and manpower resources.

Traditionally, molecular and cell biologists have a reductionist approach toward signaling pathway study: Exploring through wet-lab experiments, a given set of proteins in an animal or cell model, manipulated or not, e.g. mouse, *in vitro* cultured cells. Such approach can be successful to identify proteins and their interactions, and the organizational and mechanistic level of a pathway. However, observation of biological components in an isolated manner has limits. On the one hand, it is rarely possible to observe biological elements independently due to the intricate nature of living systems. On the other hand, it is the dynamic interactions between molecules that determine the function of a biological system [Wilkinson, 2009]. The latter requires taking into account complex changes in time and space, that is beyond the traditional thinking of experimentalists and needs a more abstract conceptualization [Nurse, 2000].

A computational model is an abstract mathematical representation of a system under study, that is then analyzed with help of computers, and by this way, helps to overcome the linearity

of Human thinking [Doerner, 1980]. It offers a complementary approach to develop and test hypotheses and make predictions regarding biological systems. Besides, when developing a computational model, one can structure the knowledge and acquires a better understanding about the system under study [Cellier, 1991].

Computational models of signaling pathways are dynamic models that depict the changes over time of the system properties [Ellner and Guckenheimer, 2006]. Thus, not only they represent proteins and genes interactions but also analyze how these interactions change over time. By this way, non linearity of the system, e.g. presence of feedback loops, and the temporal insulation are easily analyzed with computer power and the specificity of the pathway can be captured. Furthermore, integration of spatial aspects and element of insulation, e.g. compartments, protein relocation, should, ideally, be included in dynamic models [Takahashi et al., 2006, Kholodenko, 2006, Ahn et al., 2006].

Dynamic models are built based on experimental data and previous knowledge gathered about the system under study. Protein interactions can be represented as biochemical reactions, in a similar manner as biologists describe signaling pathways. Model analyses are multiple and encompass computational simulation and mathematical analyses, and are selected depending on the model characteristics.

Stochastic modeling, as described in [Gillespie, 1977], considers models in terms of multisets of molecules, representing chemical solutions, and chemical reactions rules. Molecular interactions are regarded as discrete events randomly distributed in time. Analysis of stochastic models in terms of stochastic simulation gives a picture of the component at a given time and each simulation run represents a random experiment.

Deterministic modeling studies usually transform chemical reaction rules into ordinary differential equations (ODEs) and regard concentrations instead of multisets of molecules. The equivalent to simulation in the context of ODEs is numerical integration. Studies based on ODEs form an approximation of the stochastic approach [Wilkinson, 2009]. They may neglect significant differences in the behavior of systems with some chemical species in relatively low abundance that arise from stochastic effects.

Although standards are lacking for model development [Klipp and Liebermeister, 2006], the process is usually initiated based on prior knowledge in order to design the pathway structure, the proteins involved and protein interactions. Besides, in order to depict the pathway dynamics, values for the model parameters are needed, e.g. number of molecules (or concentration), and rate constants. Ideally, these are measured directly in the system under study, as the closer kinetic parameters relate to experimental data the more reliable the results of a modeling study are.

However, gathering all model parameters from biological experiments is one of the challenges in the modeling task. The reasons are manifold: although techniques that can provide quantitative biological data are increasing, they remain time-consuming and expensive to acquire, and the obtained data can suffer from a lack of reliability [Schilling et al., 2005]. Thus, most of the values needed for model parameters are usually lacking. This lack can be overcome by parameter estimation, that aims to find value for missing parameters such that the model output fits the reference data, e.g. experimental data [Aldridge et al., 2006]. After the model is designed, a series of analyses follow that aims to verify whether the behavior of the model species meet the post hoc constraints [Aldridge et al., 2006]: the simulation data are compared to data provided from experimental analysis, e.g. data issued from microscopy, cytometry, or immunoblotting experiments. When the simulation data do not fit the experimental ones, the model structure and the parameter values, especially the estimated ones, can be questioned. Sensitivity analysis can then be used to determine which parameters have the most influence on the model behavior and by this way, determine which ones can be changed [Aldridge et al., 2006]. These model analysis are performed in an iterative manner until satisfying results are found.

Computational systems biology defines the synergistic work between wet- and dry-labs, that encompasses "“experimentation and computational modeling”" [Klipp et al., 2005, pg.14]. It is considered as a field of biology that aims at studying biological systems with their dynamics, interplays and interactions and by doing so provides an integrative view on these systems. The workflow is performed as an iterative cycle, driven from prior knowledge issued from wet-labs, biological questions and hypothesis are tested with computational modeling and subsequently in-/validated with further wet-lab experiments [Kitano, 2002, Glass et al., 2006]. As already mentioned, computational systems biology is strewn with bottlenecks, such as the lack of standards and of reliable quantitative data. Another challenge lies in the interdisciplinarity of the field, as it involves expertise in various scientific fields among which are medicine, biology, physics, mathematics and computer science. Thus, scientists involved in the field of computational systems biology must learn, and be willing to do so, the idioms from other disciplines.

1.1 ReNcell VM cells and Wnt/ β -catenin signaling pathway

ReNcell VM cell line is a recently established hNPC line [Donato et al., 2007]. The cells are issued from the ventral mesencephalon of a 10 weeks old fetus and are immortalized with v-myc. It is established that ReNcell VM cells are able to differentiate into glial cells (astro-

cytes, oligodendrocytes) and neurons [Donato et al., 2007, Morgan et al., 2009, Schmöle et al., 2010]. Furthermore, ReNcell VM cells present the advantages of a short doubling-time, i.e. time needed for a population to double, and an easy and standardized cultivation protocol that are essential for *in vitro* experimentation. The transition from proliferation to differentiation is simply performed by removal of the growth factors from the cell environment. However, this transition is not synchronous in the population due to the cell commitment to the cell cycle, i.e. process that keep the cell in proliferation [Mazemondet et al., 2011].

Wnt/ β -catenin signaling pathway, among two others, is triggered by Wnt molecules that are released by the cells and are distributed along the cell field to coordinate changes in the whole population. The Wnt/ β -catenin signaling pathway is known to participate in the proliferation and differentiation of NPCs [Castelo-Branco et al., 2003] and ReNcell VM cells [Schmöle et al., 2010, Hübner et al., 2010, Mazemondet et al., 2011]. When binding to the receptors of the Frizzled family and co-receptor Low-density lipoprotein receptor-related protein 6 (LRP6), Wnts activate the first protein relocation: transfer of Dishevelled proteins (Dvl) from the cytosol to the cell membrane. Consequently, the protein β -catenin that is no longer phosphorylated by glycogen synthase kinase 3 beta (GSK3 β), accumulates in the cytosol and shuttles into the nucleus. In the latter, β -catenin becomes a transcription factor leading to the transcription of specific genes such as AXIN2.

ReNcell VM cells are known to be receptive to Wnt/ β -catenin pathway activation or inhibition during proliferation and differentiation of ReNcell VM cells: inhibition of GSK3 β leads, to the pathway activation and to an increase of neuronal cells [Schmöle et al., 2010], and activation of the pathway during proliferation increases the transcription of target genes [Hübner et al., 2010]. However, no investigation of the pathway in a physiological context, without protein overexpression or addition, has been performed so far. Thus, establishing a kinetic profile of the intracellular signaling proteins' dynamics in their subcellular location is a first step to understand the Wnt/ β -catenin pathway involvement in the ReNcell VM cell differentiation.

1.2 Contributions

In this dissertation we investigate the dynamics of the Wnt/ β -catenin signaling pathway during differentiation of ReNcell VM cells.

The work presented shows a duality between wet- and dry-lab experiments in order to understand the dynamics of signaling proteins, especially β -catenin. Within the field of computa-

tional systems biology this dissertation illustrates a representative case of the cyclic workflow starting with *in vitro* time-course and quantitative analyses of the pathway intracellular protein expressions. In a second step, the data obtained are used to generate hypotheses regarding the dynamics of nuclear β -catenin during the first 12 hours of ReNcell VM cell differentiation. Furthermore, the obtained data provide a source of information for model evaluation and *in silico* result comparison. A computational model of the pathway in ReNcell VM cell population is created, driven by the previous *in vitro* results. It aims at testing hypotheses that arise from the *in vitro* experiments. The model built is stochastic in order to investigate the potential effects engendered by the low amount of one of the pathway components (Axin). By simulation analyses one of these hypotheses is privileged as it predicts a β -catenin behavior similar to the one observed experimentally. Thus we propose further *in vitro* experiments in ReNcell VM cells to validate our predictions and by this way we close the loop of the computational systems biology workflow.

1.2.1 Quantitative kinetics of Wnt/ β -catenin pathway signaling proteins

Our results show that the Wnt/ β -catenin signaling pathway is involved during different phases of ReNcell VM cell differentiation. The internal signaling machinery is present in the cells and presents spatio-temporal dynamics along the differentiation. A first increase of nuclear β -catenin during the early hours suggests that the pathway is active as soon as differentiation is triggered, whereas a second and later increase indicates the pathway involvement in the cell fate commitment. We show that the pathway can be active during proliferation, under exogenous stimulation with Wnt3a, however, the accumulation of β -catenin does not involve the same mechanisms as during differentiation. Finally, we propose the ReNcell VM cells as a good cell model to study specific signaling proteins, i.e. the co-receptor LRP6 and Dvl2, under Wnt/ β -catenin pathway activation, and to investigate the role of the pathway in hNPC differentiation.

By means of wet-lab experiments, such as cell culture, cell fractionation and immunoblotting, we quantify the relative amount, i.e. fold change, over time, of the main signaling proteins involved in the Wnt/ β -catenin pathway: the co-receptor LRP6, the first intracellular protein activated Dvl2, GSK3 β , and the target protein β -catenin. The focus is on the first three days of ReNcell VM cell differentiation, with a distinction between the *early differentiation*, from 0 to 8 hours, and the *late differentiation*, from 12 to 72 hours. The boundary between the two phases is due to the cell fate commitment, as after 12 hours one can distinguish within the cell population, a neuron from a glial cell. Proteins are quantified in their specific subcellular lo-

cation, i.e. membrane, cytosol, and nuclear fractions. Two sets of experiments are performed that comprise protein quantification under physiological differentiation, i.e. removal of growth factors without addition of exogenous Wnt proteins, and under differentiation in presence of exogenous Wnt3a that is known to trigger the Wnt/ β -catenin pathway.

The kinetic analyses during physiological differentiation show that signaling proteins are differently regulated depending on their location and over time. The protein dynamics present biphasic kinetics: a first regulation wave during the first three hours of differentiation and a second one after 24 hours of differentiation. The two regulation waves are separated by a phase where protein levels are equivalent to the ones during proliferation. The first wave of regulation is accelerated with the presence of exogenous Wnt3a, showing that the Wnt/ β -catenin pathway is active when ReNcell VM cells start to differentiate.

We show for the first time in hNPCs the *phosphorylation-dependent Dvl2 mobility shift* [Bryja et al., 2007b] due to Wnt3a stimulation and we found that it happens only in the cytosol. Interestingly the effects of Wnt3a on protein expression are different between proliferation and differentiation. This finding supports the theory that Wnt molecules act differently depending on the developmental phase of cells or tissues. It emphasizes the motivation to analyze the pathway characteristics in each cell type and at different moments of the cell development.

1.2.2 Computational model of the Wnt/ β -catenin pathway in ReNcell VM cells

We propose two hypotheses to explain the two waves of protein regulation. The first hypothesis concerns the asynchrony of the ReNcell VM cells toward the cell cycle during the proliferation phase [Mazemondet et al., 2011]. Indeed only 53% of the ReNcell VM cells are able to differentiate right after growth factor removal. The second wave of regulation could arise from the pathway activation in the cells that differentiate after some delay due to their cell cycle commitment. The second hypothesis is correlated to the nature of Wnt molecules: these signaling molecules are produced and secreted by cells, and move toward the neighbor cells to propagate the signal. Thus, the second wave of regulation could result from cell-cell communication occurring after some delay needed for the Wnt production and secretion. Our hypothesis favors a continuous and self-induced Wnt signal between ReNcell VM cells. Testing these two hypotheses *in vitro* has not been yet possible, thus we test them with *in silico* experiments.

Based on computational modeling, we investigate the origin of nuclear β -catenin dynamics

observed in previous *in vitro* experiments, and show that the impact of the cell cycle asynchrony is negligible when analyzing protein dynamics during ReNcell VM cell differentiation. Our results further suggest that at the same time continuous and autocrine Wnt signal has considerable impact. We also report on significant stochastic effects that directly result from model parameters provided in literature and that are not observable in deterministic investigations.

We provide a model of the intracellular Wnt/ β -catenin pathway that is derived from the reference model in literature [Lee et al., 2003]. Each ReNcell VM cell is represented with two compartments, the cytosol and the nucleus, in order to compare the *in silico* protein dynamics to the *in vitro* ones and to analyze specifically nuclear β -catenin dynamics. The model represents the pathway with the three main proteins Wnt, Axin, and β -catenin, and includes the negative feedback loop generated by Axin production. The model is expressed in terms of chemical reactions, such that we can easily switch between the deterministic and the stochastic realm only by parameter conversion. The model parameters are derived from a combination of literature data [Lee et al., 2003, Kriehoff et al., 2005, Schmöle et al., 2010, Mazemondet et al., 2011], wet-lab experiments, and parameter estimation. The model evaluation is based on a deterministic investigation: a first increase of nuclear β -catenin is reproduced that fits the β -catenin behavior proposed in the reference model [Lee et al., 2003], as well as the first increase observed *in vitro* (from 0 to 2 hours). However, since our previous Western-blot data reflect β -catenin amount in ReNcell VM cell populations and our intracellular Wnt pathway model does not reflect the impact of the cell cycle, at this point it is implicitly assumed that ReNcell VM cells are synchronized regarding the cell cycle. In order to provide a more complete characterization of the model, results of a sensitivity analysis are presented.

Stochastic investigation of the intracellular Wnt pathway model is performed. The motivation held in the reference model [Lee et al., 2003] as it appeared, in their biological system (*Xenopus* oocyte) that Axin protein is in very low amount compared to the other pathway components, possibly leading to significant stochastic deviations. Indeed stochastic simulation of the model results in high fluctuations of the nuclear β -catenin level. In order to reduce these fluctuations, two strategies are carry on by adapting parameter values while keeping low Axin amount. However, both strategies failed and therefore a new parameter set is used with a higher Axin amount. From this stochastic investigation, two hypotheses are directly derived: either Axin amount in ReNcell VM cells is higher than suggested by [Lee et al., 2003], despite the fact that *in vitro* detection of Axin in ReNcell VM cells did not succeed, or the intracellular Wnt pathway model, and thus, our understanding of the system misses an important mechanism to reduce stochastic noise, like dimerization [Bundschuh, 2003, Morishita, 2004] or additional

feedback loops [Orrell et al., 2006].

To investigate the impact of the cell cycle, the intracellular Wnt pathway model is extended to represent ReNcell VM cell populations and their heterogeneity toward the cell cycle. The main assumption is that each cell has to complete the cell cycle before it can process the Wnt signal. The ReNcell VM cell distribution over the cell cycle and the duration of each cell cycle phase are obtained by wet-lab experiments and from literature [Mazemondet et al., 2011, Schmöle et al., 2010, Alam et al., 2004], respectively. The results of simulating heterogeneous cell populations show a lower amplitude in the first increase of nuclear β -catenin than observed in the experimental data. This implies that our initial assumption of considering only homogeneous cell populations to model the Wnt/ β -catenin pathway is not feasible. More generally it means that when modeling the Wnt/ β -catenin pathway in ReNcell VM cells the cells' commitment to the cell cycle should be considered. We present an additional parameter set to fit the first increase of nuclear β -catenin in our experimental data with the simulation data in heterogeneous cell populations. The results imply that in wet-lab experiments on the Wnt/ β -catenin pathway in ReNcell VM cells, the impact of the cell cycle onto the β -catenin dynamics can be neglected. In other words, the observations of Wnt pathway in ReNcell VM cells are not biased by the cell cycle asynchrony.

We further extend our model with the process of self-induced Wnt signal, in order to propose a source of induction for the second increase of nuclear β -catenin observed *in vitro*. A reaction is introduced that models Wnt production and secretion by ReNcell VM cells. This reaction starts when cells exit the cell cycle, but consumes a certain amount of time accounting for gene expression and relocation processes that are presumably involved. Both continuous and discrete Wnt secretion are tested. The simulation results suggest that with a Wnt production process that is as fast as 2.5 hours, continuous and autocrine Wnt signaling may be an explanation for the observed behavior of nuclear β -catenin in ReNcell VM cells, as simulation results fit well the experimental ones. However, due to the standard error of the mean of some experimental data, a discrete secretion can not be excluded and will need to be further investigated, eventually by means of wet-lab experiments.

1.3 Outline

The thesis is structured in three main chapters. Chapter 2 introduces background regarding the Wnt/ β -catenin signaling pathway as well as hNPCs and ReNcell VM cells. In Chapter 3 spatio-temporal profiles of the pathway signaling proteins are presented during physiological

differentiation and differentiation with Wnt3a stimulation, in Sections 3.2 and 3.3, respectively. Chapter 4 includes computational model of ReNcell VM cell populations, in Section 4.2 and *in silico* experiments regarding β -catenin dynamics, in Section 4.5.

1.4 Bibliography note

The work presented in Chapter 3 is submitted to an international journal and the article is currently under revision.

Mazemondet, O., Hübner, R., Frahm, J., Koszan, D., Bader, B. M., Weiss, D. G., Uhrmacher, A. M., Frech, M., Rolfs, A., and Luo, J. (2011). **Quantitative and kinetic profile of Wnt/ β -catenin signaling components during human neural progenitor cell differentiation.** *Cellular and Molecular Biology Letters*, submitted January, 2011.

The model and the *in silico* experiments reported in Chapter 4 are presented in an article submitted to an international journal:

Mazemondet, O., John, M., Leye, S., Rolfs, A., and Uhrmacher, A. M. (2011). **Elucidating the sources of β -catenin dynamics in human neural progenitor cells.** *PLoS ONE*, submitted May, 2011.

The parametrization presented in Chapter 4 has been published in the conference article below, that provides a modeling study on the cell cycle dependency of the Wnt/ β -catenin signaling pathway.

Mazemondet, O., John, M., Maus, C., Uhrmacher, A. M., and Rolfs, A. (2009). **Integrating diverse reaction types into stochastic models - a signaling pathway case study in the imperative pi-calculus.** In Rossetti, M. D., Hill, R. R., Johansson, B., Dunkin, A., and Ingalls, R. G., editors. *Winter Simulation Conference*, pages 932-943, Piscataway, New Jersey. Institute of Electrical and Electronics Engineers, Inc.

Chapter 2

Biological background

2.1 Wnt signaling pathway

2.1.1 Wnt proteins

Wnt proteins form a family of 19 glycoproteins with a conserved pattern of 23-24 cysteine residues. The name *Wnt* comes from the *Drosophila* wingless (*Wg*) gene and the vertebrate *int-1* oncogene. Wnt proteins are highly conserved across species, especially within vertebrates [Sidow, 1992]. They are secreted signaling molecules that regulate cell decisions such as apoptosis, proliferation, differentiation, and polarity, but that are also involved in diseases such as diabetes and cancers [Fuerer et al., 2008].

The synthesis and secretion of Wnt proteins remain unclear processes. After synthesis, Wnt proteins undergo post-translational modifications in the endoplasmic reticulum (ER) with the influence of other proteins, e.g. Porcupine (Figure 2.1). It is also in the ER that Wnt proteins can bind chaperone proteins that help their sorting and later secretion. The intracellular traffic continues from the ER to the Golgi network and to diverse subcellular compartments before Wnt proteins are ready for secretion. The picture of Wnt secretion is incomplete, with diverse proposed mechanisms that are yet a matter of conjecture. For recent reviews see [Coudreuse and Korswagen, 2007, Hausmann et al., 2007].

When secreted, Wnt proteins act as morphogens and can impose a specific change in a cell field in both short-range, i.e. to nearest neighbor cells, and long-range signaling, i.e. to cells up to 20 cell diameters away [Zecca et al., 1996]. The latter produces a morphogen gradient from the source, i.e. the cell expressing Wnt proteins, to the receiver, i.e. the cell responding to Wnt proteins. This is defined as a paracrine signaling. Wnt proteins can also signal to the cell

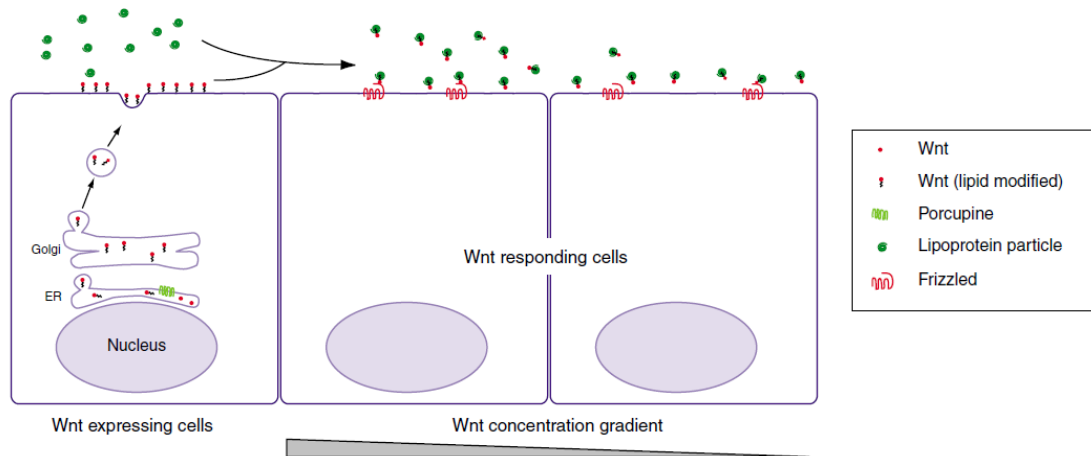


Figure 2.1: Wnt intra- and extra-cellular traffic. Adapted from [Coudreuse and Korswagen, 2007]. After their synthesis Wnt proteins undergo maturation and post-translational modifications through the endoplasmic reticulum (ER) and the Golgi network before secretion in the extracellular environment where Wnts bind to lipoproteins and move along the cell field.

that produced them. This specific signaling is called autocrine. Thus morphogens in general, and Wnt proteins in particular, are used by cells to establish communication between them, a process referred to as cell-cell communication [van den Heuvel et al., 1989]. This process is well known in *Drosophila* wing disc development [Strigini and Cohen, 2000] although how Wnt proteins are transported in the extracellular space is yet hard to answer. This is partly due to the fact that Wnt proteins are traveling close to the extracellular matrix and are thus difficult to purify [The and Perrimon, 2000]. Nevertheless, it is known that Wnt protein transport is a fast process around $50 \mu\text{m}$ in 30 minutes during the *Drosophila* wing disc development [The and Perrimon, 2000]. The cell response to morphogen reception is a downstream process of protein activation and gene transcription that define the term *signaling pathway*.

2.1.2 Wnt/ β -catenin pathway

Wnt proteins target different signaling pathways that are distinguished depending on the protein β -catenin activation. The calcium-dependent pathway and the planar-cell-polarity pathway do not involve β -catenin, in contrast to the Wnt/ β -catenin pathway, also called canonical Wnt pathway, which is the most known and studied one.

The Wnt/ β -catenin pathway mechanism is the following: In absence of Wnt proteins, cytosolic β -catenin is phosphorylated by a multi-protein complex. This complex, called *degradation*

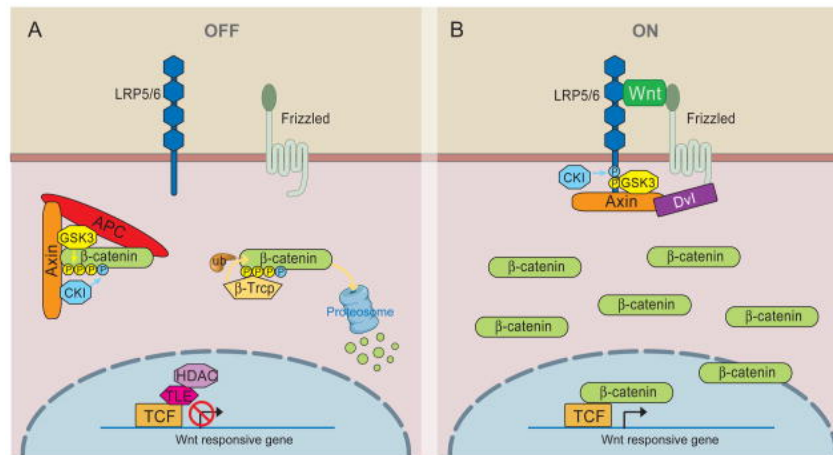


Figure 2.2: Overview of the Wnt/ β -catenin signaling pathway. (A) In absence of Wnt proteins, the degradation complex phosphorylates β -catenin which is subsequently degraded by the proteasome. (B) In presence of Wnt proteins, the receptor complex Fz-LRP6 is formed, leading to Dvl recruitment at the plasma membrane, followed by Axin, GSK3 β and CKI, resulting in LRP6 phosphorylation. As the degradation complex is dismissed β -catenin can accumulate in the cytosol and further transfers to the nucleus, where it binds TCF and activates Wnt responsive genes. Source [MacDonald et al., 2009].

complex, is constituted of four proteins called adenomatous polyposis coli (APC), Axin, casein kinase I alpha (CKI α), and glycogen synthase kinase 3 beta (GSK3 β) (Figure 2.2A). APC is the scaffold protein of the degradation complex (Figure 2.2A), Axin is the binding element, as it contains binding sites for all the complex components as well as a binding site for β -catenin. Axin refers equally to the proteins Axin1 and Axin2 as both participate to the degradation complex. GSK3 β is a multifunctional kinase, involved in numerous pathways, which is active when phosphorylated on the T-loop, on tyrosine 279 residue and inactive when phosphorylated on the serine 9 residue [Doble and Woodgett, 2003]. Inactivation of GSK3 β through phosphorylation on serine 9 is not observed during Wnt signaling transduction [Ding et al., 2000]. When GSK3 β is active its substrate β -catenin has access to the catalytic site, only if a pre-phosphorylation on the substrate serine residue is done beforehand [Meijer et al., 2004]. For β -catenin, this pre-phosphorylation is done by CKI α . Thus β -catenin phosphorylation is a hierarchical process starting with CKI α phosphorylation on β -catenin serine 45 residue, followed by GSK3 β phosphorylation on threonine 41 and serine 33 and 37 residues [Doble and Woodgett, 2003]. Phosphorylated β -catenin is tagged for ubiquitination and subsequent degradation by the proteasome (Figure 2.3).

When Wnt proteins are present in the cell environment (Figure 2.2B), they bind to one of the 10 isoforms of Frizzled receptors (Fz) and their co-receptors. The specific combination of Fz isoforms and co-receptors makes the specificity of the Wnt signal. For the Wnt/ β -catenin pathway, the co-receptor is the low-density lipoprotein receptor-related protein 6 (LRP6). Activated

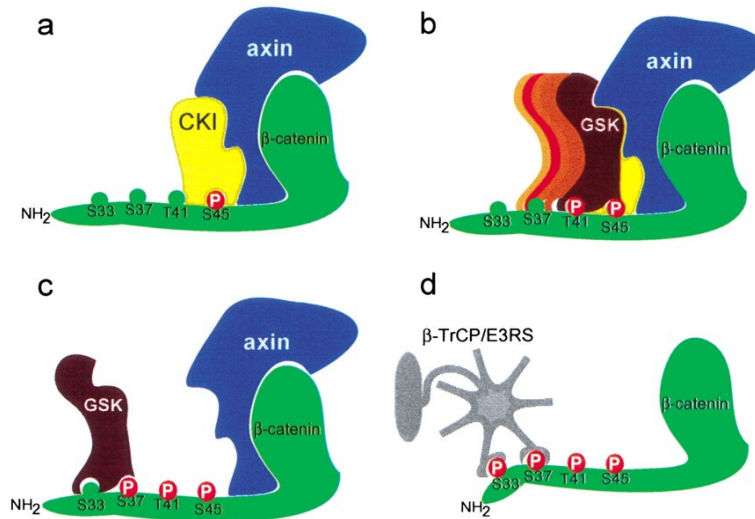


Figure 2.3: Schema of β -catenin phosphorylation and degradation cascade. Adapted from [Amit et al., 2002]. (a) Axin bound to β -catenin recruits CK1 to phosphorylate β -catenin on serine 45. (b,c) subsequently to the first phosphorylation, GSK3 β proceeds to phosphorylate in series until serine 33. (d) phosphorylation on serine 33/37 allows β -catenin ubiquitination by β -TrCp/E3RS, leading to β -catenin degradation.

Fz recruits LRP6, resulting in the signal transduction from the membrane into the cytosol. The mechanisms underlying this step remain unclear. Dishevelled (Dvl) is the first cytosolic protein family to be activated (phosphorylated) and to be recruited from the cytosol to the plasma membrane where it binds to Fz receptors. The Dvl family includes three proteins, Dvl1, Dvl2, and Dvl3. Dvl2 isoform is the most abundant in mammalian cells [Lee et al., 2008]. Although their respective roles in the activation of the pathway are not well understood, Dvl proteins are thought to play a role at the crossroad for the activation of the different Wnt signaling pathways [Boutros and Mlodzik, 1999]. The complex Dvl-Fz is thought to form a scaffold for Axin [Roberts et al., 2007], thus promoting its recruitment to the plasma membrane and leading to the degradation complex disassembly. At the plasma membrane, Axin binds to LRP6 cytoplasmic tail and generates phosphorylations of the co-receptor, especially on the serine 1460 residue [Tamai et al., 2004].

After deactivation of the degradation complex, non-phosphorylated β -catenin accumulates in the cytosol and shuttles into the nucleus. The β -catenin accumulation in both compartments is the hallmark of the pathway activation. The process governing β -catenin shuttling between cytosol and nucleus is assumed to be a facilitated diffusion combined with compartment retention as no shuttling partners have been found so far [Krieghoff et al., 2005]. Once in the

nucleus, β -catenin binds to the transcription factor T-cell factor (TCF) leading to Wnt specific gene transcription. Currently 107 genes are known to be regulated following Wnt signaling (details and updates at the Wnt homepage <http://wnt.stanford.edu>). Among these target genes, AXIN2 over-expression is the indisputable sign of Wnt/ β -catenin pathway activation [Leung et al., 2002]. Furthermore, as the protein Axin2 regulates negatively the pathway by participating to the degradation complex, AXIN2 transcription is a negative feedback loop of the Wnt/ β -catenin pathway [Leung et al., 2002].

A classification of the 19 Wnt proteins has defined Wnt1, Wnt2, Wnt3a, Wnt7a/b and Wnt8a/b as triggers of Wnt/ β -catenin pathway [Lange et al., 2006]. However, the last years of research have changed the Wnt pathways' paradigm. It has been shown that a given Wnt protein does not always trigger the same pathway. The current consensus is that more than the Wnt protein itself, it is the cell type and the receptors present at the cell membrane that determine the pathway to be activated [Mikels and Nusse, 2006]. Thus classification of each Wnt protein regarding their respective effects in different cell types and organisms remains an ongoing task. The investigation of the Wnt pathways started 27 years ago, and still some mechanisms of the signaling cascade remain unclear. How Wnt leads to LRP6 activation, and inhibits β -catenin phosphorylation [Tamai et al., 2004, He et al., 2004] ? How does the signal transduce from its receptors Fz and LRP6 at the plasma membrane, to the destruction complex in the cytosol ? How does β -catenin transfer from the cytosol to the nucleus ? Exploration of Wnt proteins and Wnt/ β -catenin pathway downstream and upstream of the signal reception are still needed to answer the remaining questions.

2.2 Human neural progenitor cells

2.2.1 ReNcell VM cell line

Human neural progenitor cells (hNPCs) are a new hope in cell replacement therapies for neurodegenerative diseases, e.g. Parkinson's and Huntington's diseases [Lindvall and Bjoerklund, 2004]. These diseases are characterized by a loss of neural cells, i.e. neurons, and more specifically dopaminergic neurons. These dopaminergic neurons are located, among several areas, in a region of the central nervous system (CNS), i.e. the brain, called mesencephalon or mid-brain [Smidt and Burbach, 2007] and are issued from neural progenitor cell differentiation. Progenitor cells, like stem cells, have the ability to maintain their proliferation state, i.e. their self-renewal. However, unlike stem cells, they are niche specific and mature in diverse cell types

specifically of their original tissue. Thus, progenitor cells issued from the CNS are committed to given cell fate, neural cells, i.e. neurons and glial cells [Hirabayashi and Gotoh, 2010].

The ventral mesencephalon (VM) contains a neurogenic niche, thus cells issued from this region are suitable for *in vitro* studies of neural progenitor cell differentiation and neurogenesis.

ReNcell VM is an immortalized cell line derived from the ventral mesencephalon, of a ten week old human embryo. The cell line is immortalized by retroviral transduction with the v-myc oncogene. Immortalization is needed to maintain cell viability as well as stable genotype and phenotype when cultivated *in vitro* [Donato et al., 2007]. The ReNcell VM cells remain in a proliferative state in the presence of growth factors such as basic fibroblast and epidermal growth factors (bFGF, EGF). After removal of the growth factors from the media, ReNcell VM cells are able to differentiate into neural cells [Donato et al., 2007], especially dopaminergic neurons [Morgan et al., 2009]. So far ReNcell VM cells remain a research cell line only and application for human therapy is not its purpose. Thus investigations of ReNcell VM cells are a first means to explore and understand the molecular mechanisms underlying hNPC proliferation and differentiation.

2.2.2 Cell cycle in ReNcell VM cell line

The cell cycle is the biological process leading to DNA duplication and cell division into two identical daughter cells. This process allows a cell population to stay in the proliferation state and to exponentially grow. The cell cycle is usually described as a succession of four different sequential phases (Figure 2.4):

1. The G1 phase (*gap 1*) is the cell growth phase, throughout which the cell undergoes morphological changes. During G1, a cell can also enter in a resting phase, called G0. While in G0 the cell remains quiescent for a long time, which can possibly be indefinitely, before coming back to G1 if it receives the appropriated signals. At the end of G1, a *restriction point* (R) will decide whether the cell remains committed to the cycle and will proceed to DNA replication and division or has to leave the cycle and starts its differentiation.
2. The S phase (*synthesis*) consists in the DNA replication.
3. The G2 phase (*gap 2*) stands between S and M phases and allows the cell to continue its growth. In the meantime the previous replicated DNA will be checked and a second *restriction point* will decide for the continuation of the cycle.

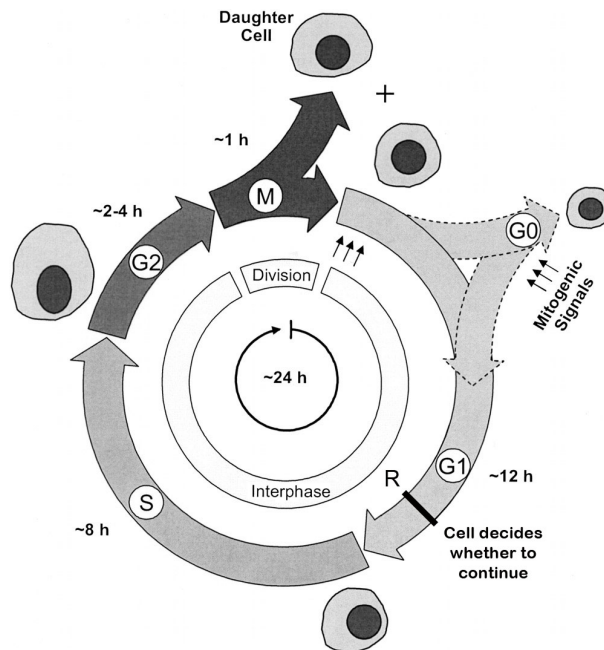


Figure 2.4: Typical cell cycle showing the four phases and their relative duration in mammalian cells. Modified from [Alam et al., 2004].

4. The M phase (*mitosis*) is the real division phase. The nucleus and its content, i.e. the chromosomes, divide equally in two, followed by the cytoplasm equal division. The M phase leads to the generation of two identical daughter cells.

On average, in mammalian cells, the cell cycle has a duration of 24 hours, with the following distribution: G1 phase lasts for 12 hours, S for 8 hours, G2 between 2 to 4 hours and about 1 hour for the M phase [Alam et al., 2004] (Figure 2.4).

The cell cycle is critical for the cell survival, and thus it is protected by intra- and extracellular signals. Intracellular signals are governed by family of proteins called cyclin-dependent kinases (Cdks) and through their binding to other proteins, known as cyclins. Extracellular signals are triggered by the presence of growth factors or mitogens, e.g. nerve or epidermal growth factors (NGF, EGF), in the cell environment. Their presence promotes cell growth and cell division through the cell cycle. To illustrate, an absence of external growth factor, will inhibit a cyclin-Cdk complex leading to the arrest of the cycle at the G1 restriction point. Thus the passage from G1 phase to S phase is feasible only in a favorable environment, i.e. in presence of growth factors. However this does not apply to the checkpoint in G2. If an error is detected during the cycle, the only alternative is death, i.e. apoptosis. Indeed a cell already committed into S, G2 or M phases can not leave the cell cycle until the division is finished. In this case, the cell will interpret the lack of growth factors only after ending the cycle, when re-entering G1 phase. The

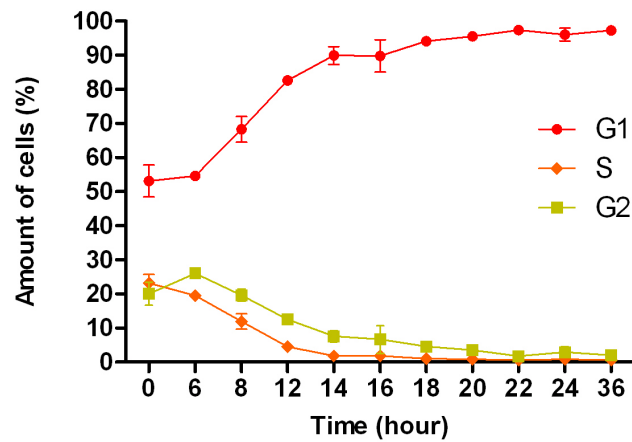


Figure 2.5: Cell cycle analyses during differentiation of ReNcell VM cells. Source [Mazemondet et al., 2011].

passage from one phase to another has been intensively studied and the probabilities for a cell to go through the checkpoints is thought, especially for G1 checkpoint, to follow an exponential distribution [Smith and Martin, 1973].

The cell cycle of ReNcell VM cells has a doubling time, i.e. the duration of one cycle, of around 19 hours and 40 minutes [Schmöle et al., 2010]. However, the cells are asynchronous in the cell cycle (Figure 2.5), i.e. the whole cell population is not encompassed in one phase but distributed all over the cell cycle. Indeed, the distribution of the ReNcell VM cells in the cell cycle is the following: about 53% of cells are in G0/G1 phase, 23% in S phase and 20% in G2 phase (Figure 2.5). Thus, when the growth factors are withdrawn from the media, only 53% of the cells will be able to start the differentiation and it will take up to 24 hours before all the cells leave the cell cycle and enter the differentiation process. Therefore, this asynchronism of the cell population should be taken into account during the study of molecular mechanisms underlying cell differentiation.

2.2.3 Wnt/ β -catenin pathway and neural progenitor cells

Wnt signaling pathways are involved in proliferation, differentiation and cell fate processes in diverse neural progenitor and stem cell lines, although a consensus regarding their real functions has not been reached. It has been first established that Wnt/ β -catenin pathway accompanies proliferation of neural stem cell derived from the CNS [Castelo-Branco et al., 2003, Zechner et al., 2003, Michaelidis and Lie, 2008]. However, evidence accumulates that the Wnt/ β -catenin pathway is equally involved in the differentiation process: Cortical neural precursors are able to differentiate into neurons under the pathway stimulation in presence [Hirabayashi et al., 2004] or

absence [Israsena et al., 2004] of growth factors. Lately, the implication of Wnt/ β -catenin pathway to promote neurogenesis and to inhibit gliogenesis, has been demonstrated in the neurosphere of neonatal forebrain in mouse [Kunke et al., 2009]. Furthermore, evidence arose that β -catenin is specifically involved in differentiation and dopaminergic neurogenesis [Castelo-Branco et al., 2004, Lange et al., 2006, Tang et al., 2009].

In ReNcell VM cells inhibition of GSK3 β is leading to an accumulation of nuclear β -catenin and an increase of neurogenesis [Schmöle et al., 2010, Lange et al., 2011], suggesting that the Wnt/ β -catenin is active in ReNcell VM cells and involved in neuron differentiation. However, the duration and the nature (autocrine or paracrine) of this signal remain unclear. Autocrine Wnt/ β -catenin signaling is known to occur in neural stem cell [Wexler et al., 2009] and brain development [Chenn and Walsh, 2002, Canning et al., 2007], respectively, but has not yet been investigated for ReNcell VM cells, in particular. It is noteworthy that ReNcell VM cell immortalization with v-myc might have some drawbacks on Wnt/ β -catenin pathway analyses as in many cell lines myc is a downstream target of the Wnt signals [Sansom et al., 2007]. Whether this is also the case in ReNcell VM cells needs future investigation.

Thus, different and opposite effects, i.e. proliferation and differentiation, of a given Wnt protein or the Wnt/ β -catenin pathway, are observed in neural progenitor and stem cell population, also depending of the stage of the CNS development. This disparity suggests that each Wnt protein has his own profile of action, in a given cell line, in relation with the cell development stage [Michaelidis and Lie, 2008].

2.2.4 Wnt3a and neural progenitor cells

Although a given Wnt protein does not always trigger the same Wnt pathway, depending on the cell type and cell state, Wnt3a is commonly referred as a trigger for Wnt/ β -catenin pathway. This is accepted since cells expressing Wnt3a have demonstrated an elevation of β -catenin level in the cytosol [Shimizu et al., 1997]. Later, Wnt3a appeared to be a ligand for the co-receptor LRP6 [Liu et al., 2003] and to phosphorylate LRP6 on its serine 1490 residue [Pan et al., 2008]. It is thought that Wnt3a signaling leads to the recruitment of Axin to LRP6, inhibiting Axin binding to β -catenin, that results in β -catenin accumulation [Yamamoto et al., 2006].

Investigation of Wnt3a impact on neural cell development established that Wnt3a is involved in the proliferation of neural progenitor cells in rat ventral midbrain [Castelo-Branco et al., 2003]. It further mediates the self-renewal of mouse neural progenitor cells [Kalanina et al., 2008] and neural progenitors derived from human embryonic stem cells [Davidson et al., 2007]. Controversially, it has been shown to promote neuronal differentiation in neural stem cell culture

[Muroyama et al., 2004].

ReNcell VM cells transfected with Wnt3a vector present an increase of TCF activity and of Wnt/ β -catenin pathway specific gene transcription, i.e. AXIN2, Cyclin D1, during proliferation [Hübner et al., 2010]. Furthermore, these transfected cells tend to differentiation into neurons rather than glial cells, suggesting a role of Wnt3a in the cell fate.

Chapter 3

in vitro exploration

This chapter presents the *in vitro* exploration of the Wnt/ β -catenin pathway in ReNcell VM cells using molecular and cellular biology techniques. Details about the methods and the procedures applied for wet-lab experiments are explained in Section 3.1. Description of *in vitro* results are given in Sections 3.2 and 3.3. First, the spatio-temporal profiles of the Wnt/ β -catenin pathway components during the first 72 hours of ReNcell VM cell physiological differentiation are detailed (Section 3.2). Second, the component profiles in presence of exogenous Wnt3a are reported during proliferation and differentiation of ReNcell VM cells (Section 3.3). These experimental results are discussed, interpreted and hypotheses regarding the protein regulation during ReNcell VM cell differentiation are proposed in Section 3.4.

3.1 Material & Methods

The following section describes molecular and cellular biology procedures carried out during wet-lab experiments to explore *in vitro* the spatio-temporal dynamics of intracellular protein within ReNcell VM cells. It documents the specialized material and experimental techniques used and aims to allow other researchers to replicate the work done if needed.

3.1.1 Solutions & Material lists

Cell culture buffers

Differentiation medium

DMEM:F12 1:1 w/o L-Glutamin	482 mL	Gibco #21331-020
B27 supplement	10 mL	Gibco #17504-044

GlutaMax I	2 nM	Gibco #35050-038
Heparin sodium salt	10 U/mL	Sigma #H 3149
Gentamycin	50 μ g/mL	Gibco #15750-037

Proliferation medium

Differentiation medium		
Epidermal Growth Factor	20 ng/mL	PeptoTech #100-15
Basic Fibroblast Growth Factor	10 ng/mL	Roche #11120417001

Trypsine/Benzonase

Trypsin-EDTA (1x in HBSS)	100 mL	Gibco #25300-054
Benzonase 250 U/ μ L	10 μ L	Merck #1.01654.0001

Trituration solution (Trit)

Soybean trypsin inhibitor	50 mg	Sigma #T-6522
DMEM:F12 1:1 w/o L-Glutamin	87.4 mL	Gibco #21331-020
Human serum albumin	4.5 mL	Octa Pharma #10542a/96
Benzonase	9.1 μ L	Merck #1.01654.0001

Cell culture products & equipments

Mouse Laminin 1 Protein 1 mg/mL	Trevigen #3400-010-01
Recombinant mouse Wnt3a reconstituted 40 μ g/mL in sterile PBS	R&D Systems #1324-WN
PBS w/o Ca^{2+} and Mg^{2+}	Biochrom AG #L 1825
HBSS w/o Ca^{2+} and Mg^{2+}	Gibco #14170-088
Phosphostop	Roche #04 906 837 001
Cell counter	CASY®, Innovatis AG
Microscope	Biozero, Keyence
ReNcell VM cells	ReNeuron, Milipore
Qproteome Cell Compartment	Qiagen #37502

Western-blot buffers

The chemicals' suppliers are the companies Calbiochem, Fluka, Merck, Sigma and Roth.

<i>TBS (pH 7.5)</i>		<i>TBST (pH 7.6)</i>	
NaCl	150 mM	TBS	100 mL
Tris-Hcl	7.7 mM	Tween 20	1%
Distilled water	1 L	Distilled water	900 mL
<i>Transfer buffer (pH 8.3)</i>		<i>Electrophoresis buffer (10 fold)</i>	
TRIS	6.06 g	TRIS	3.03 g
Glycine	28.02 g	Glycine	14.1 g
Methanol	400 mL	SDS	10 g
Distilled water	1.6 L	Distilled water	1 L
<i>Laemmli buffer (5 fold)</i>		<i>Colloidal Coomassie Dye (CCD)</i>	
SDS	1.5 g	Coomassie Brilliant	
Tris-Hcl	1 M	Blue 5% in Distilled water	10 mL
Bromphenol blue	10%	Phosphoric acid	6 mL
DTT	1.16 g	Ammonium sulfate	50 g
Glycerin	87%	Distilled water	490 mL
Distilled water	15 mL		
<i>Colloidal Coomassie Solution</i>		<i>1°Antibody buffer</i>	
CCD	200 mL	Albumin Serum in TBST	5%
Methanol	50 mL		
<i>Blocking solution I</i>		<i>2°Antibody buffer I</i>	
Skim milk powder in TBS	5%	Albumin Serum in TBST	5%
<i>Blocking solution II</i>		<i>2°Antibody buffer II</i>	
Albumin Serum in TBS	5%	Skim milk powder in TBST	5%

Western blot products & equipments

Prestained peqGOLD marker IV	PEQLAB #27-2111
Nitrocellulose membrane, Amersham Hybond-ECL	GE Healthcare #RPN303D
<i>Criterion</i> TM Precast Gels 4-15% Tris-HCl, 1.0 mm	
12+2 Well Comb, 45 μ L	BIO-RAD #345-0027
18 Well Comb, 30 μ L	BIO-RAD #345-0028
Electrophoresis chamber, Criterion Cell	BIO-RAD
Protein transfer, Trans-Blot Cell	BIO-RAD
Power supply, PowerPac HC	BIO-RAD
Protein Assay Kit <i>BCA</i> TM	Pierce #23225
Odyssey® Infrared Imaging System	LI-COR Biosciences

Cell fraction buffers

Buffers adapted from the kit *Qproteome Cell Compartment*, Qiagen #37502

Cytosol buffer	Buffer CE1 (Qiagen)	220 μ L
	Calyculin A (Upstate #19-139)	2.2 μ L
	Protease Inhibitor (Qiagen)	2.2 μ L
Membrane buffer	Buffer CE2 (Qiagen)	220 μ L
	Calyculin A (Upstate #19-139)	2.2 μ L
	Protease Inhibitor (Qiagen)	2.2 μ L
Nucleus buffer	Buffer CE3 (Qiagen)	110 μ L
	Calyculin A (Upstate #19-139)	1.1 μ L
	Protease Inhibitor (Qiagen)	1.1 μ L

3.1.2 Cell culture

The cell line ReNcell VM is derived from the ventral mesencephalon of a ten week old human fetus and is immortalized by retroviral transduction with v-Myc oncogene (ReNeuron Ltd, Guildford, UK). ReNcell VM cells were cultivated according to the previous described protocol [Hoffrogge et al., 2006]. Briefly, cells were cultured in proliferation medium with laminin (10 μ g/mL) coated cell culture flasks T75, and maintained at 37 Celsius degrees with

5% CO_2 . The medium was changed every two to three days. Proliferating cells were passaged when confluence reached approximately 80%. For initiation of differentiation cells were washed once with HBSS (15 mL) before differentiation medium was added (15 mL). For experiments with Wnt3a treatment, 100 ng/mL of recombinant mouse Wnt3a were added to proliferation or differentiation media.

Cells were harvested either in proliferating state (time point 0 hour) or at time points 0.5, 1, 2, 3, 4, 8, 12, 24, 48 and 72 hours after differentiation. Cells were detached from the flasks by addition of Trypsin-Benzoyl-L-histidine-Hydrochloride solution (2.5 mL per flask T75). The flasks were incubated at 37 degrees for three to five minutes. Addition of trituration solution (5 mL per flask) ensured to stop the effect of the Trypsin. The cells in suspension were collected and pelleted by centrifugation (1500 rpm for five minutes at room temperature). The supernatant was discarded and cells were resuspended in 5 mL of ice-cold PBS with addition of the phosphatase inhibitor Phosphostop (1 tablet/10 mL of PBS) and directly used for subcellular fractionation or stored at -80 degrees.

3.1.3 Cell volume

ReNcell VM cell volume was calculated using the cell counter CASY® device. After trypsination ReNcell VM cells are in nearly spherical shape in the solution suspension. This condition is necessary and sufficient for the device CASY® to retrieve the mean volume of the cells analyzed in the sample. As the solution Trypsin-Benzoyl-L-histidine-Hydrochloride-trituration is isotonic it does not produce cell volume changes. Cell suspension (25 μ L) was diluted in 10 mL of CasyTon buffer and analyzed by CASY®. The results given contain the mean volume (in femtolitre) of the spherical spheres passing through the capillary.

3.1.4 Subcellular fractions

Subcellular fractions were prepared using the kit Qproteome Cell Compartment (Qiagen) according to the manufacturer's instructions. However buffer volumes were adapted, see details in Section 3.1.1. Briefly, cells resuspended in 5 mL ice-cold PBS/Phosphostop were centrifuged for 5 minutes at 1200 rpm, and the pellet was resuspended in 224.4 μ L of *cytosol buffer* and incubated for 10 minutes at 4 degrees on an end-over shaker. After 10 minutes of centrifugation at 2000 rpm, the supernatant was kept and identified as the *cytosol fraction*. The pellet

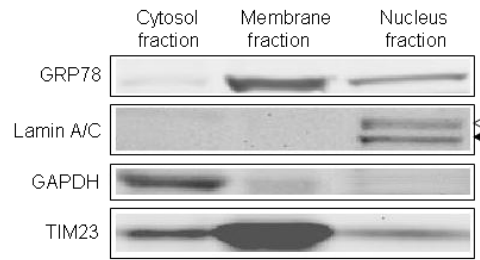


Figure 3.1: Representative Western-blot for the subcellular fractions. GRP78 and TIM23 are markers for the membrane fraction. Lamin A/C is a marker for the nucleus fraction, two bands are detected by the antibody, the upper one (white arrow head) at 74 kDa and the lower one (black arrow head) at 65 kDa. GAPDH, is mainly present in the cytosol fraction.

was resuspended in 224.4 μL of *membrane buffer* and incubated for 30 minutes at 4 degrees on an end-over shaker. After centrifugation for 10 minutes at 8000 rpm the supernatant contained the *membrane fraction*. The pellet was resuspended with 7 μL Benzonase Nuclease and 13 μL distilled water, and incubated at room temperature for 15 minutes. After addition of 112.2 μL *nucleus buffer* and incubation for 10 minutes at 4 degrees on an end-over shaker, a last centrifugation at 9000 rpm for 10 minutes separated the supernatant kept as the *nucleus fraction*. Subcellular fractions were stored at -80 degrees. Purity of the membrane, cytosol and nucleus fractions were analyzed by immunoblotting, 30 μg of proteins were loaded on a SDS-polyacrylamide gel and blotted, as described in the Section 3.1.5. Detection was made with antibodies against the specific compartmental marker proteins: the Translocase of the Inner Mitochondrial membrane (TIM23) and the glucose-regulated protein 78 (GRP78) for the membrane fraction; the glyceraldehyde-3-phosphate dehydrogenase (GAPDH) for the cytosolic fraction and the lamin A/C for the nuclear fraction. Antibodies details can be found in Table 3.3. Notice that GAPDH is also present in the membrane fractions, as mentioned by the manufacturers, but to a least extend than in the cytosolic fractions.

3.1.5 Protein determination & Western blot analysis

Protein concentrations of subcellular fractions were estimated using the protein assay kit *BCATM* (Pierce) according to the manufacturer's instructions. Afterwards, cell samples were diluted in Laemmli-buffer 5 fold and boiled at 95 degrees for five minutes. Lysates were loaded into gradient (4-15%) SDS-polyacrylamide gels (10-50 μg of proteins per lane) and separated electrophoretically (BIO-RAD, Hercules, USA) for two hours (120 Volts). The prestained pep-GOLD marker IV (PEQLAB, Erlangen, Germany) was used as molecular weight marker.

Antibody name	Reference	Dilution
Mouse anti β -catenin	Santa Cruz #7963	1:1000
Rabbit anti Dishevelled-2	Cell Signaling #3216	1:4000
Rabbit anti LRP6	Cell Signaling #2560	1:4000
Rabbit anti phospho-LRP6 (Ser1490)	Cell Signaling #2568	1:2000
Mouse anti GSK-3 β	BD Transduction Laboratories #610201	1:1000
Mouse anti GSK-3 β (pY216)	BD Transduction Laboratories #612312	1:1000
Mouse anti Tim23	BD Transduction Laboratories #611222	1:1000
Mouse anti Lamin A/C	BD Transduction Laboratories #612163	1:1000
Goat anti GRP78 (N-20)	Santa Cruz Biotechnology #1050	1:2000
Rabbit anti GAPDH	Santa Cruz Biotechnology #25778	1:2000
Rabbit anti β -actin	Delta Biolabs #070	1:1000

Table 3.3: Primary antibodies used for protein detection by Western-blot

Antibody name	Reference	Dilution
Goat anti rabbit Alexa Fluor 680	Invitrogen #A-21076	1:10000
Goat anti mouse Alexa Fluor 680	Invitrogen #A-21057	1:10000
Rabbit anti mouse Alexa Fluor 680	Invitrogen #A-21065	1:10000
Donkey anti goat Alexa Fluor 680	Invitrogen #A-21084	1:10000
Rabbit anti mouse IRDye 800	Rockland #610-431-020	1:10000
Goat anti rabbit IRDye 800	Rockland #611-131-122	1:10000
Goat anti mouse IRDye 800	Rockland #610-131-003	1:10000

Table 3.4: Secondary antibodies used for fluorescence analysis of Western-blot

Proteins separated into the gel were transferred using a wet transfer system (BIO-RAD, Hercules, USA) onto nitrocellulose membranes for one hour. After transfer, the membranes were blocked with blocking solution I or II for detection of phosphorylated proteins (details in Section 3.1.1) for one hour on a shaker, before incubation with the primary antibodies (Table 3.3). Antibodies were diluted in 1° Antibody buffer (Section 3.1.1) and membrane incubation was done overnight at 4 degrees on a shaker. Meanwhile, the blotting gels were stained with Colloidal Coomassie solution for verification of the amount of protein uploaded. Membranes were rinsed three times, for five minutes each time, with TBST and probed with appropriate fluorescent secondary antibodies (Table 3.4) diluted in 2° Antibody buffer I or II for detection of phosphorylated proteins, one hour at room temperature on a shaker and in the dark. Membranes were washed two times for five minutes each with TBST and once with TBS, before set to dry in the dark. Visualization and quantification of proteins were performed using Odyssey® Infrared Imaging System.

3.1.6 Quantification & statistics

For quantification of proteins of interest the samples were loaded onto the gel in randomized and non-chronological order to reduce systematic errors [Schilling et al., 2005]. The strategy was developed with support from Katja Rateitschak (Department of Systems Biology & Bioinformatics, University of Rostock). Expressions of β -actin or GAPDH proteins were used as loading controls to normalize the proteins of interest's expressions. Thereby relative expression levels of the target proteins were determined.

In order to be compared, the quantification of a given protein in different subcellular fractions should have the same internal standard. The use of β -actin as loading control in the membrane fraction is not possible due to the cytoskeletal changes in ReNcell VM cells during differentiation. It is noteworthy that although GAPDH is a marker for cytosol fraction (see Section 3.1.4), it is used as a loading control for both membrane and cytosol fractions, due to its ubiquitous presence [Tarze et al., 2007] and its stability in the cytosolic fraction over the kinetics of the experiments. To illustrate the stability of GAPDH in both fractions the standard error on the mean (SEM) for GAPDH, over time and for 3 independent experiments (cell passages), was calculated: SEM of 5.7 % and 7.3% are found in cytosol and membrane fractions, respectively. For every single experiment, a SEM above 10% was ground for excluding the data from the quantification.

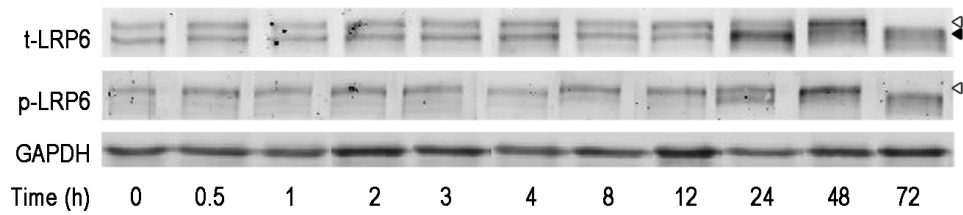
For each quantified Western-blot, the relative expression at a given time point is normalized to the mean of the time series. The resulting values were normalized to the one in proliferating cells (time point 0 hour) that is set to 1. Normalization and rescaling methods were developed with support from Yvonne Schmitz (Department of Systems Biology & Bioinformatics, University of Rostock). Results are expressed as means \pm SEM. Experiments were reproduced at least three times: three independent cell passages and at least three independent Western-blot for each cell passage. Statistical evaluation was carried out using a two-tailed Student's *t-test* for normally distributed data. Difference was considered to be statistically significant when p-value was inferior to 0.05 ($p \leq 0.05$).

3.2 Spatio-temporal dynamics of Wnt signaling proteins

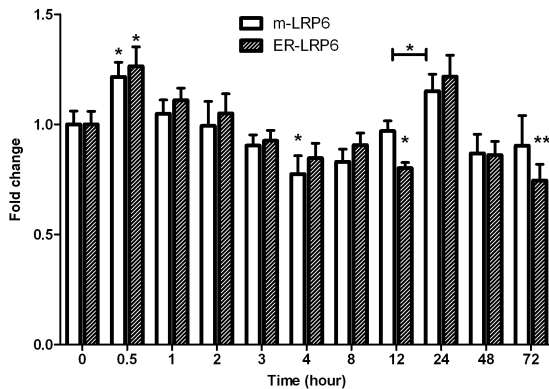
In attempt to analyze Wnt/ β -catenin pathway activity during the pivotal passage from proliferation to differentiation of ReNcell VM cells, investigation of the spatio-temporal dynamics of the main signaling proteins is performed. The proteins of interest are the co-receptor LRP6, the enzyme GSK3 β , Dvl2 and β -catenin. This choice is due, on one hand, to the importance and specificity of these proteins for Wnt signaling (see Section 1), and on the other hand, to their inaccessibility via the experimental techniques described previously (see Section 3.1, i.e. the protein Axin could not be detected with Western-blot in ReNcell VM cell fractions.). Diverse protein states are investigated with the help of different antibodies (details in Table 3.3): total LRP6 (t-LRP6) and LRP6 phosphorylated on serine 1490 residue (p-LRP6), total GSK3 β (t-GSK3 β) and GSK3 β phosphorylated on tyrosine 216 residue (p-GSK3 β), total Dvl2 distinguish mature Dvl2 form (m-Dvl2) and phosphorylated Dvl2 (p-Dvl2), and total β -catenin. To observe the spatial dynamics these proteins are quantified in their specific subcellular locations: t-LRP6 and p-LRP6 in the membrane fraction, t-GSK3 β in the cytosol fraction, total Dvl2 and p-GSK3 β in the membrane and cytosol fractions, and total β -catenin in the cytosol and nucleus fractions. The temporal dynamics are investigated by quantification of the protein expressions, in their respective locations, along the first three days of differentiation. After three days of proliferation (time point 0 hour) in presence of growth factors, the cells were incubated with differentiation media (without growth factors) before their collection after 0.5, 1, 2, 3, 4, 8 hours (*early differentiation*), and after 12, 24, 48, and 72 hours (*late differentiation*). The temporal distinction between early and late differentiation is done regarding ReNcell VM cell fate commitment as proposed by [Bader, 2010]: during *early differentiation* no distinction between neurons and glial cells is yet possible, in contrast to the *late differentiation*. The data presented are relative changes over time, compared to the amount at time 0 hour (proliferation) which is set to 1. Each protein has been quantified in a minimum of four independent cell samples with at least three quantitative Western-blot per cell sample.

3.2.1 Early regulation during the first hours of differentiation

Total LRP6 (t-LRP6) is already detectable in proliferation with two specific bands: the lower one at 180 kilodalton (kDa) represents LRP6 in the endoplasmic reticulum (ER) (ER-LRP6, black arrowhead on Figure 3.2a), and the upper band at 190 kDa shows the mature LRP6 (m-LRP6, white arrowhead, Figure 3.2a) in the membrane fraction. As early as 0.5 hour after differentiation, t-LRP6 increases significantly to 1.25 fold compared to the proliferation control.



(a) t-LRP6 and p-LRP6



(b) Quantification of t-LRP6

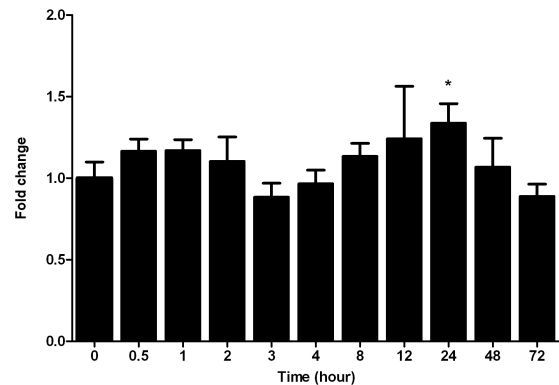
(c) Quantification of p-LRP6_{ser¹⁴⁹⁰}

Figure 3.2: Analyses of LRP6 protein in the membrane fraction during ReNcell VM cell differentiation. (a) Representative Western-blot of t-LRP6 and p-LRP6 in membrane fraction. For t-LRP6 white arrowhead point to mature LRP6 (m-LRP6) and black arrowhead points to LRP6 in endoplasmic reticulum (ER-LRP6). (b,c) Quantified Western-blot analyses of total LRP6 (t-LRP6) (b) and LRP6 phosphorylated on serine 1490 (p-LRP6) (c) in membrane fraction. Time point 0 hour stands for control using proliferating cells. GAPDH is used as a loading control. The signal intensity at 0 hour is set to 1 and used to normalized the intensity for the other time points. Values are presented as mean \pm SEM from at least 3 independent experiments. For statistical significance '*' stands for p-value <0.05, and '**' for p-value <0.01 compared to control (0 hour).

It is followed by a slow decrease reaching a level of 0.77 fold after 4 hours that remains almost constant until 12 hours of differentiation (Figure 3.2b). The detection of p-LRP6 shows a weak expression during proliferation that remains stable along the first 12 hours of differentiation (Figure 3.2c).

Dvl2 is also detected in Western-blot with two bands [Bryja et al., 2007b, Hübner et al., 2010]: The upper one, the phosphorylated Dvl2 at 95 kDa (p-Dvl2, white arrowhead on Figure 3.3a and 3.10d), and the lower one, the mature Dvl2 at 90 kDa (m-Dvl2, black arrowhead, Figure 3.3a and 3.10d). It is noticeable that in the membrane fraction, more than two bands are detected for Dvl2, which might be due to various forms of Dvl2 contained in diverse membrane-enclosed organelles. In the membrane fraction the level of Dvl2 is very low during proliferation but increases significantly from 0.5 to 12 hours. Two peaks are observed at 2 hours and 12 hours with similar levels for p-Dvl2 and m-Dvl2, i.e. 1.75 and 1.57 fold increase, respectively (Figure

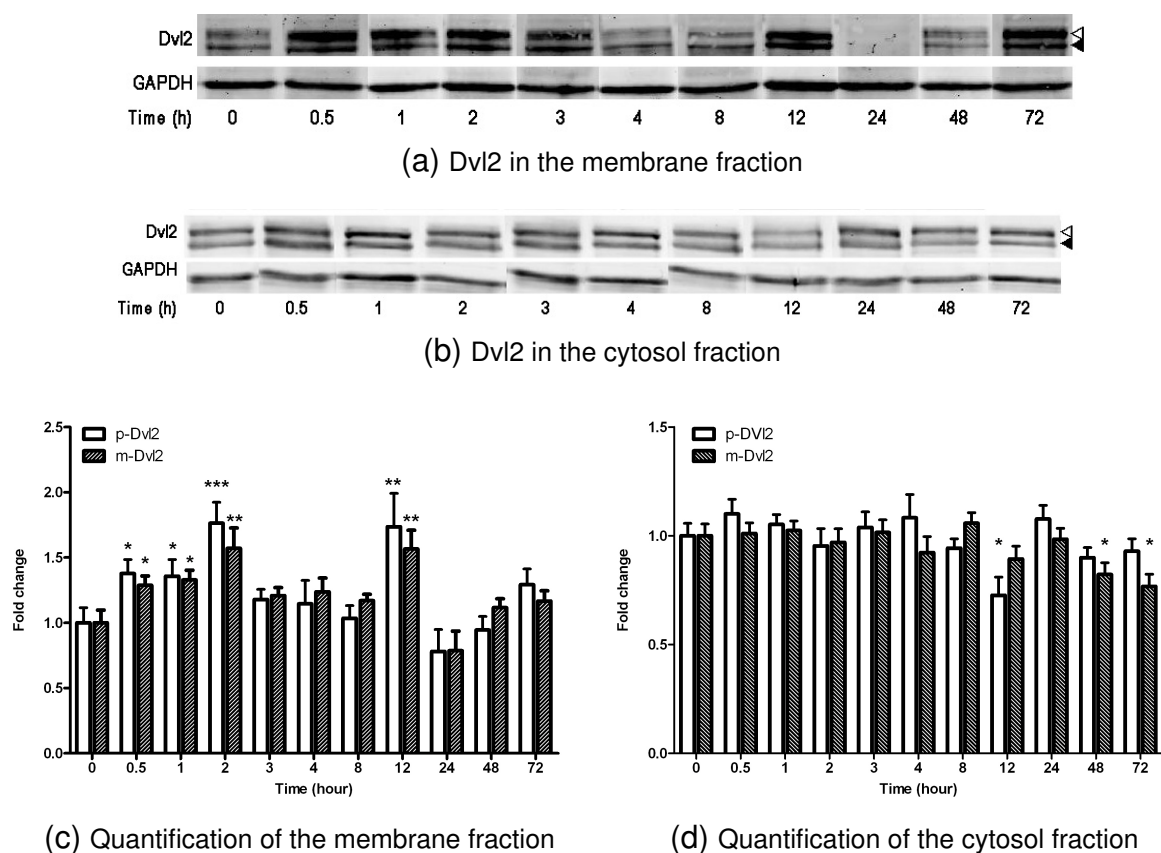


Figure 3.3: Analyses of Dvl2 protein in the membrane and cytosol fractions during ReNcell VM cell differentiation. (a,b) Representative Western-blot of Dvl2 in membrane (a) and cytosol (b) fractions. White arrowheads point phosphorylated Dvl2 (p-Dvl2) and black arrowheads point mature Dvl2 (m-Dvl2). (c,d) Quantified Western-blot analyses of p-Dvl2 and m-Dvl2 in membrane (c) and cytosol (d) fractions. GAPDH is used as a loading control. Normalization and statistical analyses were performed as described in Figure 3.2.

3.3c). Contrarily, in the cytosol fraction, the level of Dvl2 stays stable along the first 8 hours of differentiation, and in response to the increase at 12 hours in the membrane, a decrease to 0.73 fold of p-Dvl2 in the cytosol is observed (Figure 3.3d).

Analyses of total GSK3 β do not show variation over time in the cytosol fraction (Figure 3.4b). This could be expected since GSK3 β is a kinase and it is its level of in/activation that is expected to change rather than the total amount of molecules [Papkoff and Aikawa, 1998]. Detection of active-phosphorylated GSK3 β on tyrosine 216 amino acid with a specific antibody (see Table 3.3) reveals two bands: the upper one is GSK3 α phosphorylated on tyrosine 279 at 51 kDa (p-GSK3 α), the lowest one is GSK3 β phosphorylated on tyrosine 216 at 47 kDa (p-GSK3 β) [Kotliarova et al., 2008]. In the membrane fraction, a significant decrease of p-GSK3 β at 3 and 8 hours is observed (Figure 3.5c), as well as an increase of p-GSK3 α in the cytosol fraction at 3 hours (Figure 3.5d).

Total β -catenin varies in the different compartments. In the cytosol fraction a first significant

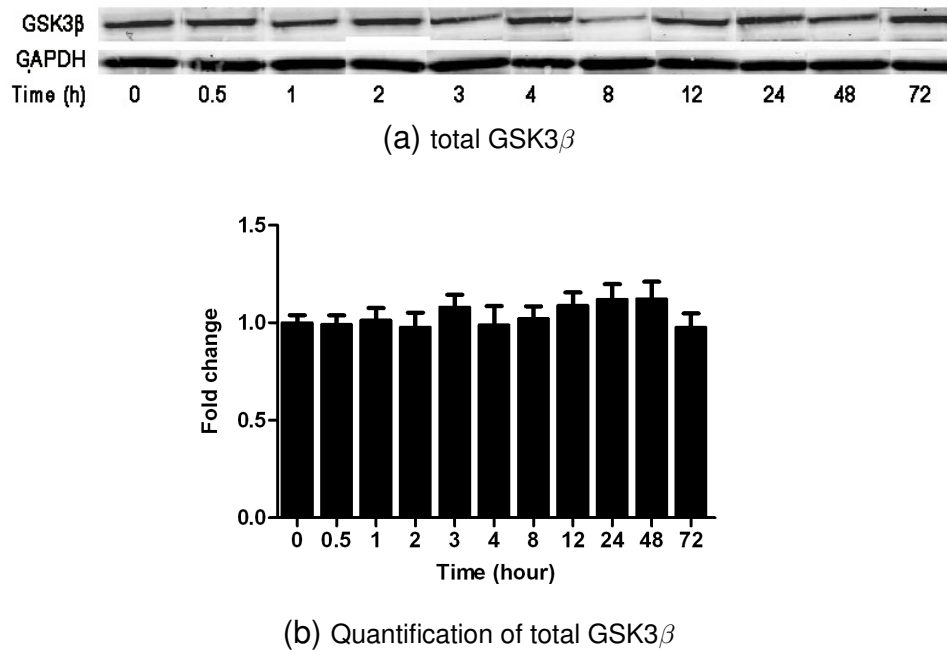


Figure 3.4: Analyses of GSK3 β protein in the cytosol fraction during ReNcell VM cell differentiation. (a) Representative Western-blot of total GSK3 β in the cytosol fraction. (b) Quantified Western-blot analyses of total GSK3 β in cytosol fraction. GAPDH is used as a loading control. Normalization and statistical analyses were performed as described in Figure 3.2.

decrease to 0.79 fold is observed after 1 hour of differentiation (Figure 3.6c), whereas in the nucleus fraction β -catenin level increases, at the same time point, up to 1.47 fold (Figure 3.6d). Afterwards, the level of cytosolic β -catenin stays stable around the proliferation level until 8 hours of differentiation. Nuclear β -catenin declines at 2 hours, before a gradual increase which reach 1.53 fold at 8 hours and 1.72 fold at 12 hours.

3.2.2 Late response during the first days of differentiation

After 24 hours of differentiation, LRP6 shows a significant increase compared to the level at 12 hours (Figure 3.2b), and p-LRP6 rises of 1.34 fold (Figure 3.2c). Besides, a change of LRP6 is observed as the ER-form (band at 180 kDa) increases at 24 hours, and at 72 hours the two bands are close to each other around 180 kDa. An equivalent change is observed for p-LRP6, with the detection on the Western-blot of a second band at 24 hours, and a shift of the band from 200 kDa to 190 kDa at 72 hours. In the membrane fraction, both m-Dvl2 and p-Dvl2 are expressed at very low level, close to proliferation level, between 24 and 72 hours (Figure 3.3c). Similarly, in the cytosol fraction, m-Dvl2 and p-Dvl2 levels are low and below the proliferation level from 24 hours onward (Figure 3.3d). Only at 72 hours, in the membrane fraction, a decrease of pGSK3 α

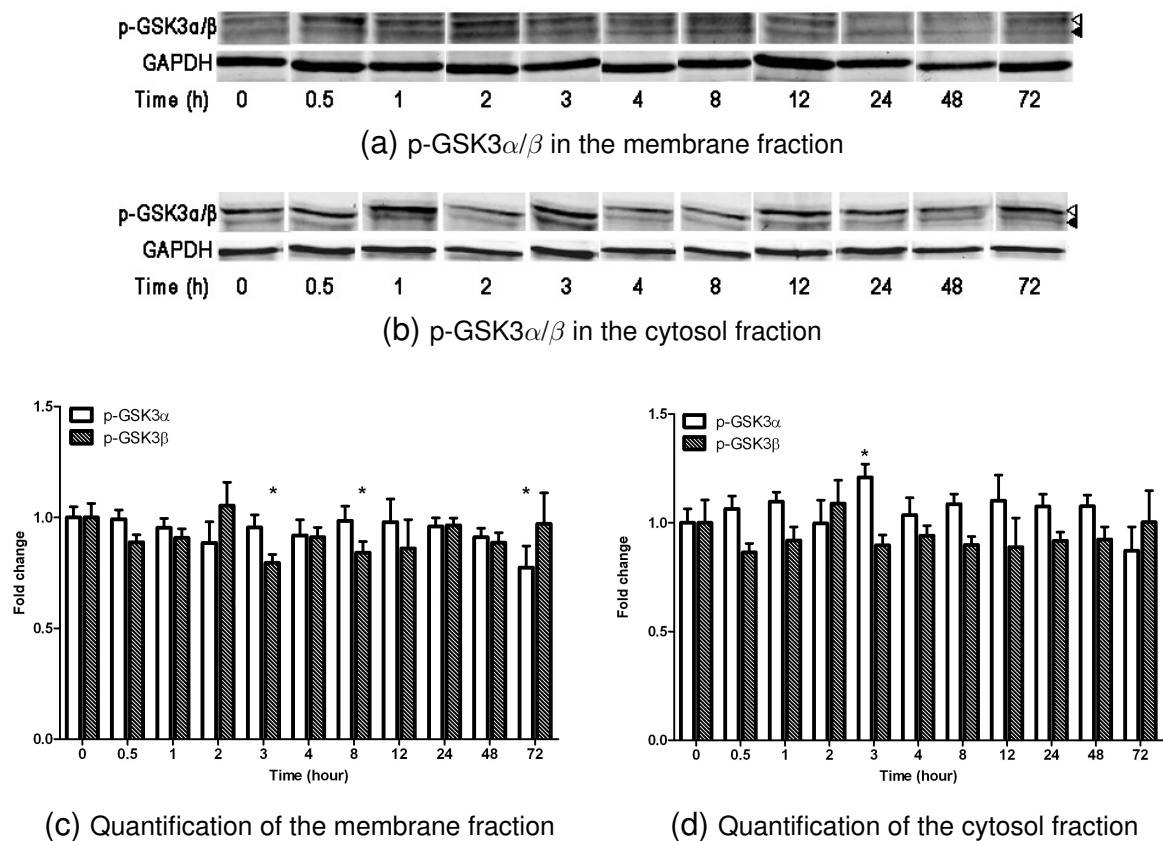


Figure 3.5: Analyses of phosphorylated GSK3 α/β proteins in the membrane and cytosol fractions during ReNcell VM cell differentiation. (a) Representative Western-blot of phosphorylated GSK3 α/β proteins, white arrowhead points to p-GSK3 α , and black arrowhead points to p-GSK3 β . (b,c) Quantified Western-blot analyses of p-GSK3 α and p-GSK3 β in membrane (b) and cytosol (c) fractions. GAPDH is used as a loading control. Normalization and statistical analyses were performed as described in Figure 3.2.

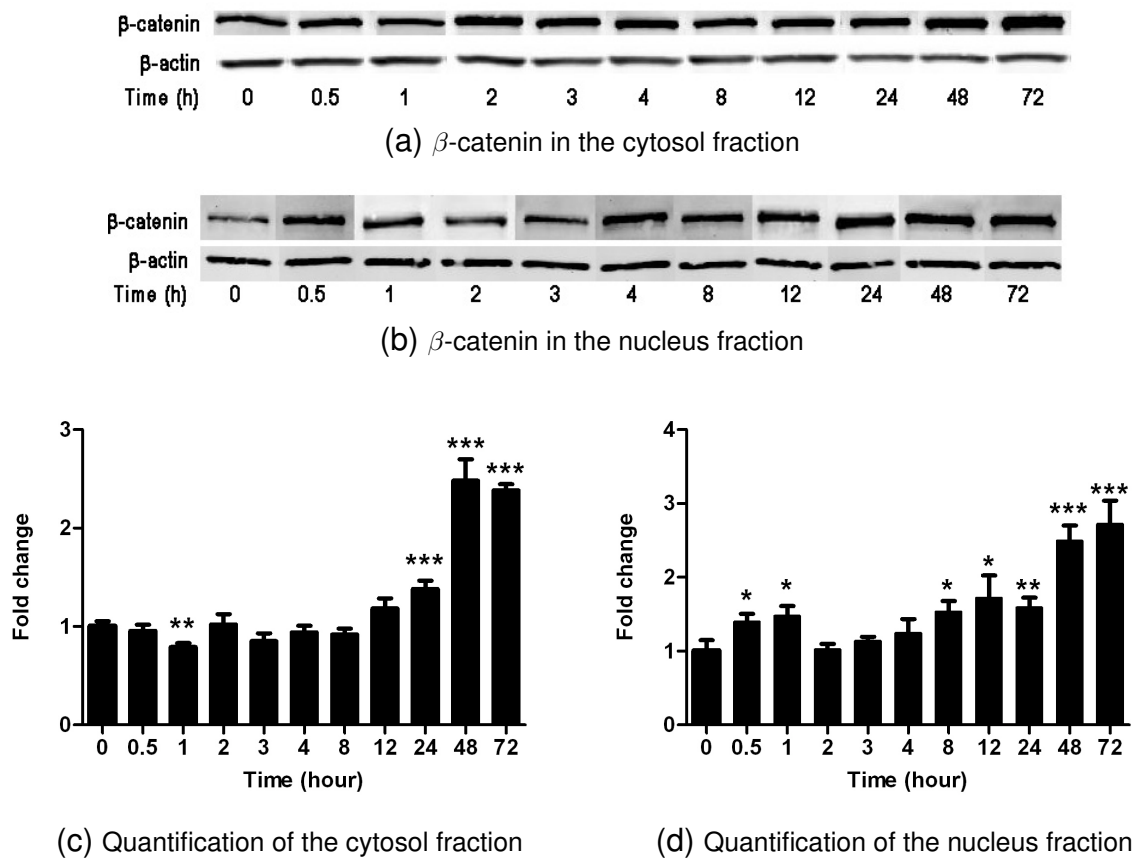


Figure 3.6: Analyses of β -catenin protein in the cytosol and nucleus fractions during ReNcell VM cell differentiation. (a,b) Representative Western-blot of β -catenin in the cytosol (a) and nuclear (b) fractions. (c,d) Quantified Western-blot analyses of β -catenin protein in cytosol (c) and the nucleus (d) fractions. β -actin is used as a loading control. Normalization and statistical analyses were performed as described in Figure 3.2.

is observed (Figure 3.5c). Finally, cytosolic β -catenin is increasing from 24 hours onward, to reach a peak around 2.5 fold at 72 hours (Figure 3.6c). In the nucleus, the increase, already visible at 8 hours, endures to reach 1.6 fold increase at 24 hours, and 2.7 fold at 48 and 72 hours (Figure 3.6d).

3.3 Protein dynamics under Wnt3a stimulation

In a second set of experiments the protein dynamics were analyzed under the pathway stimulation with Wnt3a, known to trigger Wnt/ β -catenin pathway. The changes in response to Wnt3a stimulation are compared to the physiological response in order to understand the effects of Wnt3a stimulation on protein abundance and relocation. ReNcell VM cells were treated with Wnt3a (100 ng/ml) during proliferation and differentiation. After three days of proliferation, the cells were collected for control (proliferation, time 0 hour), and either incubated in proliferation media with Wnt3a for 3 hours (proliferation with Wnt3a), or incubated in differentiation media with Wnt3a for 0.5, 1, 3, 24 and 48 hours and harvested after the respective incubation time. The rest of the experimental setting stays as described previously in Section 3.2.

3.3.1 Wnt3a influences during proliferation

Three hours after proliferation with Wnt3a, no significant changes are detected for LRP6, p-LRP6, and Dvl2 in the membrane fraction compared to the control (proliferation without Wnt3a) (Figures 3.7a-3.7d, and 3.7b- 3.7e). The same holds true for the level of p-GSK3 α and p-GSK3 β , both in membrane and cytosol fractions (data not shown). In contrast, in the cytosol fraction, a hyper-phosphorylation of Dvl2 is observed with the mobility shift resulting in the absence of m-Dvl2 (90 kDa) and the increase of p-Dvl2 (95 kDa) (Figures 3.7b, 3.7e). It is accompanied by an increase of β -catenin to 1.36 fold in the cytosol, and to 1.6 fold in the nucleus (Figures 3.7c, 3.7f). It is noticeable that the cell proliferation is not affected by Wnt3a presence, and that no differentiation's phenotype, e.g. cell elongation, can be seen during the three hours of Wnt3a treatment.

3.3.2 Wnt3a influences during differentiation

The detection of t-LRP6 in the membrane fraction shows the same temporal dynamics during differentiation with and without (control) Wnt3a (Figure 3.8). On the contrary, a quick increase of p-LRP6 is observed at 0.5 hours (1.64 fold) and remains high until 3 hours after

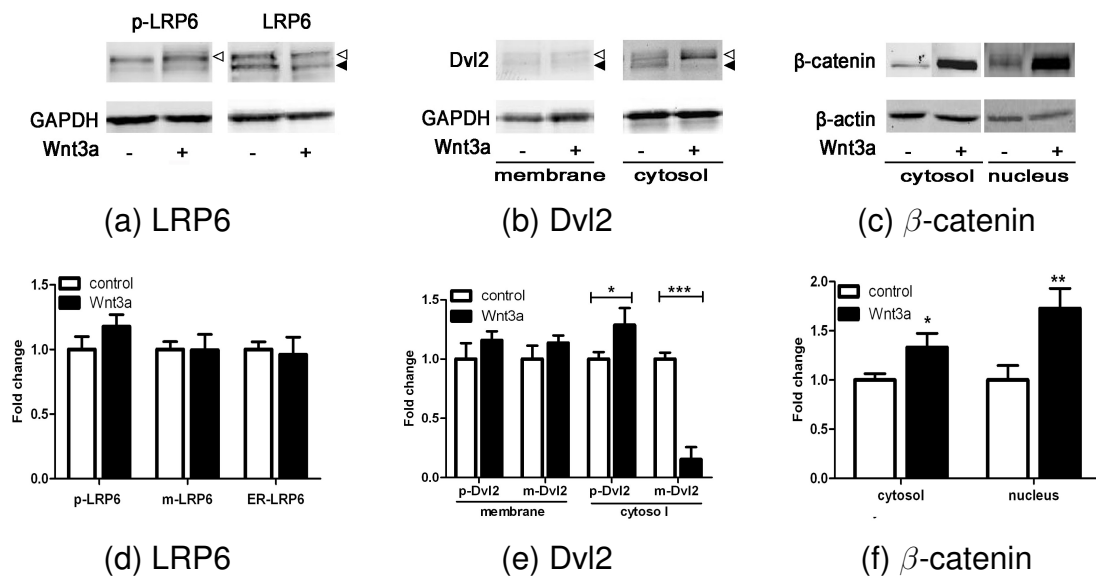


Figure 3.7: Protein expression during ReNcell VM cell proliferation with Wnt3a. (a,b,c) are representative Western-blot images of the proteins under proliferation with Wnt3a treatment (100ng/ml) (+) or without Wnt3a (-), GAPDH or β -actin are used as loading control. (a) detection of LRP6 phosphorylated on serine 1490 residue (p-LRP6) shows a band at 200 kDa (white arrowhead) in the membrane fraction and detection of total LRP6 (LRP6) shows 2 bands, one at 190 kDa (white arrowhead) for the ER form (ER-LRP6) and one at 180 kDa (black arrowhead) for the mature form (m-LRP6). (b) Dvl2 detected in the membrane and cytosol fractions, presents a band at 95 kDa (white arrowhead) for the phosphorylated form (p-Dvl2), and a band at 90 kDa (black arrowhead) for the mature form (m-Dvl2). For Dvl2 in the cytosol fraction under Wnt3a treatment, no mature form is detected. (c) detection of total β -catenin in cytosol and nucleus fractions. (d,e,f) Quantified Western-blot analyses during proliferation with (Wnt3a) or without Wnt3a (control) treatment. The signal intensity at proliferation without Wnt3a is the control for each protein and its value is set to 1. Values are presented as mean \pm SEM from at least 3 independent experiments. For statistical significance '*' stands for p-value <0.05, '**' for p-value <0.01, and '***' for p-value <0.001 compared to control (proliferation without Wnt3a).

differentiation (Figure 3.9a). This intensification of p-LRP6 signal is accompanied by the shift of the original band at 190 kDa to 210 kDa [Khan et al., 2007]. After 8 hours and during the late differentiation the level of p-LRP6 declines down to 0.67 fold (Figure 3.9b).

In the membrane fraction, p-Dvl2 presents two transient peaks at 0.5 and 3 hours (1.46 and 1.38 fold increase), whereas m-Dvl2 shows a single increase at 0.5 hours and remains afterwards close to the control level (at time 0 hour). In the cytosol fraction, p-Dvl2 dynamic does not differ from the physiological differentiation, whereas m-Dvl2 presents a highly regulated dynamic in presence of Wnt3a: as early as 0.5 hours m-Dvl2 decreases and reaches a level of 0.33 fold at 3 hours. Later, at 8 and 48 hours m-Dvl2 exhibits two increases to 1.8 and 1.5 fold, respectively.

In the membrane fraction p-GSK3 α and p-GSK3 β increase significantly after 0.5 hours of Wnt3a treatment during differentiation. It is followed by a decrease of p-GSK3 α after 1 hour of differentiation with Wnt3a and at 24 and 48 hours for p-GSK3 β . In the cytosol fraction, significant decreases of p-GSK3 α occur at 1 and 3 hours compared to the differentiation without Wnt3a at the same time points. Inversely, p-GSK3 α increases significantly at 48 hours after Wnt3a treatment. Two limited increases of p-GSK3 β are observed at 8 and 48 hours of differentiation with Wnt3a treatment.

Wnt3a influences the level of β -catenin as early as 0.5 hours after treatment with a significant decrease down to 0.7 fold observed in the cytosol (Figure 3.12c) that contrasts with a significant increase in the nucleus to 2.1 fold (Figure 3.12d). Levels of β -catenin increase in the cytosol and in the nucleus to reach a level of 1.47 fold after 3 hours of differentiation with Wnt3a. For the late differentiation, at 24 and 48 hours, β -catenin in both compartments accumulates as observed during differentiation without Wnt3a (Figures 3.12a-3.12d).

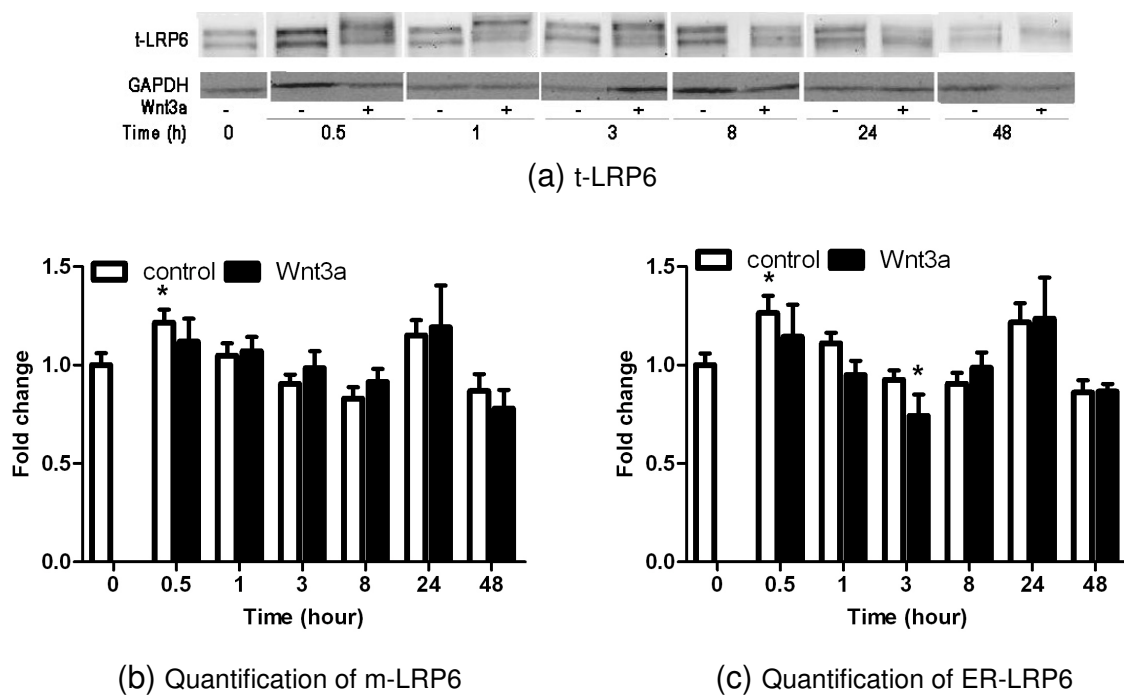
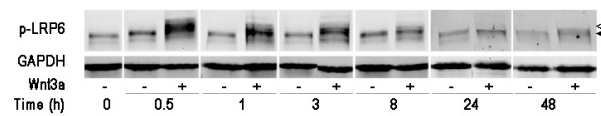
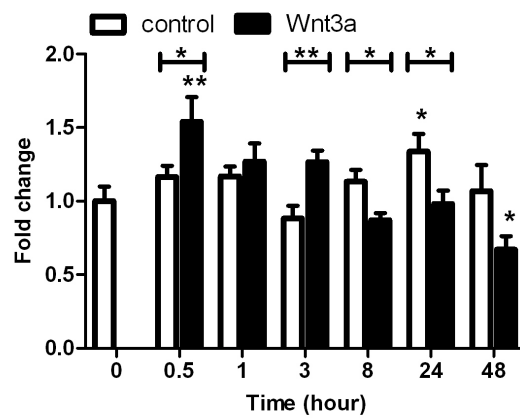


Figure 3.8: Analyses of t-LRP6 protein in the membrane fraction during ReNcell VM cell differentiation with Wnt3a. (a) Representative Western-blot of t-LRP6. (b,c) Quantified Western-blot analyses of LRP6 mature form (m-LRP6) (b) and ER form (ER-LRP6) (c) in membrane fraction. GAPDH is used as a loading control. Time point 0 hour stands for control using proliferating cells without Wnt3a. The signal intensity at 0 hour is set to 1 and used to normalized the intensity for the other time points. Values are presented as mean \pm SEM from at least 3 independent experiments. For statistical significance ‘*’ stands for p-value <0.05 , and ‘**’ for p-value <0.01 compared to control (proliferation without Wnt3a).



(a) p-LRP6



(b) Quantification of p-LRP6

Figure 3.9: Analyses of p-LRP6 protein in the membrane fraction during ReNcell VM cell differentiation with Wnt3a. (a) Representative Western-blot of p-LRP6, white arrowhead points to the band at 210 kDa, and the black arrowhead points to the band at 190 kDa. (b) Quantified Western-blot analyses of phosphorylated LRP6 (p-LRP6) in membrane fraction. GAPDH is used as a loading control. Normalization and statistical analyses were performed as described in Figure 3.8.

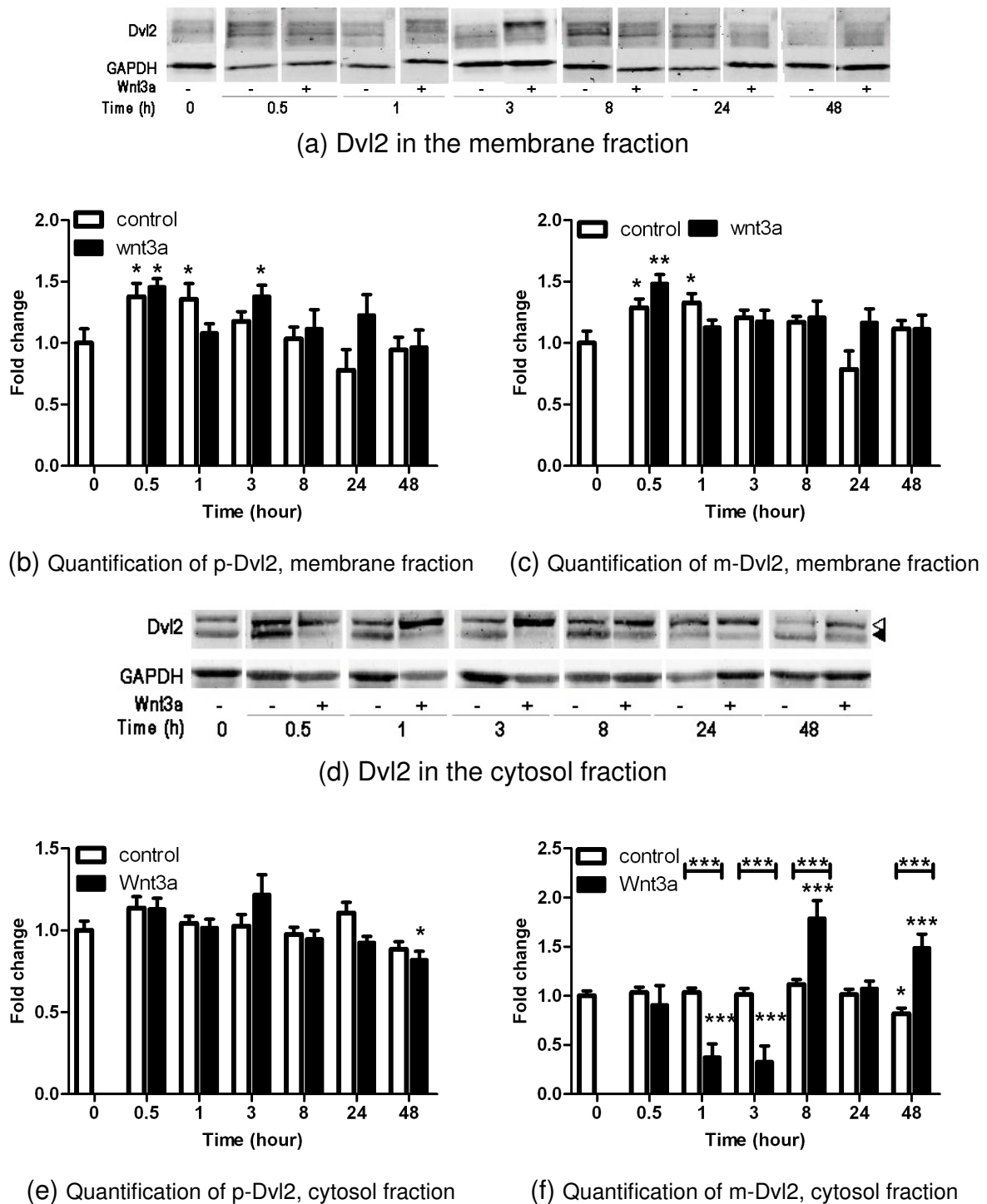


Figure 3.10: Analyses of Dvl2 protein in the membrane and cytosol fractions during ReNcell VM cell differentiation with Wnt3a. (a,d) Representative Western-blot images of Dvl2 in the membrane (a) and the cytosol (d) fractions. (b,c,e,f) Quantified Western-blot analyses of phosphorylated (p-Dvl2) (b,e) and mature (m-Dvl2) (c,f) dishevelled 2 protein, in membrane (b,c) and cytosol (e,f) fractions. GAPDH is used as a loading control. Normalization and statistical analyses were performed as described in Figure 3.8.

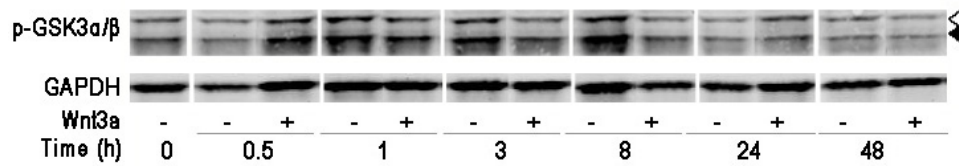
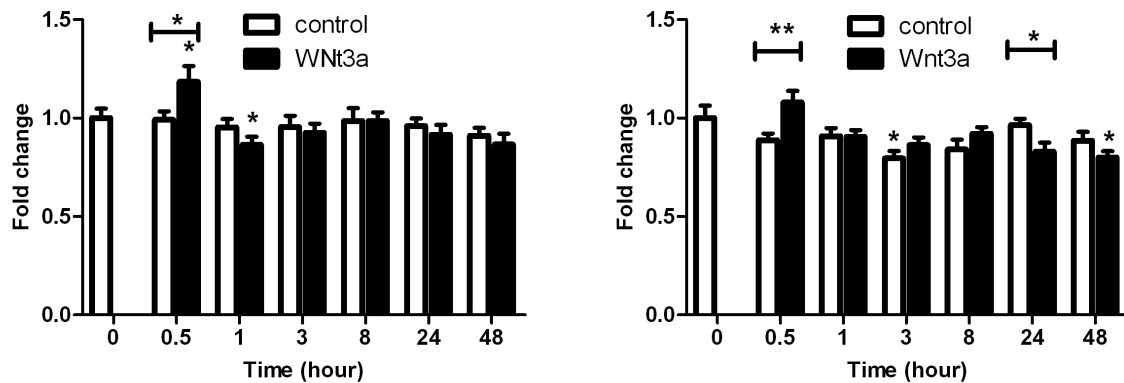
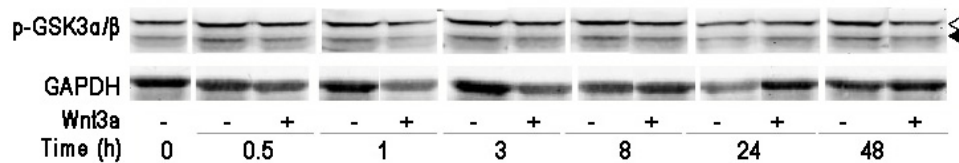
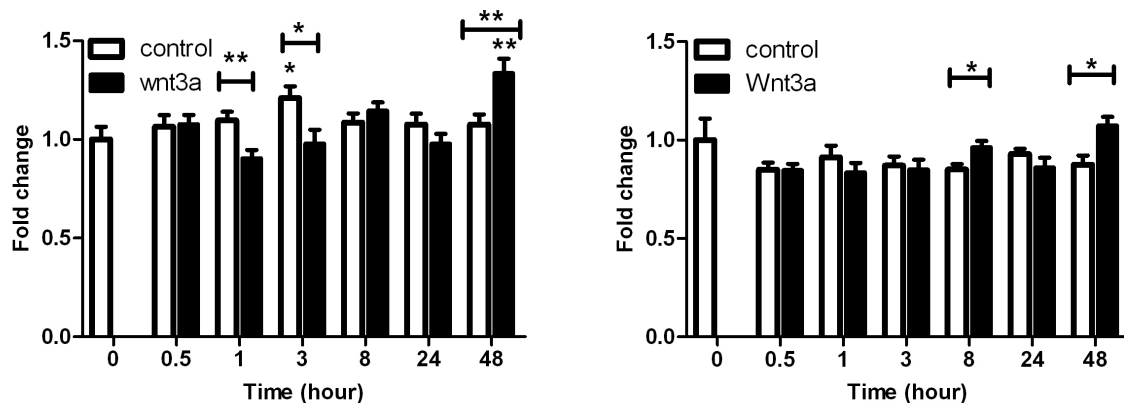
(a) p-GSK3 α/β in the membrane fraction(b) Quantification of p-GSK3 α , membrane fraction (c) Quantification of p-GSK3 β , membrane fraction(d) p-GSK3 α/β in the cytosol fraction(e) Quantification of p-GSK3 α , cytosol fraction (f) Quantification of p-GSK3 β , cytosol fraction

Figure 3.11: Analyses of phosphorylated GSK3 α/β proteins in the membrane and cytosol fractions during ReNcell VM cell differentiation with Wnt3a. (a,d) Representative Western-blot of phosphorylated GSK3 α/β in the membrane (a) and cytosol (d) fractions, white arrowhead points to p-GSK3 α , and black arrowhead points to p-GSK3 β . (b,c,e,f) Quantified Western-blot analyses of p-GSK3 α (b,e), and p-GSK3 β (c,f) in membrane (b,c) and cytosol (e,f) fractions. GAPDH is used as a loading control. Normalization and statistical analyses were performed as described in Figure 3.8.

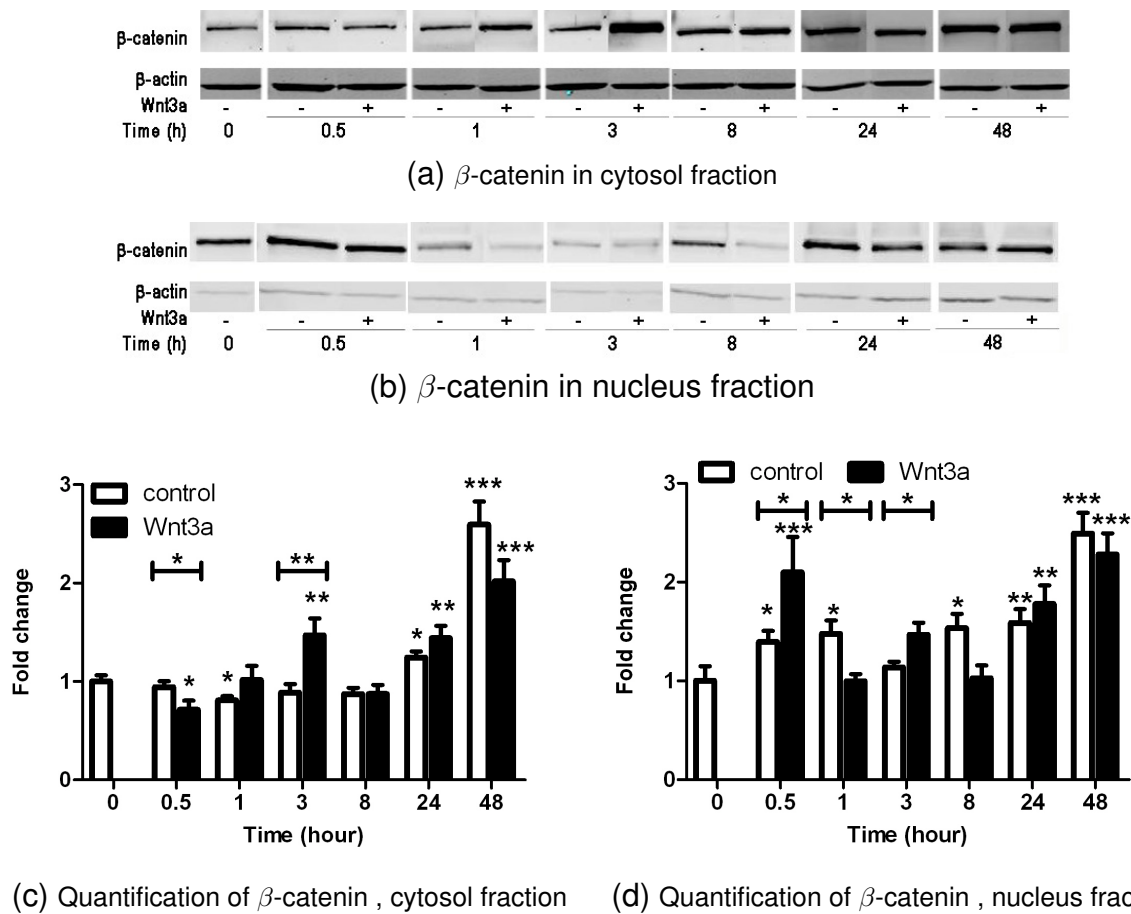


Figure 3.12: Analyses of β -catenin protein in the cytosol and nuclear fractions during ReNcell VM cell differentiation with Wnt3a. (a,b) Representative Western-blot of β -catenin in the cytosol (a) and in the nucleus (b) fractions. (c,d) Quantified Western-blot analyses of β -catenin in the cytosol (c) and nucleus (d) fractions. β -actin is used as a loading control. Normalization and statistical analyses were performed as described in Figure 3.8.

3.4 Discussion

The present study reports on the spatio-temporal dynamics of Wnt/ β -catenin signaling proteins along the differentiation process of human neural progenitor cells, ReNcell VM cells. The quantitative kinetic investigation of the signaling proteins shows their regulation during the first three days of physiological differentiation and differentiation under Wnt3a treatment, a trigger of Wnt/ β -catenin pathway. The four proteins of interest are the co-receptor LRP6, Dvl2, GSK3 β , and β -catenin due to their prominent roles in the Wnt/ β -catenin signaling pathway.

The present study focuses on protein dynamics at the physiological level. This is not a standard approach as some components are endogenously expressed at low level in cells and thus, can be detected only with difficulty, e.g. Axin [Lee et al., 2003], and LRP6 [Khan et al., 2007]. However, any attempt to overexpress these components would invalidate the observed results. Thus, there is a need to analyze the proteins regulation at physiological level. During physiological differentiation, the protein dynamics follow biphasic kinetics with a first phase during the first three hours of differentiation, and a second one between 24 and 72 hours of differentiation, both separated by an intermediate steady level (Figure 3.13). The involvement of the pathway is observed under physiological differentiation through the presence of the co-receptor LRP6, the activation of Dvl2 at the membrane level, and the accumulation of β -catenin in the cytosol and the nucleus. Wnt3a stimulation during differentiation increases protein abundance and relocation as well as the nucleo-cytosolic shuttling of β -catenin.

3.4.1 Protein dynamics during differentiation

Phosphorylation of LRP6 on the PPP(S/T)P motifs is thought to trigger the pathway activation [Tamai et al., 2004]. In the membrane fraction of the ReNcell VM cells, phosphorylation of LRP6 on serine 1490 (p-LRP6) is observed only after 24 hours whereas an increase is observed after 0.5 hours in presence of Wnt3a. Thus, an augmentation of serine 1490 phosphorylation might not be necessary for Wnt signal transduction, as proposed by [Beagle et al., 2009, Wolf et al., 2008] and p-LRP6 increase might occur only subsequently to Wnt3a stimulation. It is noteworthy that the absence of signal can also be due to the sensitivity of the antibody used that is too low to detect physiological levels of LRP6 phosphorylation. In the second phase of protein dynamics, after 24 hours, t-LRP6 and p-LRP6 show significant changes. At the same time point an increase of LRP6 mRNA is found by real-time PCR in ReNcell VM cells [Hübner, 2010, Mazemondet et al., 2011]. These results suggest that the increase of the ER form of LRP6 at 24 hours reflects the receptor synthesis and turn-over. Furthermore, this rise of LRP6

abundance can explain the presence of the second band detected by p-LRP6 antibody at 24 hours. Thus, the ReNcell VM cells are a good cell model to study the dynamics of the co-receptor LRP6 in the regulation of the Wnt/ β -catenin signaling pathway.

The massive increase of Dvl2 in the membrane fraction subsequent to differentiation reflects the protein activation and recruitment in order to trigger the intracellular signaling cascade in response to the Wnt signal [Axelrod et al., 1998]. In ReNcell VM cells this recruitment is subject to dynamic regulation as shown by the biphasic kinetics with peaks at 2 and 24 hours. These observations suggest that Wnt signaling pathways are active at diverse stages of ReNcell VM cell development, i.e. early and late differentiation. Thus, the apparent absence of Dvl2 in the membrane fraction during proliferation and after 24 hours of differentiation appears to be associated with the pathway inactivity. Indeed, in mouse neuron-like dopaminergic cells, the absence of Dvl2 is associated to an inhibition of the Wnt ligand endocytosis, leading to a down-regulation of the signaling pathway [Bryja et al., 2007a]. Hence, the disappearance of Dvl2 after 24 hours that accompanies the change of LRP6, especially the low detection of the mature form, can illustrate a negative feedback as proposed by [Bryja et al., 2007a], shown here for the first time in human neural progenitor cells. In comparison to the physiological differentiation, the presence of Wnt3a during differentiation does not impact the dynamics of Dvl2 in the membrane. In contrast, Wnt3a affects Dvl2 in the cytosol. As shown in dopaminergic neuronal cell line [Bryja et al., 2007b], Wnt3a induces the *phosphorylation-dependent Dvl mobility shift* as observed by the presence of a single band in the Western-blot at the level of p-Dvl2. Interestingly, in ReNcell VM cells this mobility shift of Dvl2 is similar to the one observed previously. However, the present analyses show that such event occurs only in the cytosol.

The amount of GSK3 β does not change over time as it is often the case for kinases: the kinase pool remains constant and only the enzymatic activity varies. However, during physiological differentiation, no significant changes in the amount of active GSK3 α/β have been found. Thus, the activation of GSK3 α/β in the T-loop might not be necessary for the transduction of the Wnt signal.

β -catenin is submitted to high spatio-temporal dynamics during ReNcell VM cell differentiation. The increase of nuclear β -catenin during the first hour of differentiation is correlated to the decrease at the same time point in the cytosol, predicting a shuttle of β -catenin from the cytosol to the nucleus activated quickly after the beginning of differentiation. It is known that this trafficking is observable in kinetic studies previously to β -catenin accumulation [Hendriksen et al., 2008]. Interestingly, no accumulation of β -catenin in the cytosol prior to 24 hours could be detected, which leads to the hypothesis that non-phosphorylated β -catenin shuttles im-

mediately to the nucleus, whereas accumulation happens in the late differentiation phase, after 24 hours.

An overview of the protein spatio-temporal dynamics during ReNcell VM cell physiological differentiation is shown in Figure 3.13.

3.4.2 Pathway dynamics under Wnt3a stimulation

Due to the short half-life of Wnt3a (1.9 hours), its effects are observable mainly during the early differentiation of ReNcell VM cells. The spatio-temporal dynamics of the signaling proteins under Wnt3a stimulation have been investigated in mouse F9 teratocarcinoma cells [Yokoyama et al., 2007] and the results differ from the one observed here. This emphasizes the importance of investigating these aspects in every specific cell line, as the pathway is differently regulated in each cell type and at different stages of cell development. However, the common effect of Wnt3a on the protein kinetics, in ReNcell VM cells as well as in F9 cells, is the acceleration of protein recruitment and activation such as the acceleration of β -catenin transfer from the cytosol to the nucleus. Also, the early increase of β -catenin in the nucleus after 0.5 hours of Wnt3a stimulation has been observed in diverse cell systems [Yokoyama et al., 2007, Hendriksen et al., 2008]. Differences in protein activation are observed between physiological and Wnt3a-stimulated differentiation. In the latter a significant protein activation is observed as early as 0.5 hours after addition of Wnt3a with an increase of p-GSK3 α/β , p-LRP6 and Dvl2 in the membrane fraction and of nuclear β -catenin associated with a decrease of cytosolic β -catenin (Figure 3.14). Effects of Wnt3a are still visible after 3 hours of treatment with a second peak of nuclear β -catenin, in this case associated with an increase of cytosolic β -catenin and the *phosphorylation-dependent Dvl2 mobility shift* in the cytosol. Treatment for 3 hours with Wnt3a in proliferating or differentiating ReNcell VM cells leads to different effects: equivalent increases of β -catenin in cytosol and nucleus are observed during both cellular processes. However, these accumulations seem to result from diverse processes as during proliferation no significant phosphorylation of LRP6 is observed in contrary to differentiation. This suggests that Wnt3a can trigger both phosphorylated LRP6 dependent and independent activation of β -catenin in the same cell line depending of the cell-stage. Thus, high amount of Wnt3a (100 ng/ml) significantly seems to change the dynamics of signaling proteins that can influence cell phenotype. However, this hypothesis should be subject to future investigations in ReNcell VM cells in order to be confirmed.

An overview of the protein spatio-temporal dynamics during ReNcell VM cell differentiation in presence of Wnt3a is shown in Figure 3.14.

3.4.3 Nuclear β -catenin dynamics

During ReNcell VM cell differentiation, the signaling proteins of the Wnt/ β -catenin pathway are subject to dynamic regulations especially nuclear β -catenin. After one hour of differentiation an increase is observed subsequent to the Wnt signal as confirmed by the experiments with Wnt3a. However, it remains unclear if the later increase, starting after 8 hours is due to a second signal of Wnt molecules or due to some other changes in the cell environment.

A first hypothesis arises with the other observations made in ReNcell VM cells. As mentioned previously (see Section 2.2.2), the ReNcell VM cells do not start their differentiation at the same time after growth factor removal. This is due to the asynchrony of the cell population, i.e. the heterogeneity regarding their progression in the cell cycle. Indeed when the growth factors are removed from the media, only 53% of the cells can start their differentiation and be sensitive to the presence of Wnt molecules in the environment. Between 12 and 24 hours of differentiation all the remaining cells, i.e. 43%, reach G1 phase and can then be receptive to Wnt signal. Does this asynchrony explain the second increase from 8 hours onward observed for nuclear β -catenin? Further experiments on ReNcell VM cells, such as cell synchronization with the chemical molecule nocodazole, have been tested (oral communication with Dr. M. Frech). Although the synchronization of the cells was successful the collateral damages, e.g. cell instability, and high death rate, made the synchronized ReNcell VM cells not suitable for *in vitro* exploration. Thus, so far, *in vitro* exploration of the ReNcell VM cell asynchrony effects onto nuclear β -catenin dynamics cannot be performed.

Another explanation for this second increase of nuclear β -catenin could be a self-induced Wnt signal. As morphogens, Wnt molecules are produced by the cells and exported in the cell field to propagate their signal (see Section 2.1.1 for details). In ReNcell VM cells, production of Wnt molecules such as Wnt5a or Wnt7a mRNA increases between 6 and 24 hours of differentiation [Mazemondet et al., 2011]. Thus, the second increase of nuclear β -catenin could reflect an increase of Wnt molecules production, secretion, and propagation in the population leading a second response of the cells to Wnt signal. However, isolation and analysis of endogenous Wnt proteins in the cell medium are nontrivial experiments.

As an alternative to time and fund consuming experiments, and in order to test the accuracy and validate the two given hypotheses, a computational model of the Wnt pathway in ReNcell VM cell populations is built to further investigate nuclear β -catenin dynamics.

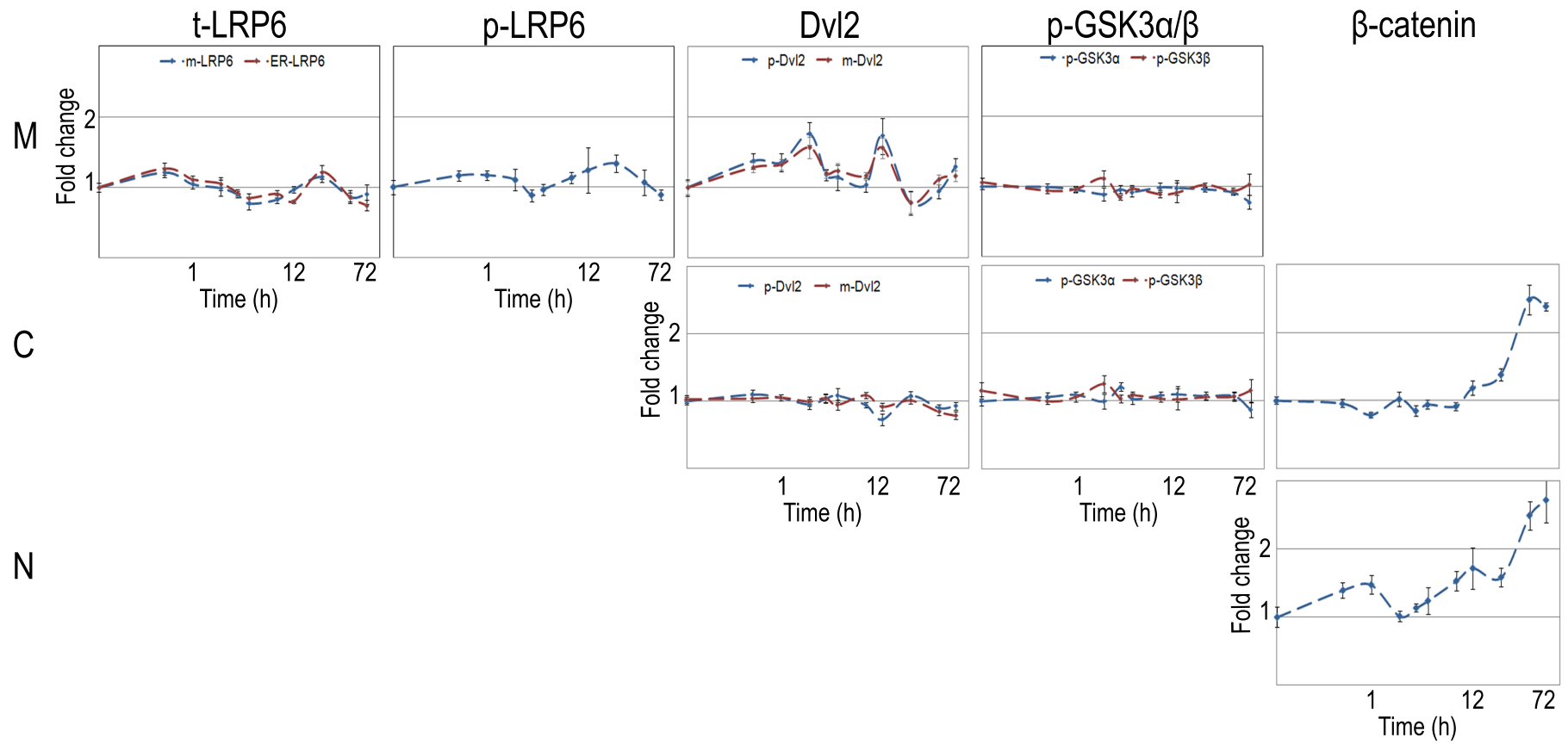


Figure 3.13: Overview of protein dynamics during physiological differentiation of ReNcell VM cells. Plots are ordered depending on the protein quantification in the respective subcellular location: M stands for the membrane, C for the cytosol, and N for the nucleus fractions. The scale of the X-axis is logarithmic.

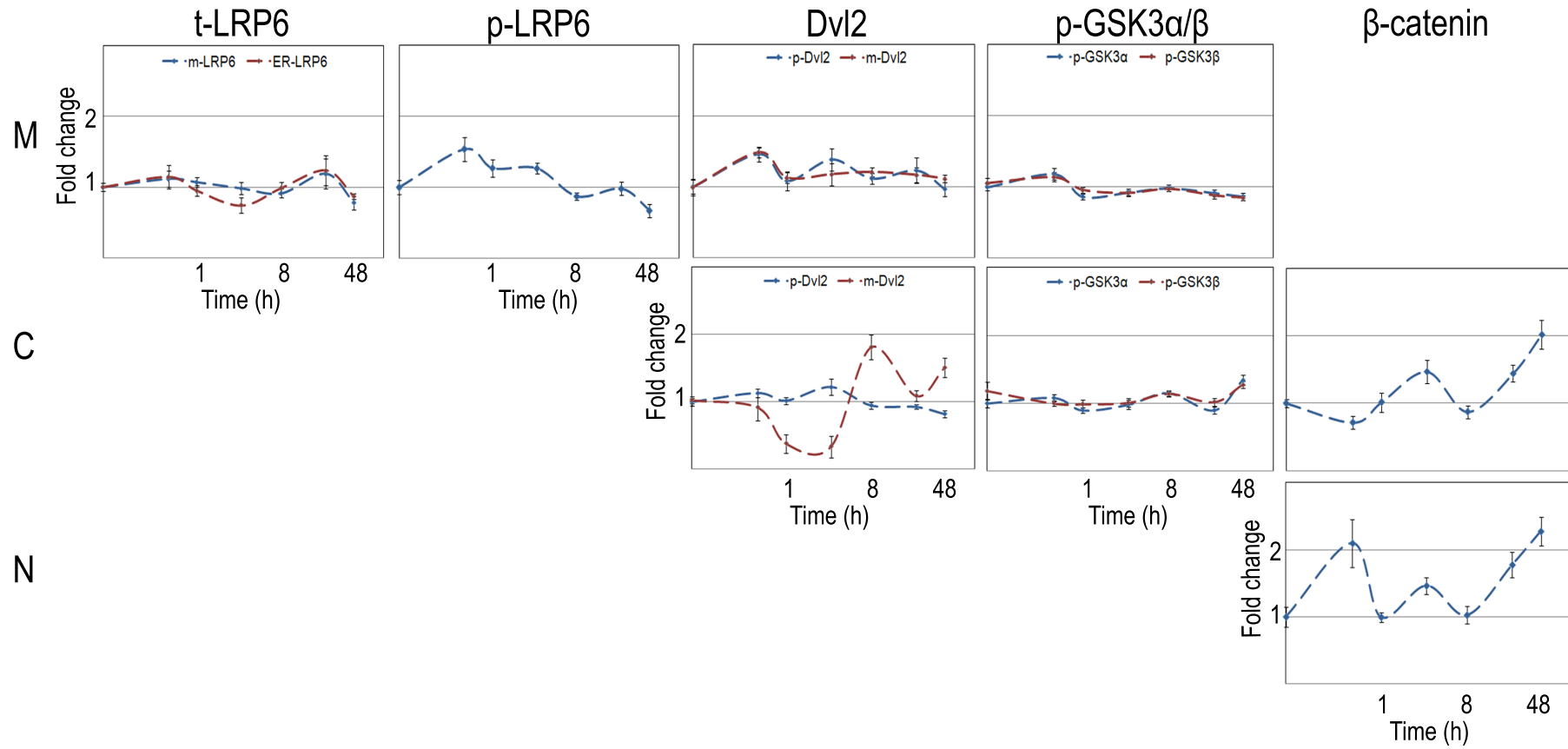


Figure 3.14: Overview of protein dynamics during differentiation of ReNcell VM cells with Wnt3a. Plots are ordered depending on the protein quantification in the respective subcellular location: M stands for the membrane, C for the cytosol, and N for the nucleus fractions. The scale of the X-axis is logarithmic.

Chapter 4

in silico validation

In this chapter a computational model of the Wnt/ β -catenin pathway in ReNcell VM cell populations is presented. It aims to explore the impact of the cell cycle and of self-induced Wnt signal, on the nuclear β -catenin dynamics observed *in vitro* (see Section 3). Section 4.1 presents the related work and the reference model. The model of the intracellular Wnt/ β -catenin pathway in ReNcell VM cells is presented in Section 4.2. Section 4.3 shows the methods used to obtain the model parameters. Sections 4.4 and 4.4.3, respectively, present the model evaluation and the parameters' impact on the model behavior. Stochastic analyses of the model and the results of the *in silico* experiments are provided in Section 4.5.

4.1 Existing Wnt/ β -catenin pathway models

4.1.1 Lee et al. (2003)

Due to its complexity and the lack of published quantitative data, the Wnt signaling pathway was not the first choice for modeling experts. Nevertheless, in 2003, Krüger and Heinrich proposed the first mathematical and deterministic model of the Wnt/ β -catenin pathway, in the *Xenopus* oocyte. In the following, it will be referred as the *Lee model*. Moreover, the originality of this model resides in the combination of estimated, experimentally retrieved and derived kinetic parameters. The use of *Xenopus* oocyte, as an experimental system, presents the advantages to be essentially cytoplasm, well-stirred and synchronous, the way a cell population is not.

The *Lee model* describes the pathway reaction network, in a single cell with one compartment, expressed as a set of ordinary differential equations (ODEs). Initially composed of 15 ODEs, the model is reduced to 7 ODEs and 8 algebraic equations using approximations and

assumptions described in [Krueger and Heinrich, 2004].

The *Lee model* contains the following species: Dishevelled (called *Dsh* in *Xenopus*), GSK3 β , APC, Axin, β -catenin (total and phosphorylated), and TCF (Figure 4.1). The events happening at the plasma membrane are omitted and the pathway activation via Wnt is represented by the activation of Dsh (*reaction 1* in Figure 4.1). All the species concentrations, except phosphorylated β -catenin, were determined experimentally by Western-blot. The concentrations of Dsh, GSK3 β , APC and TCF are considered to be constant over time. Only Axin and β -catenin are the two species constantly produced and degraded.

The reactions between species describe the following processes: protein synthesis and degradation, de-/phosphorylation, and protein complex dis-/assembly. These reactions follow different kinetics: the synthesis of *Axin* and β -catenin are described as flux. They are respectively represented by the constant rates v_{12} and v_{14} (Figure 4.1). The unimolecular reactions (single headed arrows in Figure 4.1) follow mass action kinetics, described by a first order rate constant. Simplification is made for the reversible steps (double headed arrows in Figure 4.1): it is assumed that the binding step is faster than the unbinding one. Thus, a reversible reaction is only characterized by the dissociation step and only the dissociation constant is needed to describe the reaction. This limits the amount of parameters needed, leaving aside the ability to describe the reaction kinetics.

Among the model results, the authors show that their model predictions are fitting experimental data performed in the *Xenopus* oocyte. The main insight concerns the role of Axin, proposed as the crucial component of the degradation complex. Indeed, the quantitative experiments done by Lee and co-authors measured a lower concentration of Axin compared to the other species of the degradation complex, i.e. 0.02 nM versus 50 nM for GSK3 β and 100 nM for APC. The *in silico* experiments show that Axin turnover affects the amplitude and duration of β -catenin level under transient Wnt stimulation. Thus, according to the *Lee model* Axin is the limiting factor in β -catenin degradation process.

4.1.2 *Lee model* extensions

The *Lee model* is a reference regarding Wnt pathway's computational modeling approach, and is used as a basis for further model attempts.

Cho et al. (2006) A first extension was done by [Cho et al., 2006], who added the negative feedback loop due to Axin production (referred as Axin2 in the paper). Whereas the *Lee model* only refers to the binding of β -catenin to TCF, Cho and co-authors assume that the species

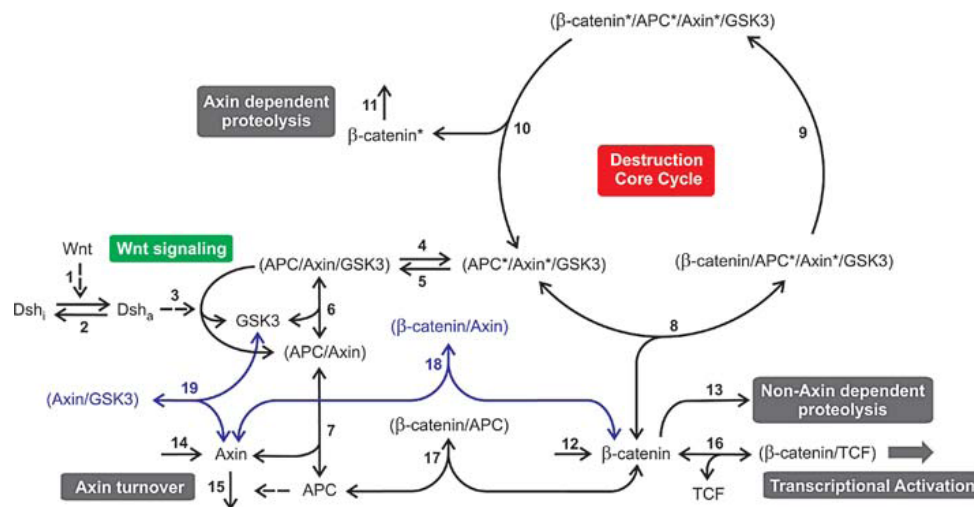


Figure 4.1: The reaction steps of the Wnt pathway (reproduced from [Lee et al., 2003], Figure 1). Protein complexes are denoted by the names of their components. Phosphorylated components are marked by an asterisk. Single-headed solid arrows characterize reactions taking place only in the indicated direction. Double-headed arrows denote binding equilibrium. The broken arrows indicate that the components mediate, but do not participate in, the reaction scheme. The irreversible reactions 2, 4, 5, 9-11, and 13 are unimolecular, and reactions 6, 7, 8, 16, and 17 are reversible binding steps.

β -catenin and β -catenin/TCF are inducing Axin synthesis. This reaction follows mass action kinetics. This model aims to observe the impact of various APC mutations, as these are associated to colon cancer. The mutations are represented by a variation of the parameter values. The authors conclude that the APC mutations are selected based on an optimal level of β -catenin which is determined by a specific balance between its increase consecutively to the pathway activation and its decrease due to Axin feedback. Limitations of this model include the assumption that both free β -catenin and β -catenin complexed to TCF produce Axin: in biological systems only the second holds true.

Wawra et al. (2007) Hereby, the authors propose a robustness analysis and an extension of the *Lee model* [Wawra et al., 2007]. The robustness of the *Lee model* is tested by single and multiple parameter perturbations as well as initial condition variation. These analyses reveal robustness of the steady-state and dynamic shape of β -catenin time plots.

With their extension the authors aim to test whether intrinsic oscillations of the Wnt/ β -catenin pathway can occur. They refer to vertebrate somitogenesis, i.e. formation of vertebral column and muscles during early development, a process during which oscillating Wnt pathway is observed.

Similar to the *Cho model*, the extension of this model concerns the addition of negative feedback loops, as they are known to down-regulate the signaling cascade, and have been proposed

to produce oscillation [Kholodenko, 2000]. However, their approach differs from the previous one in the more detailed description of the two feedback loops engendered by production of Axin and of a pathway inhibitor protein, such as Dickkopf 1 (*Dkk1*). The gene transcription is assumed to be a cooperative activation and is described by sigmoidal Hill function. The model integrates the intermediate products of the reactions, such as *Axin RNA* and *Dkk1 RNA*. The authors add delays to represent the time needed by the biological processes for transcription (copy of the DNA into RNA), splicing (modification of the RNA), translation (RNA transformation into protein), and diffusion (passage of the RNA from the nucleus to the cytosol). Thus, the addition of delays turns the system of ODEs into a system of delay differential equations (DDEs).

The analysis of this extended model, with the original parameters of the *Lee model*, under permanent Wnt signal, does not show stable oscillations. Furthermore, the steady-state of β -catenin is decreasing of 38% compared to the level observed in the *Lee model*, i.e. from 25.01 nM to 15.51 nM. These primary observations lead to the conclusion that a higher turn-over of β -catenin and Axin is necessary to reach an oscillation threshold. The modification of the corresponding parameters, i.e. an increase between 2 and 20 fold of the values provided in the *Lee model*, leads to oscillations of β -catenin and β -catenin/TCF, *Axin2 RNA* and *inhibitor RNA*. However, the authors report that compared to the oscillations observed *in vivo*, the ones observed *in silico* are longer, and this can be due to additional mechanisms not included in the model. Through their model, Wawra and co-authors show that oscillations of the Wnt/ β -catenin pathway can occur independently of the environment and external influences.

van Leeuwen et al. (2007) This model focuses on β -catenin and the balance between its adhesion and transcription functions [van Leeuwen et al., 2007]. A set of ODEs describes the different conformations and binding states of β -catenin. As in the *Lee model*, the reactions take place in a single cell compartment although in biological systems β -catenin functions are subcellular location-dependent: adhesion occurs at the plasma membrane and transcription occurs in the nucleus. Via *in silico* experiments, the authors tested two hypotheses concerning β -catenin fate between these two functions: either the proteins binding to β -catenin determine the fate, or it is governed by the conformational change of β -catenin itself. Their analyses suggest that the second hypothesis is the most probable.

Mirams et al. (2010) The authors propose a systematic asymptotic analysis of the *Lee model* [Mirams et al., 2010]. This mathematical analysis aims to reduce the number of parameters

used in the model. Thus, the original set of ODEs from the *Lee model* is reduced to a single simplified ODE, that represents the dynamics of β -catenin (denoted as X_{11}) over time with Wnt signal dependency. Only three reactions are considered around β -catenin: the synthesis flux of β -catenin is conserved as in the *Lee model*, represented by the constant rates v_{12} (*reaction 12* in figure 4.1) as well as the β -catenin decay non-axin dependent, represented as a mass action reaction with the rate k_{13} (*reaction 13* in figure 4.1). The third reaction is the Axin dependent degradation of β -catenin. As the usual object of interest, regarding Wnt pathway activity, is β -catenin, the authors propose to add a second equation representing the complex β -catenin/TCF (denoted as X_{14}) to complete the model. The authors show that, taken together, the ODE for β -catenin and the equation for β -catenin/TCF, form a simplified version of the *Lee model*. The same is done to simplify the *Cho model* [Cho et al., 2006], resulting in the β -catenin ODE including the Axin feedback loop.

All the models described above are deterministic and continuous models represented by ODEs or DDEs. Their limitations include the difficulty to proceed to stochastic and discrete simulations. Also none of the models integrate explicitly space as no volume parameter enter in the calculation. For a complete review of the existing Wnt models, especially regarding cross-talks and Wnt during animal development, that are not relevant for the present work, see [Kofahl and Wolf, 2010].

4.1.3 Tymchyshyn et al. (2008)

The first stochastic model of the Wnt/ β -catenin signaling pathway is proposed by [Tymchyshyn and Kwiatkowska, 2008]. The analysis of the pathway is a support to explore the applicability of methods from the field of concurrency programming, i.e. the stochastic π -calculus [Priami, 1995, Priami et al., 2001], to the realm of stochastic modeling of biological systems. The model is represented by discrete reaction rules implemented with the stochastic π -calculus language, and simulated using BioSPI simulation platform (www.wisdom.weizmann.ac.il/~biospi/).

The biological system of interest is the intestinal crypt cells. The model aims to identify the factors controlling the ability of intestinal cells to keep the balance between division and differentiation, and to answer whether the Wnt/ β -catenin pathway is one of these factors. It is a multi-scale model combining the pathway and the cellular decision between proliferation and differentiation processes. The representation of the cells in the intestinal crypt is abstract in a one-dimensional space, where a cell has only an upper neighbor. The diffusion of Wnt is

simulated by calculating its concentration at each cell position. Wnt is produced by the cells at the bottom and transported by diffusion. The model of the intracellular pathway contains four species that represent β -catenin, the activated receptor complex, and the active and inactive degradation complex abstracted by Axin and phosphorylated Axin, respectively. The authors include the negative feedback loop that produces Axin as it confers robustness toward parameter variation. Further details of the model and its parametrization can be found in [Schaeffer, 2008]. However, discrepancies appear in parameter numerical values that occurred from the parameter conversion, i.e. the conversion from concentration to protein number does not take into account the cell or compartment volumes.

Stochastic simulations of the model validate the hypothesis that transient activation of β -catenin triggers cell proliferation while a prolonged signal triggers differentiation of intestinal crypt cells. A combination of continuous deterministic and discrete stochastic model analyses [Schaeffer, 2008] show oscillations of β -catenin under Wnt stimulation: at low Wnt levels β -catenin activity presents stochastic outbreaks, whereas regular oscillations are observed with increased stimulus. The model analysis propose that Wnt/ β -catenin pathway ensures the cell fate determination of the intestinal epithelium. These results have been validated against experimental results: mRNA Axin2 expression was quantified in HeLa cells (immortal cell line derived from cervical cancer) after treatment for 24 hours with Wnt3a-conditioned medium. The Axin2 expression shows oscillations with a period of 12 hours.

4.2 Model

Subsequent to the *in vitro* experiments and observations (see Section 3.2), two hypotheses are proposed regarding the dynamics of nuclear β -catenin during the *early differentiation* of ReN-cell VM cells: β -catenin dynamics are influenced by (1) the ReNcell VM cells' asynchrony toward the cell cycle, (2) a self-induced Wnt signal that occurs during cell differentiation. By means of computational modeling, these two hypotheses are tested through *in silico* experiments. The model represents a population of ReNcell VM cells with the intracellular Wnt/ β -catenin pathway in each cell. To represent each of the two hypotheses, two additional reactions are added to the intracellular Wnt pathway model.

4.2.1 The intracellular Wnt/ β -catenin pathway model

A ReNcell VM cell is modeled with two compartments, the cytosol and the nucleus, that are assumed to be two concentric spheres (Figure 4.2). The three main proteins, Wnt, β -catenin, and Axin, are represented by five species. Two species represent β -catenin to illustrate its cellular location: β_{cyt} and β_{nuc} , in the cytosol and in the nucleus respectively, and two species for Axin reflecting the phosphorylation state, $AxinP$ and $Axin$, both located in the cytosol. Wnt is represented by the species Wnt located extracellularly. Based on [Tymchyshyn and Kwiatkowska, 2008] (see Section 4.1.3), Axin is representing the whole degradation complex: the species $Axin$ and $AxinP$ representing the inactive and active degradation complex, respectively.

The model's reactions are presented in Table 4.1 and depicted in Figure 4.2. $Axin$ can either decay (r_6, k_{A_d}) or phosphorylate into $AxinP$ ($r_4, k_{A \rightarrow Ap}$). The latter can dephosphorylate into $Axin$ ($r_3, k_{Ap \rightarrow A}$), decay (r_5, k_{Ap_d}), or degrade β_{cyt} ($r_7, k_{\beta d}$).

Wnt-dependent deactivation of the degradation complex is represented by Wnt promoting $AxinP$ dephosphorylation into $Axin$ ($r_2, k_{Ap \Rightarrow A}$), and thereby, indirectly increasing the amount of β_{cyt} ($r_7, k_{\beta d}$). Only by this reaction ($r_2, k_{Ap \Rightarrow A}$), Wnt signal influences β -catenin dynamics. If injecting an initial amount of Wnt , the effect of the signal decreases over time, since Wnt decays (r_1, k_{W_d}) and is not further produced.

For β_{cyt} there exists a constant flux of production ($r_8, k_{\beta \uparrow}$) and decay (r_9, k_{β_d}), in the cytosol. Furthermore, β_{cyt} travels between the cytosol and the nucleus, to become in the latter β_{nuc} ($r_{10}, k_{\beta in}$, and $r_{11}, k_{\beta out}$). β_{nuc} produces $Axin$ ($r_{12}, k_{A \uparrow}$), representing the pathway negative feedback loop. All the reactions follow mass-action kinetics (β_{cyt} production ($r_8, k_{\beta \uparrow}$) is a zero order kinetics).

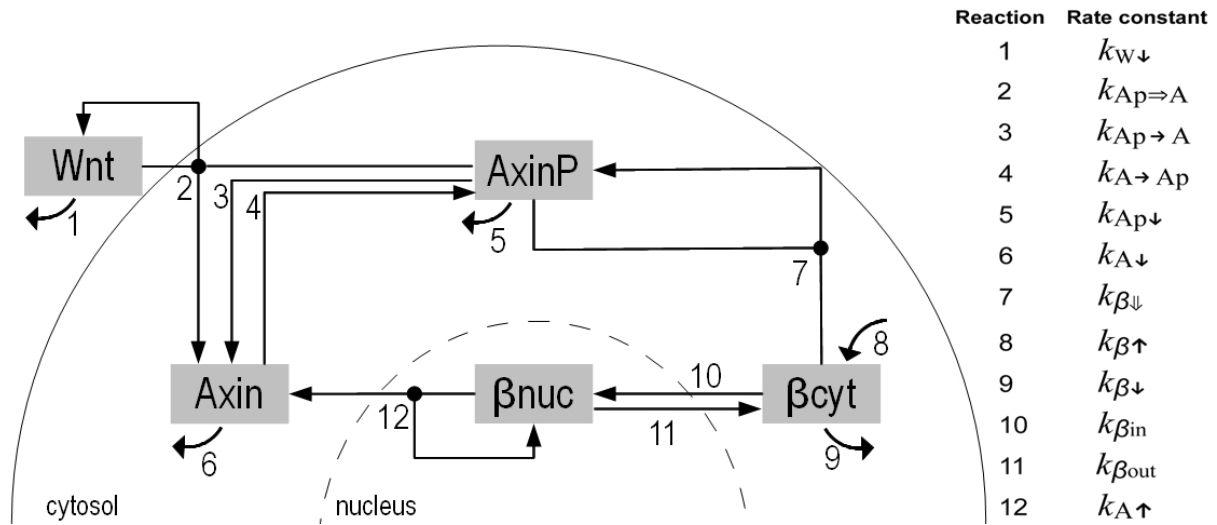


Figure 4.2: Model of the intracellular reactions of Wnt/ β -catenin pathway. The two compartments cytosol and nucleus are separated by the dashed lane. The five species are framed. For a given reaction, an arrow-less line shows the reactant(s), and an arrow points to the product(s). Bended arrows represent protein production (flux) for reaction 8 or protein decay (mass-action) for reactions 1, 3, 6, and 7.

4.2.2 Assumptions

The degradation complex is abstracted by only one of its component, Axin. This is possible since Axin is the limiting factor of the degradation complex due to its low amount in comparison to the other three components, GSK3 β , APC and CKI α [Lee et al., 2003] (see also Section 4.1.1). The binding of Wnt molecules to the membrane receptors is not represented as it still remains, biologically, poorly understood. Thus, the events' cascade following the signal reception at the plasma membrane is omitted. The reaction of *Wnt decay* (r_1) represents its consumption and deactivation after signaling. The mechanism governing β -catenin shuttling between the cytosol and the nucleus remains unclear. In the model, β -catenin motion is a facilitated diffusion as proposed in [Schmitz et al., 2011], with rate constants based on experimental data [Kriehoff et al., 2005, Kriehoff, 2006]. As suggested by the previous *in vitro* experiments (see Section 3.2), the model considers that the Wnt molecules are already present extra-cellularly, and that the passage from cell proliferation to differentiation is accompanied cell reception of the Wnt signal. The compartment volumes, as well as the ratio between them, are considered constant over time.

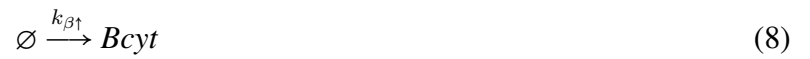
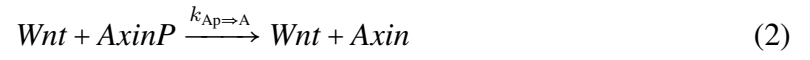


Table 4.1: Reactions of the intracellular Wnt/ β -catenin pathway model. All reactions are following mass-action kinetics, but β -catenin production is a constant flux. The reaction numbers correspond to the ones in the model schema (Figure 4.2).

4.3 Parametrization & Methods

4.3.1 Spatial parameters

Cell & Compartment volumes

The volume is a prerequisite for calculating stochastic parameters as the reaction speed is dependent on the probability of molecules to collide. As the cell volume and thus the compartment volumes might change along cell differentiation, the volume measurement is restricted to the proliferating ReNcell VM cells, as at this stage their general shape is regular, in a cobblestone pattern [Donato et al., 2007]. The global volume of proliferating ReNcell VM was determined using the electric cell counter CASY® (Innovatis AG, Germany) which uses impedance technique. The ReNcell VM cells were cultivated according to the protocol previously described in section 3.1.2. The cells were detached from the coated cell culture flask with addition of Trypsin-Benzoyl-L-glutamate solution (2.5ml/flask) followed by trituration solution (5ml/flask) (solutions are described in Section 3.1.1). As the two solutions are isotonic, they do not cause cell volume changes. After trypsination ReNcell VM cells are in nearly spherical shape within the solution suspension. This condition is necessary and sufficient for the device CASY® to retrieve the mean volume of the cells analyzed in the sample. Cell suspension (25 μ l) was diluted in 10 ml of CasyTon buffer and analyzed by CASY®. The analysis results contain the mean volume of the spherical cells passing through the capillary.

The mean of 79 cell samples, from cell passage 9 to 27, gives the average volume of ReNcell VM cells,

$$V_{VM} = 1.365 \cdot 10^{+3} \pm 0.0495 \text{ fl} = 13.65 \cdot 10^{-16} \text{ m}^3.$$

To obtain the compartment volumes, the average area of the cytosol and nucleus in proliferating cells, was measured via microscopy. The cytosol represents an average of 64% of the cell surface, whereas the nucleus represents 26% of the cell surface. These values were considered to hold true for the volume proportions, leading to:

$$\begin{aligned} V_{cyto} &= 0.64 \cdot 1.365 \cdot 10^{+3} = 0.873 \cdot 10^{+3} \text{ fl} = 8.73 \cdot 10^{-16} \text{ m}^3, \\ V_{nucl} &= 0.26 \cdot 1.365 \cdot 10^{+3} = 0.355 \cdot 10^{+3} \text{ fl} = 3.55 \cdot 10^{-16} \text{ m}^3. \end{aligned}$$

Stochastic diffusion constants

The approach follows the one described in [Elf and Ehrenberg, 2004], i.e. the compartments are considered to be separated containers, called sub-volumes, between which molecules diffuse in

a discrete event manner. A diffusion event describes the motion of one particle from the center of one compartment to the center of the other. Thereby, the cytosol and the nucleus form a structure of two concentric spheres, the first surrounding the latter, see Figure 4.2. The rate constants of diffusion events (diffusion constants) are determined starting off with Fick's first law

$$J = -D \frac{d\Phi}{dx}, \quad (13)$$

that describes the diffusive flux J in $[mol \cdot m^{-2} \cdot min^{-1}]$ through the unit area. It depends on the diffusivity D of the diffusing species in $[m^2 \cdot s]$ and the concentration gradient $d\phi/dx$ in $[mol \cdot m^{-4}]$, with the direction of the latter being against the motion. The focus is on the rate constant of a single particle moving, such that a difference of one particle between the two compartment centers is considered. Therefore, the gradient to $d\phi/dx = -1/x$ is set, where x is the absolute distance between the compartment centers. Notice, that by this step, the gradient is converted from a concentration difference over some distance with unit $[mol \cdot m^{-4}]$ into a difference of particle numbers over some distance with unit $[m^{-1}]$. Since J is given for the unit area, multiplication by the area A connecting the cytosol and the nucleus is needed. Under consideration of the volume V of the compartment where the molecule starts, the stochastic diffusion constant obtained is

$$D_{sto} = \frac{D \cdot A}{x \cdot V}, \quad (14)$$

with the intended units s^{-1} in its final result. Notice, however, that in the following model the time unit min is used, and not s , such that further conversions are required.

In the case of β -catenin diffusion between the two compartments, cytosol and nucleus, the various variables of this formula are obtained as follow:

1. The diffusivity, D , can be calculated based on experiments carried out by the Fluorescence Recovery After Photobleaching (FRAP) technique, and is retrieved following the formula, $D = \frac{w^2}{4 \cdot HRT}$, where w is the width of the laser beam used to bleach the biological sample, and HRT is the half-recovery time. As presented in [Krieghoff, 2006] the HRT

of β -catenin is $HRT_{\beta} = 2 : 12 \text{ min}$ and the width of the laser beam used is $w = 3 \cdot 10^{-6} \text{ m}$. Thus, the diffusivity of β -catenin is

$$D_{\beta} = \frac{(3 \cdot 10^{-6})^2}{4 \cdot 2.2} = 1.023 \cdot 10^{-12} \text{ m}^2 \cdot \text{min}^{-1}. \quad (15)$$

2. The diffusion distance, x , of β -catenin between the two compartments, results from the compartment model with two concentric spheres,

$$x = r_{nucl} + \frac{r_{cyto} - r_{nucl}}{2}. \quad (16)$$

The two compartments are assumed to be spherical and their respective radius are retrieved from the compartment volumes mentioned in Section 4.3.1.

Following the formula for a sphere, where $radius = \sqrt[3]{\frac{V}{4\pi}}$, the radius of both compartments are $r_{cyto} = 5.93 \cdot 10^{-6} \text{ m}$, and $r_{nucl} = 4.39 \cdot 10^{-6} \text{ m}$, resulting in the distance $x = 5.16 \cdot 10^{-6} \text{ m}$.

3. The diffusion surface, A , corresponds to the surface of the nucleus. The detail of the surface with the amount of pores on the nuclear envelop is not taken into account, as this amount is not exactly known, and as the pore diffusion surface changes over time and in different conditions. Thus, the nucleus surface is

$$A_{nucl} = 4 \cdot \pi \cdot r_{nucl}^2 = 2.42 \cdot 10^{-10} \text{ m}^2 \quad (17)$$

4. The volume, V , from which the molecule starts to diffuse is retrieved as presented in Section 4.3.1:

diffusion from the cytosol to the nucleus, $V_{cyto} = 8.73 \cdot 10^{-16} \text{ m}^3$,

diffusion from the nucleus to the cytosol, $V_{nucl} = 3.55 \cdot 10^{-16} \text{ m}^3$.

The stochastic diffusion constant for the shuttle of β -catenin from the cytosol to the nucleus is

$$k_{\beta in} = \frac{D_{\beta} \cdot A_{nucl}}{x \cdot V_{cyto}} = 0.0549 \text{ min}^{-1}, \quad (18)$$

and the stochastic diffusion constant for the shuttle of β -catenin from the nucleus to the cytosol is

$$k_{\beta out} = \frac{D_{\beta} \cdot A_{nucl}}{x \cdot V_{nucl}} = 0.135 \text{ min}^{-1}. \quad (19)$$

4.3.2 Molecule number & Stochastic rate constants

Essential parameters of stochastic models are the initial number of molecules and stochastic rate constants. As described in [Kuttler and Niehren, 2006], they are obtained from initial concentrations and kinetic rate constants. In [Lee et al., 2003] concentrations are given in nM (nmol/l), i.e. amount of molecules per volume. Thus the molecules' number of the model species are calculated as follow:

$$N = C \cdot N_A \cdot V$$

where C is the concentration, N_A the Avogadro constant ($N_A \approx 6.023 \cdot 10^{23}$) and V is the volume of the cell or compartment.

The stochastic rate constant $k_{sto}^{(0)}$ of zero order reactions, i.e. reactions without reactants, is calculated based on the volume, the Avogadro constant, and the kinetic rate constant k:

$$k_{sto}^{(0)} = k \cdot N_A \cdot V$$

For first order reactions, the kinetic and the stochastic rate constant coincide. For second order reactions, i.e. reactions with two reactants, the stochastic rate constant $k_{sto}^{(2)}$ is calculated by:

$$k_{sto}^{(2)} = \frac{k}{N_A \cdot V}$$

4.3.3 Duration and distribution of cell cycle phases

The duration of the cell cycle of ReNcell VM cells is given in [Schmöle et al., 2010] with a doubling time of 19.8 ± 0.6 hours. The single phase durations are retrieved according to [Alam et al., 2004] (see Figure 2.4) that describes, in mammalian cells, a relative duration of 50% for G1, 33.3% for S and 16.7% for G2/M of the entire duration of the cell cycle. Thus, the delay for G2/M phase $d_{G2} = 198.4$ minutes and for S phase $d_S = 395.6$ minutes.

The amount of ReNcell VM cells committed in the cell cycle were retrieved experimentally as described in [Mazemondet et al., 2011] and in Figure 2.5): around 20% of ReNcell VM cells are in G2 phase and around 23% in S phase when differentiation is induced (time 0 hour).

4.3.4 Delays

The delays are modeled by introducing for each delay d a species S and a reaction $r : \emptyset \xrightarrow{d} S$. Initially the number of S is set to 0. Reaction r produces a single instance of S to denote the end of the delay. Reactions that are supposed not to happen before the delay has ended are equipped with an additional reactant and product of species S , e.g. reaction $r : A \xrightarrow{k_B} B$ is transformed to $r_B : A + S \xrightarrow{k_B} B + S$. Notice that when ensuring that the number of S is always 1, the rate of reactions with mass-action kinetics is not affected by this modification. Reaction r cannot be directly mapped to a stochastic reaction since it is required to happen only once and at a time point not exponentially distributed but normally distributed in time that denotes the end of delay d . This is achieved by using the next-reaction method [Gibson and Bruck, 2000] version of the stochastic simulation algorithm [Gillespie, 1977] that schedules the time point of each reaction in an event queue. The firing of a reaction at a fixed time point that models the end of a delay can thus be just scheduled as an additional event. It is assumed that the end time points of a delay are drawn from a normal distribution on the length of the delay with a standard deviation that is estimated to be 5% (without direct relation to the phase passage). Similar ideas have already been presented in [Ciocchetta, 2009]. Alternatively, one can also approximate events at normally distributed time points with sets of fast, intermediate reactions [Schlicht and Winkler, 2008].

4.3.5 Parameter estimation & Simulation

The parameter estimation for the unknown values of rate constants was done using the tool COPASI [Hoops et al., 2006]. The method chosen is Hooke & Jeeves [Hooke and Jeeves, 1961], that uses a direct search algorithm. The parameter estimation aimed to find the appropriate parameter values in order to fit the model output to the data used for evaluation, i.e. the *Lee model* or the *in vitro* data. The *Lee model* simulations were performed using the online tool *JWS Online* (<http://jjj.biochem.sun.ac.za/>) [Olivier and Snoep, 2004]. Deterministic simulations were also done with the tool COPASI [Hoops et al., 2006] using the deterministic LSODA method. Notice that deterministic simulations does not include delays and were only performed for the model without delays. Stochastic simulations were performed using a small extension of the stochastic simulation algorithm, the version presented in [Gibson and Bruck, 2000], that allows to directly reflect normally distributed delays, see Section 4.3.4. This extension performs stochastic simulation experiments based on the modeling and simulation framework JAMESII [Himmelspach and Uhrmacher, 2007].

4.4 Model Evaluation

In the following section, the intracellular Wnt/ β -catenin pathway model is evaluated against the reference *Lee model* in order to compare the model behavior with the data used for the parametrization. A second evaluation is done by comparing the model prediction with data that were not used for parametrization, in this case the *in vitro* data obtained previously (Section 3).

4.4.1 Against the *Lee model*

The *Lee model* [Lee et al., 2003] is taken as a reference model for model evaluation as it includes model species concentration retrieved experimentally (see Section 4.1.1), as its robustness has been shown [Wawra et al., 2007] (see Section 4.1.2), and as it is the main reference for Wnt/ β -catenin modeling. As the *Lee model* concerns a single cell with a single compartment, a single ReNcell VM cell is modeled and simulated. The dynamics of total β -catenin in the *Lee model* are compared to the dynamics of nuclear β -catenin (β_{nuc}) in the intracellular model, as it is the species of interest due to its transcription role.

The initial species concentrations are taken from the *Lee model*, as they were retrieved from experiments. A few reactions are conserved from the *Lee model*: β -catenin decay (k_{β_d} , r_9) and production (k_{β_t} , r_8), and Axin decay (k_{Ax} , r_6). Table 4.2 presents the parameters' names and values as used in the *Lee model* and their respective names in the intracellular model, as well as the conversion of the deterministic values into stochastic ones. For the remaining reactions, kinetic rates are either taken from literature, e.g. r_{10} , r_{11} (see Section 4.3.1), or estimated (Section 4.3.5). The parameters used are displayed in Table 4.4 (set 1).

An exception forms the concentration of *Wnt* as, in the *Lee model*, it was not measured experimentally and as Wnt signal is modeled as a transient decay. In order to compare the dynamics of β -catenin, the same Wnt signal should be applied to the intracellular model. In the *Lee model*, Wnt signal is represented by a function of time, $W(t)$, where $0 \leq W \leq 1$ decays exponentially following: $W(t) = \exp(-0.133 \cdot t/20)$. In the intracellular model, Wnt signal is represented by a number (dimensionless) of Wnt molecules (*Wnt*) that decays over time following mass action kinetics (r_1). The kinetic rate value for this reaction is obtained from the above function: $k_{w_d} = -0.133/20 = 6.65 \cdot 10^{-3} \cdot \text{min}^{-1}$.

The steady-state analysis of the intracellular model, in absence of Wnt signal, leads to the adaptation of a few parameters that are estimated in order to fit the steady-state level proposed in the *Lee model*: k_{β_d} and k_{β_t} were both reduced, whereas k_{Ax} was increased (Table 4.4 (set 1)). Following this parameter adaptation, the steady-state of β_{nuc} is similar to the one of total β -

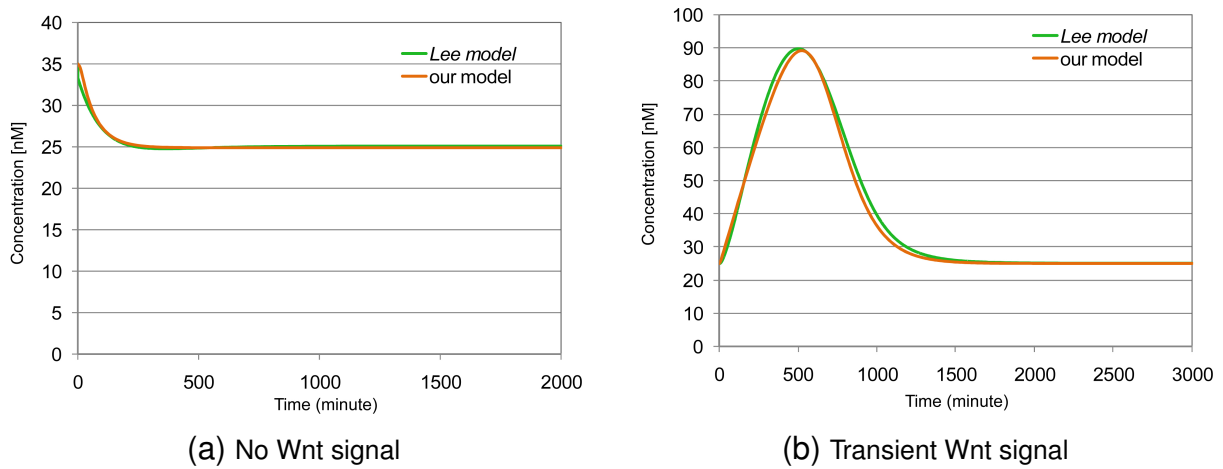


Figure 4.3: Comparison of β -catenin dynamics with the *Lee model*. (a) In absence of Wnt signal, the concentration of nuclear β -catenin (β_{nuc}) is equivalent to the one of total β -catenin in the *Lee model*, ca. 25 nM. (b) Under transient Wnt signal, the dynamics of β_{nuc} and total β -catenin are corresponding and are quantitatively in good agreement.

catenin in the *Lee model* and reaches around 25 nM (Figure 4.3a). Under transient Wnt signal, β_{nuc} increases in a similar way than total β -catenin, reaching a maximum increase of around 90 nM (Figure 4.3b). Small variations can be observed between the two curves, and these can result from the differences between the two models, e.g. in the *Lee model* Axin production is a flux, whereas in the intracellular Wnt model it is mass action kinetics. Nevertheless, the intracellular model, especially β_{nuc} , behaves in a similar manner as the reference *Lee model*.

4.4.2 Against the *in vitro* data

In a second set of experiments the intracellular model is evaluated against the experimental data that were not used for parametrization. For this purpose a homogeneous, i.e. synchronized, ReNcell VM cell population is assumed, in order to verify whether this condition alone is sufficient to obtain, *in silico*, β_{nuc} dynamics equivalent to the *in vitro* ones (see Figure 3.6d).

In order to fit the *in vitro* data, parameter values need to be adjusted (Table 4.4, set 2). This is not surprising since the two data sets (from *Lee model* and our *in vitro* experiments) are retrieved in different organisms, i.e. *Xenopus* and Human, where the enzyme activities can vary widely, thus leading to different rate constants. However, the species initial values, in absence of Wnt signal, remain as previously, leading to steady-state levels in the same range as the previous ones.

The simulation data are in perfect agreement with the experimental ones for the first four time points (Figure 4.4). After two hours of differentiation, β_{nuc} remains constant and no second

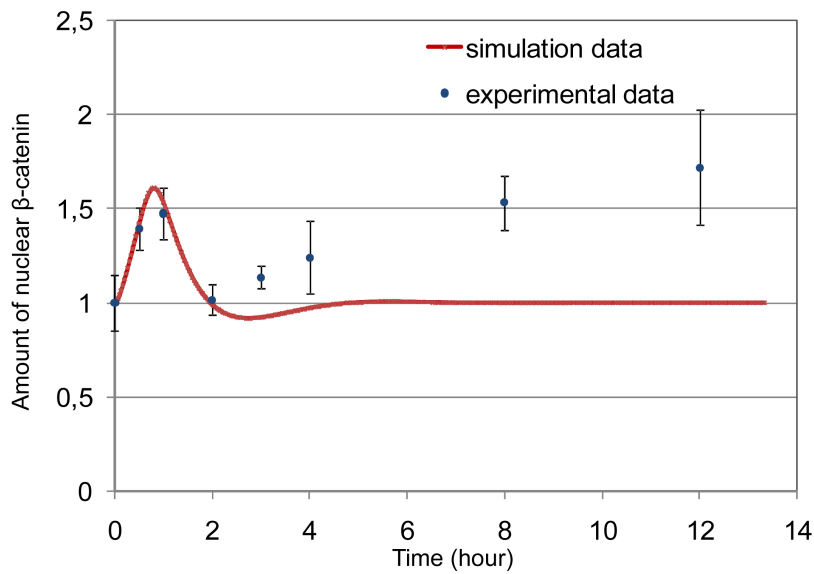


Figure 4.4: Model evaluation in comparison to the experimental data. Comparison of the model time course to the experimental data for nuclear β -catenin dynamics. The simulation data fit the experimental ones for the first time points, until 2 hours of differentiation.

increase can be observed. Thus, a homogeneous cell population in which a Wnt signal is only induced at the beginning of the differentiation does not reproduce the experimentally observed second increase of nuclear β -catenin .

4.4.3 Sensitivity analysis

Following the model evaluation, a sensitivity analysis of the last parameter set is performed to determine which parameters have the most influence on β_{nuc} dynamics. The analysis is performed by calculating the Euclidean distance between a simulation run and the experimental data. The results are shown in Table 4.3. For each parameter it displays the relative change needed for the parameter value in order to obtain a change of 10% in the simulation data with a confidence of 95%. The results show that the amount of *Axin* and *AxinP* have a high influence on β_{nuc} dynamics.

<i>Lee model</i>		<i>Intracellular Wnt/β-catenin pathway model</i>	
Parameter	Deterministic values	Parameter	Stochastic values
<i>Species initial values</i>			
X_{11}	35 nM	β_{cyt}	18390 mol.
		β_{nuc}	7483 mol.
X_{12}	0.02 nM	<i>Axin</i>	11 mol.
		<i>AxinP</i>	11 mol.
<i>W</i>	$0 \leq W \leq 1$	<i>Wnt</i>	100 (dimensionless)
<i>Rate constants</i>			
v_{12}	$0.423 \text{ nM} \cdot \text{min}^{-1}$	$k_{\beta\uparrow}$	222 min^{-1}
<i>W(t)</i>	$\exp(-0.133 \cdot t/20)$	$k_{W\downarrow}$	$6.65 \cdot 10^{-3} \text{ min}^{-1}$
k_{15}	0.167 min^{-1}	$k_{Ap\downarrow}$	0.167 min^{-1}
		$k_{A\downarrow}$	0.167 min^{-1}
k_{13}	$2.57 \cdot 10^{-4} \text{ min}^{-1}$	$k_{\beta\downarrow}$	$2.57 \cdot 10^{-4} \text{ min}^{-1}$

Table 4.2: Parameters from the *Lee model* [Lee et al., 2003] used in the model and their stochastic conversion. Parameters' names and values are given as in [Lee et al., 2003]. Their corresponding names in the intracellular Wnt model are given with their stochastic values. The stochastic values for the species initial values are given in number of molecules (*mol.*).

Parameter	relative change	Parameter	relative change
$n\beta_{nuc}$	0.0001	$k_{\beta in}$	0.18
$nAxin$	0.016	$k_{A \rightarrow Ap}$	0.23
$nAxinP$	0.018	$k_{W\downarrow}$	0.25
$k_{\beta\uparrow}$	0.019	$k_{Ap \Rightarrow A}$	0.28
$nWnt$	0.036	$k_{Ap\downarrow}$	0.37
$k_{\beta\downarrow}$	0.04	$k_{\beta out}$	0.46
$k_{Ap \rightarrow A}$	0.042	$k_{A\uparrow}$	0.58
$k_{A\downarrow}$	0.072	$k_{\beta\downarrow}$	0.91
$n\beta_{cyt}$	0.098		

Table 4.3: Sensitivity analysis of the model parameters. The parameter values used for this analysis are given in Table 4.4 (set 2).

Parameter name	Deterministic values		Stochastic values	
	Set 1	Set 2	Set 3	Set4
Species initial values no Wnt signal				
n β cyt		35 nM	18390 mol.	
n β nuc		35 nM	7483 mol.	
nAxin		0.02 nM	252 mol.	
nAxinP		0.02 nM	219 mol.	
nWnt		0	0	
Species initial values Under Wnt signal				
n β cyt	24.9 nM	23.6 nM	11145 mol.	12989 mol.
n β nuc	24.9 nM	23.6 nM	4532 mol.	5282 mol.
nAxin	0.007 nM	0.051 nM	144 mol.	252 mol.
nAxinP	0.042 nM	0 nM	125 mol.	219 mol.
nWnt	100	1000	1000	1000
Rate constants				
$k_{\beta\uparrow}$	0.232*	0.571*	420	600
$k_{W\downarrow}$	$6.65 \cdot 10^{-3}$	0.27	0.6	0.27
$k_{Ap\Rightarrow A}$	7	10	10	20
$k_{Ap\rightarrow A}$	0.3	0.0182		0.03
$k_{A\rightarrow Ap}$	3	$1.619 \cdot 10^{-3}$		0.03
$k_{Ap\downarrow}$		0.167		$4.48 \cdot 10^{-3}$
$k_{A\downarrow}$	0.367	0.0167	$2.4 \cdot 10^{-3}$	$4.48 \cdot 10^{-3}$
$k_{\beta\downarrow}$	$4.17 \cdot 10^{-4}$ *	52.5*	$3 \cdot 10^{-4}$	$2.1 \cdot 10^{-4}$
$k_{\beta\downarrow}$	$9.98 \cdot 10^{-5}$	$1.13 \cdot 10^{-4}$		$1.13 \cdot 10^{-4}$
$k_{\beta\text{in}}$		0.0549		0.0549
$k_{\beta\text{out}}$		0.135		0.135
$k_{A\uparrow}$	$9.3 \cdot 10^{-5}$	$9.9 \cdot 10^{-5}$	$2 \cdot 10^{-4}$	$4 \cdot 10^{-4}$

Table 4.4: List of model parameters. Parameters used in the different *in silico* experiments. Sets 1 and 2 are used in Sections 4.4.1 and 4.4.2, respectively. Set 3 is used in Section 4.5.1, and set 4 in Sections 4.5.2 and 4.5.3. The stochastic values for the species initial values are given in number of molecules (*mol.*). All rate constants are in min^{-1} but the ones indicated by "*": the deterministic values of $k_{\beta\uparrow}$ are given in $\text{nmol} \cdot \text{L}^{-1} \cdot \text{min}^{-1}$, and the deterministic values of $k_{\beta\downarrow}$ are given in $\text{L} \cdot \text{min}^{-1} \cdot \text{nmol}^{-1}$.

4.5 Results & Discussion

4.5.1 Stochastic effects

In this section, the results of a stochastic investigation exploring the effect of the low Axin amounts, as suggested in the *Lee model* [Lee et al., 2003], are presented. In the *Lee model*, Axin impacts β -catenin through its role in the degradation complex that corresponds in the intracellular model to the impact of *AxinP* on β -catenin, as it represents the activated degradation complex. This study requires a transformation of the concentrations and kinetic rate constants in Table 4.4 (set 2), into molecule numbers and stochastic rate constants. The details of this transformation are presented in Section 4.3.

Figures 4.5a and 4.5b show the numbers of βnuc and *AxinP* over time, in absence of the Wnt signal, as the result of a single simulation run. Large fluctuations in the βnuc amount can be observed that were not visible in the deterministic investigations presented previously (Section 4.4.2). Along with the fluctuations, only small differences in the number of *AxinP* are observed, that underline the high impact of *AxinP* changes on the βnuc population. This impact results from a comparatively high rate of *AxinP*-dependent β -catenin degradation ($k_{\beta\downarrow}$) that is necessary to fit the experimental data. The stochastic fluctuations contradict with the previous *in vitro* results, since they do not allow for a clear transient peak of βnuc in response to the Wnt signal.

Only two strategies to change the model parameters in order to lower stochastic fluctuations while maintaining the amounts of *AxinP* and βnuc seem to be plausible: (i) the first is to decrease the rate constant of *AxinP*-dependent β -catenin degradation ($k_{\beta\downarrow}$) and maintaining the β -catenin level by simultaneously decreasing the flux of βcyt production ($k_{\beta\uparrow}$), that would be in accordance with the sensitivity analysis results (see Section 4.4.3). However, already small modification of this kind has a high impact on βnuc dynamics and prevents βnuc from increasing in response to Wnt signal (results not shown). (ii) The second strategy is to deploy the inertia of β -catenin reacting on *AxinP* number changes. Since the number of β -catenin is relatively high, observable changes due to differences in *AxinP* number can only take place with a certain delay. The quantity of *AxinP* is impacted only by its decay ($k_{Ap\downarrow}$) and its de-/phosphorylation ($k_{Ap\rightarrow A}$, $k_{A\rightarrow Ap}$). Instead of increasing one of the corresponding rate constants separately, which would result in a change in the overall amount of *AxinP*, one can increase the rate constants for de-/phosphorylation simultaneously. Figures 4.5c and 4.5d show the results when increasing the rate constants for dephosphorylation ($k_{Ap\rightarrow A}$) by about 1000 times and the one for phosphorylation ($k_{A\rightarrow Ap}$) accordingly. Changes in *AxinP* numbers happen much faster.

However, although they are lower, the stochastic fluctuations in the βnuc dynamics are still too high. Raising the dephosphorylation rate ($k_{Ap \rightarrow A}$) even more seems not plausible biologically, since then changes on the few *AxinP* molecules happen in periods of milliseconds.

Therefore, it is convincing that in the intracellular Wnt pathway model, with low *AxinP* level as derived from [Lee et al., 2003], stochastic fluctuations in the βnuc level cannot be limited to fit the experimental data. This indicates that either ReNcell VM cells contain higher level of Axin than suggested for the *Xenopus* oocyte by [Lee et al., 2003] or that the pathway model, and thus the understanding of the system, may miss an important mechanism to reduce stochastic noise, such as dimerization [Bundsuh, 2003, Morishita, 2004] or an additional negative feedback loop [Orrell et al., 2006].

Additional parameter fitting experiments are performed, thereby stepwise increasing the amount of *AxinP* and *Axin*. It results in a parameter set with acceptable stochastic fluctuations at an initial amount of *AxinP* of 125, when starting experiments in presence of Wnt signal, see Table 4.4 (set 3). In Figure 4.6a, the dynamics of βnuc over time for 10 simulation runs are shown, where the Wnt signal is switched off. One can see that the fluctuations in βnuc levels have been effectively decreased. The t-test provides that at the time point of maximum deviation around 7 hours (ca. 426 minutes), the mean value of βnuc numbers in the 10 simulation runs lies in the interval of 254.13 (ca. 5.5% of the simulated mean value) around the simulated mean value with a confidence of 95%. Figure 4.6b shows the dynamics of βnuc over time for 10 simulation runs, when the Wnt signal is on. The simulation data show a transient peak within the standard deviation of the experimental data.

4.5.2 Impact of the cell cycle on β -catenin dynamics

In this section, the impact of the cell cycle on the overall amount of β -catenin in ReNcell VM cell populations is investigated. Therefore, heterogeneous cell populations are considered with an individual cell cycle state assigned to each cell. The detailed processes of the cell cycle are not reflected, only its impact on the Wnt/ β -catenin pathway is taken into account. Also, as the M phase is really fast (less than an hour) and not represented in the data available (see Figure 2.5), the phase G2 abstracts both G2 and M phases.

The cell cycle is modeled as a delay on the start time of Wnt degradation ($k_{w \downarrow}$) and Wnt-dependent Axin dephosphorylation ($k_{Ap \rightarrow A}$). That is the corresponding reactions r_1 and r_2 are ensured not to happen before a fixed time point has passed. This time point is drawn from a normal distribution on the length of the delay with a standard deviation that we assume to be 5%. Cells that are already in the G1 phase at the beginning of a simulation experiment, i.e. at

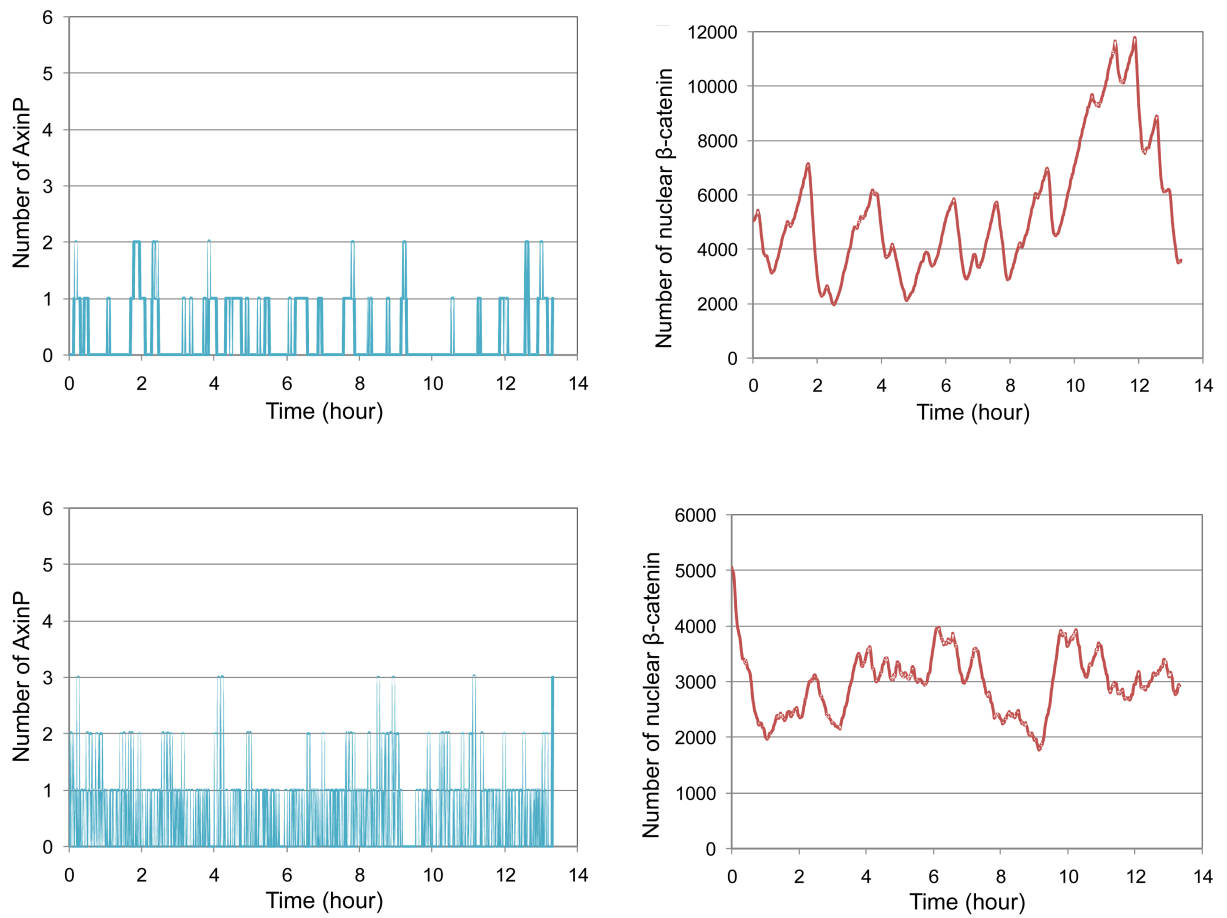


Figure 4.5: Effects of *AxinP* on nuclear β -catenin dynamics according to stochastic simulation. In absence of Wnt signal, small variations of *AxinP* (a) impact β_{nuc} dynamics (b) leading to high variance. The parameter values used for these simulations are converted from the Table 4.4 (set 2). Increase of $k_{Ap \rightarrow A}$ and $k_{A \rightarrow Ap}$ by 1000 accelerate *AxinP* changes (c) but β_{nuc} fluctuations still remain too high (d).

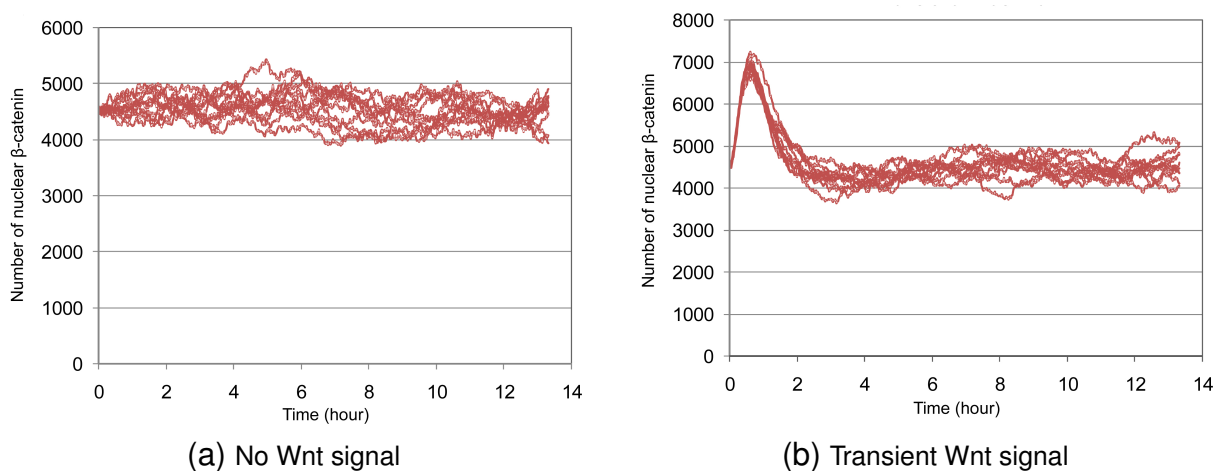


Figure 4.6: Nuclear β -catenin dynamics with higher number of *AxinP*. Stochastic simulation of β_{nuc} in absence of Wnt signal (a), and under transient Wnt signal (b). The parameter values used for these simulations are in Table 4.4 (set 3).

time 0 hour, start to perform their reactions without any delay. The integration of delays into the model is presented in Section 4.3.4.

Cell cycle states, i.e. G1, S, and G2, are assigned following the distribution of cells over the cycle phases as shown in Figure 2.5 and Section 4.3.4. For example in a population of n cells, $0.23 * n$ cells are assigned to state S . Potential rounding problems are solved by randomly assigning states to remaining cells with probabilities to be in certain states again following the experimental data.

The delay for each cell is computed in the following way: cells are assumed to be equally distributed over their respective states. That is, to a cell in state $G2$ a delay $t = \kappa * d_{G2}$ is assigned, where κ is equally distributed in $[0, 1]$ and d_{G2} is the duration of phase $G2$. Similarly, since each cell in state S has to additionally pass state $G2$, the delay of a cell in state S is given by $t' = d_{G2} + \kappa * d_S$, with d_{G2} being the duration of phase $G2$.

In Figure 4.7a the relative amount of nuclear β -catenin (β_{nuc}) for a single simulation run with 100 cells is presented, based on the parameters given in Table 4.4 (set 3). The simulation data presented are calculated in the same manner as the Western-blot data (see Section 3.1.6). Briefly, the sum of β_{nuc} amounts for the 100 cells for each time points. The resulting values are normalized to the one at time point 0 hour, that is set to 1. Similar to the results presented in the previous section, a single transient increase is observed. This peak is however lower than expected. The maximum β -catenin increase as obtained from the experiments (Figure 3.6d, Section 3.2.1) is 1.48 at 1 hour. However, the peak in Figure 4.7a is about 1.28 at 36 minutes, i.e. only 86% of the expected amount is reached. The reason can be seen in Figure 4.7b, where

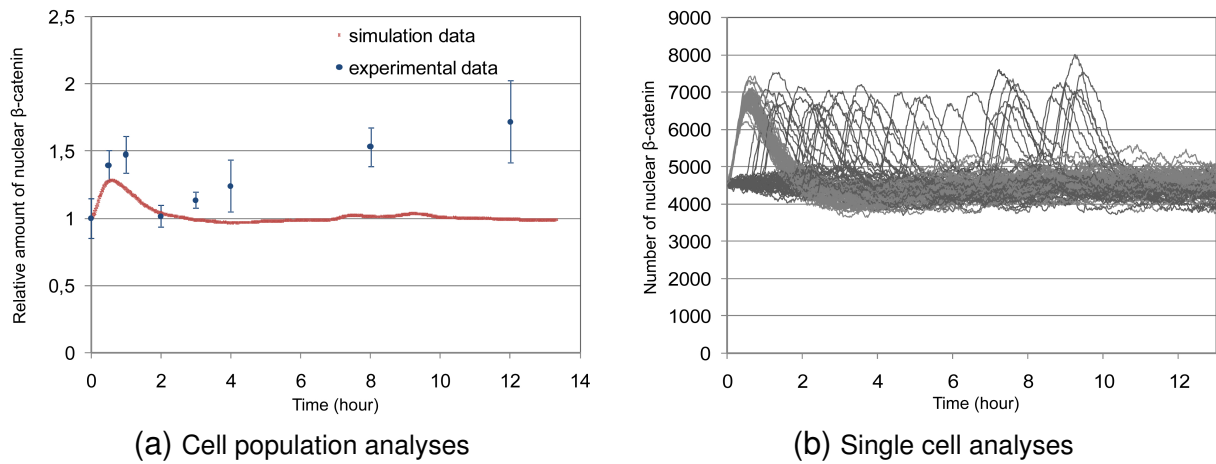


Figure 4.7: Dynamics of nuclear β -catenin in heterogeneous cell population. Population of 100 cells is simulated and compared to the experimental data. (a) The total cell population is analyzed, the simulation data do not correlate with the experimental ones. (b) Single cell analysis shows the delay in β -catenin dynamics due to the cell cycle asynchrony. Parameters used are given in Table 4.4 (Set 3).

β *nuc* dynamics are shown for the 100 cells, separately. The β -catenin amounts in most of the cells initially dedicated to the cell cycle, start to increase not before 30 minutes, i.e. after the time of the first peak is over. Thus, only about 60% of the cells contribute to the first peak, resulting in the limited increase. This shows that when modeling the Wnt/ β -catenin pathway in ReNcell VM cells the cells' commitment to the cell cycle should be considered.

Further parameter fitting experiments are performed and Table 4.4 (set 4) shows the obtained parameter set. Only a few parameters are adjusted compared to the previous parameter set. Figure 4.8a shows the corresponding simulation results. It can be seen that with the new parameter set, the first increase of nuclear β -catenin is well-fitted.

The simulation results presented in Figure 4.8a indicate that when studying the Wnt pathway in ReNcell VM cells by wet-lab experiments the impact of the cell cycle on the β -catenin amount can be neglected. The reason for this becomes obvious when looking at the dynamics of β -catenin for each cell separately, as presented in Figure 4.7b. Although, all the cells that are initially dedicated to the cell cycle start their β -catenin increase comparatively late, they do not perform it simultaneously but rather widely distributed over time (between 0.5 and 10 hours). Thus, summing up over all cells the individual peaks only lead to small deviations. It is important to notice here that this observation is rather independent from the particular design decisions of the model but most directly results from the distribution of ReNcell VM cells over the cell cycle as it is obtained experimentally (see Figure 2.5) and the basic knowledge about the Wnt/ β -catenin pathway as represented in the model.

4.5.3 Self-induced Wnt signaling

To model self-induced Wnt signaling, the intracellular Wnt/ β -catenin pathway model is extended with a single reaction representing both Wnt production and secretion in a rather abstract way. This reaction occurs with a given delay after cells exit the cell cycle. The delay is to reflect the time necessary to induce the signal. It is implemented in the same way as the one for the cell cycle reaction (details in Section 4.3.4). The time delay is selected in a broad range of values, since it encompasses various biological processes, i.e. gene transcription of Wnt molecules, their subsequent intracellular trafficking, post-translational modifications [Coudreuse and Korswagen, 2007, Lorenowicz and Korswagen, 2009], secretion of Wnt in the extracellular environment, and their binding to the cell receptors, Fz, and LRP6 (see Figure 2.1).

Two ways of self-induction are tested: a discrete and a continuous Wnt signal. For the discrete signal, once the delay is over, each cell produces 1000 Wnt for itself, i.e. autocrine signaling. For the continuous one, also after the time delay, each cell continuously produces, for itself, Wnt molecules with rate constant $k_{w_1} = 0.05 \text{ min}^{-1}$. Simulation experiments are performed with a cell population of 100 cells. Delays selected for the signal induction are 450 and 150 minutes for the discrete and continuous signal, respectively. In Figures 4.8b and 4.8c the results of a single simulation run are presented. The first peak (0 to 2 hours) of β_{nuc} is still fitting the experimental data, in both cases. However, the simulation data of the continuous signal is the only one to fit all the other experimental time points, i.e. 3, 4, 8, and 12 hours.

These results suggest that continuous and autocrine Wnt signaling occurs in ReNcell VM cells during the *early differentiation*, from 2.5 to 8, and potentially at the beginning of the *late differentiation*, i.e. 12 hours.

However, the *in vitro* data feature a substantial standard error at the time points 4 and 12 hours. That is, a plateau between 2 and 4 hours is plausible followed by the second increase around 8 hours. Although the simulation data for the discrete signal do not fit exactly the experimental ones, this hypothesis can not be excluded.

The model abstraction does not distinguish between Wnt production and secretion, it remains, nevertheless, essential to know which mechanism is involved, in order to understand the pathway functioning. Production of Wnt molecules has been investigated in ReNcell VM cell at 3, 6, and 24 hours of differentiation [Hübner, 2010, Mazemondet et al., 2011]. Only for the latter time point an increase of Wnt mRNA level (Wnt5a and Wnt7a) has been observed, leading to the conclusion that Wnt production does not occur during the early differentiation of ReNcell VM cells. However, due to the only few time points investigated this conclusion is questionable and will need further experimental analyses to be verified.

Nevertheless, supposing that Wnt production is performed before differentiation starts, the continuous and autocrine Wnt signal hypothesis can still hold true when considering continuous Wnt molecule secretion. An alternative mechanism for Wnt signaling in ReNcell VM cells can arise from Wnt molecule production prior to differentiation, that are subsequently stored in cytosolic vesicles (see Figure 2.1). The vesicles can fuse continuously with the membrane in order to release Wnt molecules outside of the cell inducing signaling [Coudreuse and Korswagen, 2007]. In order to be validated, continuous Wnt secretion can be tested *in vitro*: a continuous inhibition of the Wnt/ β -catenin pathway, e.g. inhibition with Dickkopf 1, Mesd (both inhibitors of Wnt receptors), or Porcupin [Semënov et al., 2001, Lu et al., 2010, Coudreuse and Korswagen, 2007], followed by kinetic analysis of nuclear β -catenin between 4 and 12 hours of differentiation, could be performed.

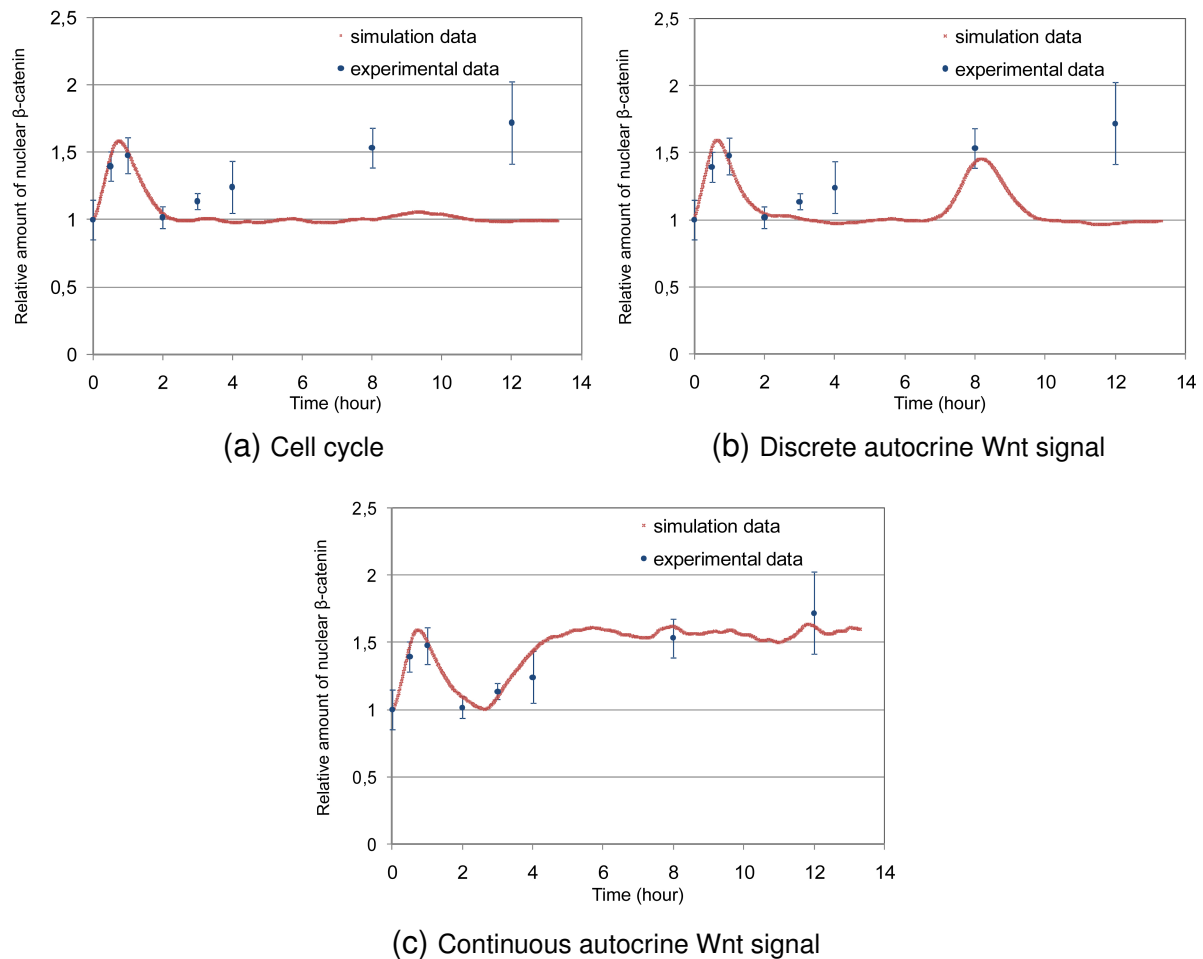


Figure 4.8: Simulation results for the time-course of nuclear β -catenin (β_{nuc}). Population of 100 cells is simulated and simulation data are compared to the experimental data. (a) The cell population asynchrony toward the cell cycle does not give rise to a second increase of nuclear β -catenin after 2 hours. In addition to the cell cycle asynchrony, a self-induced Wnt signal is added. A discrete and autocrine Wnt signal (b) does not fit all the experimental time points, whereas a continuous and autocrine Wnt signal (c) gives simulation data is perfect agreement to the experimental ones. Parameters used for these experiments are given in Table 4.4 (Set 4). The simulation data presented are calculated in the same manner as the Western-blot data (see Section 3.1.6). Briefly, the sum of β_{nuc} amounts for the 100 cells for each time points. The resulting values are normalized to the one at time point 0 hour, that is set to 1.

Chapter 5

Conclusions and Future Work

In this dissertation, computational systems biology is employed to elucidate the dynamics of Wnt/ β -catenin in ReNcell VM cell differentiation. The work encompasses both wet-lab experiments and computational modeling that results in two findings: signaling proteins of the Wnt/ β -catenin pathway present a biphasic kinetic regulation, and the asynchrony of ReNcell VM cells during differentiation does not impair the *in vitro* observations.

Quantitative Western-blot analyses show that the signaling proteins, i.e. LRP6, Dvl2, and β -catenin, are highly regulated during the *early differentiation*, i.e. 0 to 3 hours, and the *late differentiation*, i.e. after 24 hours, of ReNcell VM cells. These results underline the importance of Wnt/ β -catenin pathway during ReNcell VM cell differentiation. Furthermore, it illustrates the need to investigate protein dynamics over time and space, as in various subcellular locations protein are differently regulated, e.g. β -catenin in the nucleus and in the cytosol. These results are a first step toward understanding the role of the Wnt/ β -catenin signaling pathway in hNPC differentiation into neurons.

A stochastic computational model of ReNcell VM cell population is built to evaluate the sources of the biphasic kinetic, especially regarding nuclear β -catenin. Simulation data show that the cell asynchrony during differentiation does not impair the observations made previously *in vitro*. Furthermore, a continuous and autocrine Wnt signal is proposed as a mechanism responsible for the second phase of nuclear β -catenin accumulation, that would need to be validated by performing further wet-lab experiments. Furthermore, stochastic analyses of the model reveal discrepancies with deterministic ones, that provide insights regarding the Wnt/ β -catenin pathway in ReNcell VM cell population.

Molecular biologists commonly explore signaling pathways by influencing their behavior

under external inhibition or activation, e.g. inhibition of GSK3 β to activate Wnt/ β -catenin pathway [Schmöle et al., 2010]. Although widely and successfully used, these manipulations result in a truncated picture of the system and need to be supported by physiological experiments, i.e. without external influence. The present work illustrates such dual investigation, and shows that activation of the pathway with addition of Wnt3a leads to phenomena not observable in physiological condition, e.g. the *phosphorylation-dependent Dvl2 mobility shift*. Both approaches, physiological and manipulated explorations, done in synergy, are needed to fully understand biological systems.

Kinetic studies are challenging due, on the one hand to the time scale of molecular events (from nanosecond to hour), and on the other hand to technical limitations and manpower skills. Determining the relevant time points to study the behavior of signaling pathway during cellular process remains challenging, and necessitates a clear definition of the processes to be observed, e.g. to follow protein phosphorylation, kinetic analyses in a time frame of second are needed.

Western-blot technique has been used over the past thirty years [Towbin et al., 1979, Burnette, 1981]. Its simplicity combined to its large field of application are making it a broadly used technique in biology. Since quantitative Western-blotting is available [Wang et al., 2007] and in constant improvement [Kiyatkin and Aksamitiene, 2009], the data issued from this technique are used in the context of computational systems biology. However, as these data are issued from cell population analyses, their use for modeling is less favored than data issued from single cell analysis [Anselmetti, 2009, pg.VI]. These two different approaches and investigations of biological systems are complementary and should be performed in a synergistic manner in order to provide a complete picture of the systems. As presented in this work, the use of Western-blot data for modeling purposes is still valuable and allows exploration of the diversity in cell populations that needs to be taken into account when performing wet-lab experiments.

In order to close the loop of the computational systems biology workflow, a couple of wet-lab experiments can be performed to in-/validate the predictions obtained from *in silico* experiments. As Western-blot technique failed to detect Axin in ReNcell VM cells, other methods such as immunostaining and microscopy could be used. Alternatively, immunoprecipitation and concentration of cell lysates before Western-blotting, could succeed to quantify Axin amounts. By doing so, answer about the source of stochastic fluctuations in the intracellular Wnt pathway model, could be retrieved. So far, chemical synchronization of ReNcell VM cells is too armful to be followed by further experiments. However, using other techniques such as flow cytometry could circumvent chemical synchronization. Flow cytometry can be used to sort the cells depending on their cell cycle phases. By this way, cells in G1 phase could be selected and cultured

to perform differentiation experiments with synchronized cells. However, as ReNcell VM cells, like other stem and progenitor cells, are delicate to handle and might suffer from such manipulation. In order to confirm that the second increase of nuclear β -catenin is due to self-induced Wnt signal, *in vitro* experiments should be performed. As proposed in Section 4.5.3, constant inhibition of the pathway, e.g. in presence of exogenous proteins like Dickkopf 1, Mesd, or Porcupin [Semenov et al., 2001, Lu et al., 2010, Coudreuse and Korswagen, 2007], followed by kinetic analyses at time points between 8 and 12 hours, would provide data to compare to the simulation ones.

The lack of quantitative and reliable data remains the major bottleneck for the modeling of dynamic systems. Gathering parameter values from different sources is a tedious task that might lead to discrepancies in the model behavior, and necessitates particular attention if conversion between deterministic and stochastic values are needed [Mazemondet et al., 2009]. Although parameter estimation aims to overcome this deficiency, it is not a perfect solution as it might lead to another problem: the over-fitting of the simulation data to the experimental ones. Various data sets might result in data fitting during the model evaluation, but produce different model predictions.

Model reuse is another challenge in computational systems biology [Uhrmacher et al., 2005]. The model presented in this dissertation can easily be reused and extended as it is expressed in terms of chemical reactions. Among possible extension, analyze of the Wnt/ β -catenin pathway impact on neighbor cells can be performed by assigning position to each cell. This would allow *in silico* investigation of paracrine Wnt signal, as well as Wnt gradient in the cell field, and give insights into the mechanisms of Wnt morphogens in the cell-cell communication.

In order to make modeling task accessible to biologists, the development of modeling languages that support modeling with chemical reactions is needed. Efforts in this direction already started than need to be continued, e.g. κ -calculus [Danos and Laneve, 2004, Krivine et al., 2009], Bionetgen [Faeder et al., 2005], or React(C) [John et al., 2011]. There is also a need for these languages to be expressive in order to support delays that are an important feature of biological systems, e.g. delay for transcription process. First efforts are made in this direction [Caravagna and Hillston, 2010] but most of the languages for stochastic modeling do not support reaction delays. A clear framework for modeling development that answers biologist needs and expectations, and not computer scientists needs, is needed so that computational modeling can be established as one of the routine tool for biologists and experimentalists. This emphasizes, once more, the challenge for communication and understanding between scientists from various fields involved in the process of computational systems biology, and also its difficulty.

Glossary

Autocrine signaling	Type of cell signaling in which a cell secretes signal molecules that act on itself or on other adjacent cells of the same type [Alberts et al., 2002].
Differentiation	Process by which a cell undergoes a change to an overtly specialized cell type [Alberts et al., 2002].
Endoplasmic Reticulum	Labyrinthine membrane-bounded compartment in the cytoplasm of eucaryotic cells, where lipids are synthesized and membrane-bound proteins and secretory proteins are made [Alberts et al., 2002].
Growth factors	Extracellular polypeptide signal molecule that can stimulate a cell to grow or proliferate, such as epidermal growth factor (EGF) [Alberts et al., 2002].
Half-life	Time required for half the quantity of a substance deposited in a living organism to be eliminated.
Half-recovery time	Time required for a bleach area to recover half of its initial intensity.
Protein kinase	Enzyme that transfers the terminal phosphate group of ATP to a specific amino acid of a target protein [Alberts et al., 2002].
Mass-action kinetics	Define chemical reaction rates as a product of a rate constant and the concentrations of the reactants [Aldridge et al., 2006].
Morphogen	Signal molecule that can impose a pattern on a field of cells by causing cells in different places to adopt different fates [Alberts et al., 2002].
Negative feedback loop	Counteracts the effect of a stimulus and abbreviates and limits the level of the response, making the system less sensitive to perturbations [Alberts et al., 2002].
Ordinary differential equations (ODEs)	Describe functions of one independent variable (e.g. time t) [Klipp et al., 2005].
Phosphorylation	Reaction to which a phosphate group becomes covalently coupled to another molecule [Alberts et al., 2002].
Proliferation	Process of cell growth and division.
Restriction point	Commitment point during the cell cycle.

Robustness

Ability to maintain biological function despite external variation, internal fluctuations, or failure of system parts [Klipp et al., 2005].

Transcription

Copying of one strand of DNA into a complementary RNA sequence by the enzyme RNA polymerase [Alberts et al., 2002].

Translation

Process by which the sequence of nucleotides in a messenger RNA molecule directs the incorporation of amino acids into protein [Alberts et al., 2002].

Bibliography

- [Ahn et al., 2006] Ahn, A. C., Tewari, M., Poon, C.-S., and Phillips, R. S. (2006). The limits of reductionism in medicine: could systems biology offer an alternative? *PLOS Medicine*, 3(6):e208.
- [Alam et al., 2004] Alam, S., Sen, A., Behie, L. A., and Kallos, M. S. (2004). Cell Cycle Kinetics of Expanding Populations of Neural Stem and Progenitor Cells In Vitro. *Biotechnology and bioengineering*, 88:332–347.
- [Albert and Oltvai, 2007] Albert, R. and Oltvai, Z. N. (2007). Shaping specificity in signaling networks. *Nature Genetics*, 39:286–287.
- [Alberts et al., 2002] Alberts, B., Johnson, A., Lewis, J., Raff, M., Roberts, K., and Walter, P. (2002). *Molecular Biology of The Cell*. Garland Science, fourth edition edition.
- [Aldridge et al., 2006] Aldridge, B. B., Burke, J. M., Lauffenburger, D. A., and Sorger, P. K. (2006). Physicochemical modelling of cell signalling pathways. *Nature Cell Biology*, 8(11):1195–1203.
- [Alon, 2007] Alon, U. (2007). *Introduction to systems biology: design principles of biological circuits*. Chapman & Hall/CRC Mathematical & Computational Biology. Chapman and Hall/CRC.
- [Amit et al., 2002] Amit, S., Hatzubai, A., Birman, Y., Andersen, J. S., Ben-Shushan, E., Mann, M., Ben-Neriah, Y., and Alkalay, I. (2002). Axin-mediated CK1 phosphorylation of β -catenin as Ser 45: a molecular switch for the Wnt pathway. *Genes Development*, 16:1066–1076.
- [Anselmetti, 2009] Anselmetti, D., editor (2009). *Single cell analysis: Technologies and Applications*. Wiley-Blackwell.

- [Axelrod et al., 1998] Axelrod, J. D., Miller, J. R., Shulman, J. M., Moon, R. T., and Perrimon, N. (1998). Differential recruitment of Dishevelled provides signaling specificity in the planar cell polarity and Wntless signaling pathways. *Genes Development*, 12:2610–2622.
- [Bader, 2010] Bader, B. M. (2010). *Spatio-temporal control of Wnt/ β -catenin signaling during fate commitment of human neural progenitor cells*. PhD thesis, Universität Rostock.
- [Bardwell et al., 2007] Bardwell, L., Zou, X., Nie, Q., and Komarova, N. L. (2007). Mathematical models of specificity in cell signaling. *Biophysical Journal*, 92:3425–3441.
- [Beagle et al., 2009] Beagle, B., Mi, K., and Johnson, G. V. (2009). Phosphorylation of PPP(S/T)P motif of the free LRP6 intracellular domain is not required to activate the Wnt/ β -Catenin pathway and attenuate GSK3 β activity. *Journal of Cellular Biochemistry*, 108:886–895.
- [Boutros and Mlodzik, 1999] Boutros, M. and Mlodzik, M. (1999). Dishevelled: at the crossroads of divergent intracellular signaling pathways. *Mechanisms of Development*, 83:27–37.
- [Brandman and Meyer, 2008] Brandman, O. and Meyer, T. (2008). Feedback loops shape cellular signals in space and time. *Science*, 322(5900):390–395.
- [Bryja et al., 2007a] Bryja, V., v_Cajánek, L., Grahn, A., and Schulte, G. (2007a). Inhibition of endocytosis blocks Wnt signalling to β -catenin by promoting dishevelled degradation. *Acta Physiologica*, 190(1):55–61.
- [Bryja et al., 2007b] Bryja, V., Schulte, G., and Arenas, E. (2007b). Wnt-3a utilizes a novel low dose and rapid pathway that does not require casein kinase 1-mediated phosphorylation of Dvl to activate β -catenin. *Cellular Signalling*, 19:610–616.
- [Bundschuh, 2003] Bundschuh, R. (2003). The Role of Dimerization in Noise Reduction of Simple Genetic Networks. *Journal of Theoretical Biology*, 220(2):261–269.
- [Burnette, 1981] Burnette, N. W. (1981). "western blotting": electrophoretic transfer of proteins from sodium dodecyl sulfate–polyacrylamide gels to unmodified nitrocellulose and radiographic detection with antibody and radioiodinated protein A. *Analytical Biochemistry*, 112(2):195–203.
- [Canning et al., 2007] Canning, C. A., Lee, L., Irving, C., Mason, I., and Jones, C. M. (2007). Sustained interactive Wnt and FGF signaling is required to maintain isthmus identity. *Developmental Biology*, 305(1):276–286.

- [Caravagna and Hillston, 2010] Caravagna, G. and Hillston, J. (2010). Modeling biological systems with delays in Bio-PEPA. In Ciobanu, G. and Koutny, M., editors, *Membrane Computing and Biologically Inspired Process Calculi (MeCBIC)*, pages 85–101.
- [Castelo-Branco et al., 2004] Castelo-Branco, G., Rawal, N., and Arenas, E. (2004). GSK-3beta inhibition/beta-catenin stabilization in ventral midbrain precursors increases differentiation into dopamine neurons. *Journal of Cell Science*, 117:5731–5737.
- [Castelo-Branco et al., 2003] Castelo-Branco, G., Wagner, J., Rodriguez, F. J., Kele, J., Sousa, K., Rawal, N., Pasolli, H. A., Fuchs, E., Kitajewski, J., and Arenas, E. (2003). Differential regulation of midbrain dopaminergic neuron development by Wnt-1, Wnt-3a, and Wnt-5a. *PNAS*, 100(22):12747–12752.
- [Cellier, 1991] Cellier, F. E. (1991). *Continuous System Modeling*.
- [Chenn and Walsh, 2002] Chenn, A. and Walsh, C. A. (2002). Regulation of cerebral cortical size by control of cell cycle exit in neural precursors. *Science*, 297:365.
- [Cho et al., 2006] Cho, K.-H., Baek, S., and Sung, M.-H. (2006). Wnt pathway mutations selected by optimal beta-catenin signaling for tumorigenesis. *FEBS Letters*, 580:3665–3670.
- [Ciocchetta, 2009] Ciocchetta, F. (2009). Bio-pepa with events. *Transactions on Computational Systems Biology*, XI:45–68.
- [Coudreuse and Korswagen, 2007] Coudreuse, D. and Korswagen, H. C. (2007). The making of Wnt: new insights into Wnt maturation, sorting and secretion. *Development*, 134:3–12.
- [Danos and Laneve, 2004] Danos, V. and Laneve, C. (2004). Formal molecular biology. *Theoretical Computer Science*, 325(1):69 – 110. Computational Systems Biology.
- [Davidson et al., 2007] Davidson, K. C., Jamshidi, P., Daly, R., Hearn, M. T., Pera, M. F., and Dottoria, M. (2007). Wnt3a regulates survival, expansion, and maintenance of neural progenitors derived from human embryonic stem cells. *Molecular and Cellular Neuroscience*, 36:408–415.
- [Ding et al., 2000] Ding, V. W., Chen, R.-H., and McCormick, F. (2000). Differential regulation of Glycogen Synthase Kinase 3 β by Insulin and Wnt signaling. *The Journal of Biological Chemistry*, 275:32475–32481.

- [Doble and Woodgett, 2003] Doble, B. W. and Woodgett, J. R. (2003). GSK-3: tricks of the trade for a multi-tasking kinase. *Journal of Cell Science*, 116:1175–1186.
- [Doerner, 1980] Doerner, D. (1980). On the difficulties people have in dealing with complexity. *Simulations & Games*, 11(1):87–106.
- [Donato et al., 2007] Donato, R., Miljan, E. A., Hines, S. J., Aouabdi, S., Pollock, K., Patel, S., Edwards, F. A., and Sinden, J. D. (2007). Differential development of neuronal physiological responsiveness in two human neural stem cell lines. *BMC Neuroscience*, 8:36.
- [Elf and Ehrenberg, 2004] Elf, J. and Ehrenberg, M. (2004). Spontaneous Separation of Bi-Stable Biochemical Systems into Spatial Domains of Opposite Phases. *Systems Biology, IEE Proceedings*, 1(2):230–236.
- [Ellner and Guckenheimer, 2006] Ellner, S. P. and Guckenheimer, J. (2006). *Dynamics Models in Biology*. Princeton University Press.
- [Faeder et al., 2005] Faeder, J. R., Blinov, M. L., Goldstein, B., and Hlavacek, W. S. (2005). Rule-based modeling of biochemical networks. *Complexity*, 10(4):22–41.
- [Fuerer et al., 2008] Fuerer, C., Nusse, R., and ten Berge, D. (2008). Wnt signaling in development and disease. *European Molecular Biology Organization*, 9(2):134–138.
- [Gibson and Bruck, 2000] Gibson, M. A. and Bruck, J. (2000). Efficient exact stochastic simulation of chemical systems with many species and many channels. *Journal of Physical Chemistry*, 104:1876–1889.
- [Gillespie, 1977] Gillespie, D. T. (1977). Exact stochastic simulation of coupled chemical reactions. *Journal of Physical Chemistry*, 81:2340–2361.
- [Glass et al., 2006] Glass, A., Karopka, T., and Wolkenhauer, O. (2006). Bioinformatics and the virtual cell. *Information Technology*, 48:44.
- [Hausmann et al., 2007] Hausmann, G., Bänziger, C., and Basler, K. (2007). Helping wingless take flight: how WNT proteins are secreted. *Nature reviews. Molecular cell biology*, 8:331–336.
- [He et al., 2004] He, X., Semenov, M., Tamai, K., and Zeng, X. (2004). LDL receptor-related proteins 5 and 6 in Wnt/ β -catenin signaling: Arrows point the way. *Development*, 131:1663–1677.

- [Hendriksen et al., 2008] Hendriksen, J., Jansen, M., Brown, C. M., van der Velde, H., van Ham, M., Galjart, N., Offerhaus, G. J., Fagotto, F., and Fornerod, M. (2008). Plasma membrane recruitment of dephosphorylated β -catenin upon activation of the Wnt pathway. *Journal of Cell Science*, 121:1793–1802.
- [Himmelspach and Uhrmacher, 2007] Himmelspach, J. and Uhrmacher, A. (2007). Plug'n simulate. In *Proc. of the Annual Simulation Symposium*, pages 137–143. IEEE Computer Society.
- [Hirabayashi and Gotoh, 2010] Hirabayashi, Y. and Gotoh, Y. (2010). Epigenetic control of neural precursor cell fate during development. *Nature Reviews Neuroscience*, 11:377–388.
- [Hirabayashi et al., 2004] Hirabayashi, Y., Itoh, Y., Tabata, H., Nakajima, K., Akiyama, T., Masuyama, N., and Gotoh, Y. (2004). The Wnt/beta-catenin pathway directs neuronal differentiation of cortical neural precursor cells. *Development*, 131:2791–2801.
- [Hoffrogge et al., 2006] Hoffrogge, R., Mikkat, S., Scharf, C., Beyer, S., Christoph, H., Pahnke, J., Mix, E., Berth, M., Uhrmacher, A. M., Zubrzycki, I. Z., Miljan, E., Voelker, U., and Rolfs, A. (2006). 2-DE proteome analysis of a proliferating and differentiating human neuronal stem cell line (ReNcell VM). *Proteomics*, 6:1833–1847.
- [Hooke and Jeeves, 1961] Hooke, R. and Jeeves, T. A. (1961). "direct search" solution of numerical and statistical problems. *Journal of the Association for Computing Machinery*, 8:212–229.
- [Hoops et al., 2006] Hoops, S., Sahle, S., Gauges, R., Lee, C., Pahle, J., Simus, N., Singhal, M., Xu, L., Mendes, P., and Kummer, U. (2006). COPASI-a COMplex PATHway SIMulator. *Bioinformatics*, 22(24):3067–3074.
- [Hübner, 2010] Hübner, R. (2010). *Role of Wnt signaling in proliferation and differentiation of human neural progenitor cells (ReNcell VM)*. PhD thesis, Universität Rostock.
- [Hübner et al., 2010] Hübner, R., Schmöle, A.-C., Liedmann, A., Frech, M. J., Rolfs, A., and Luo, J. (2010). Differentiation of human neural progenitor cells regulated by Wnt-3a. *Biochemical and Biophysical Research Communications*, 400(3):358–362.
- [Israsena et al., 2004] Israsena, N., Hu, M., Fu, W., Kan, L., and Kessler, J. A. (2004). The presence of FGF2 signaling determines whether beta-catenin exerts effects on proliferation or neuronal differentiation of neural stem cells. *Developmental Biology*, 268:220–231.

- [John et al., 2011] John, M., Lhoussaine, C., Niehren, J., and Versari, C. (2011). Biochemical reaction rules with constraints. In *Proceedings of the European Symposium on Programming*, pages 338–357.
- [Kaliania et al., 2008] Kaliania, M. Y. S., Cheshier, S. H., Cord, B. J., Bababeygy, S. R., Vogel, H., Weissman, I. L., Palmer, T. D., and Nusse, R. (2008). Wnt-mediated self-renewal of neural stem/progenitor cells. *PNAS*, 4(44):16970–16975.
- [Khan et al., 2007] Khan, Z., Vijayakumar, S., de la Torre, T. V., Rotolo, S., and Bafico, A. (2007). Analysis of endogenous LRP6 function reveals a novel feedback mechanism by which Wnt negatively regulates its receptor. *Molecular and Cellular Biology*, 27(20):7291–7301.
- [Kholodenko, 2000] Kholodenko, B. N. (2000). Negative feedback and ultrasensitivity can bring about oscillations in the mitogen-activated protein kinase cascades. *European Journal of Biochemistry*, 267(6):1583–1588.
- [Kholodenko, 2006] Kholodenko, B. N. (2006). Cell-signalling dynamics in time and space. *Nature Reviews Molecular Cell Biology*, 7:165–176.
- [Kitano, 2002] Kitano, H. (2002). Systems biology: A brief overview. *Science*, 295:1662–1664.
- [Kiyatkin and Aksamitiene, 2009] Kiyatkin, A. and Aksamitiene, E. (2009). Multistrip western blotting to increase quantitative data output. *Methods in Molecular Biology*, 536:149–161.
- [Klipp et al., 2005] Klipp, E., Herwig, R., Kowald, A., Wierling, C., and Lehrach, H. (2005). *Systems Biology in Practice, Concepts, Implementation and Application*. Deutsche Nationalbibliothek. ISBN : 3-527-31078-9.
- [Klipp and Liebermeister, 2006] Klipp, E. and Liebermeister, W. (2006). Mathematical modeling of intracellular signaling pathways. *BMC Neuroscience*, 7(1):S10.
- [Kofahl and Wolf, 2010] Kofahl, B. and Wolf, J. (2010). Mathematical modelling of Wnt/ β -catenin signalling. *Biochemical Society Transactions*, 38(5):1281–1285.
- [Kotliarova et al., 2008] Kotliarova, S., Pastorino, S., Kovell, L. C., Kotliarov, Y., Song, H., Zhang, W., Bailey, R., Maric, D., Zenklusen, J. C., Lee, J., and Fine, H. A. (2008). Glycogen synthase kinase-3 inhibition induces glioma cell death through c-myc, nuclear factor- κ b, and glucose regulation. *Cancer Research*, 68(16):6643–6651.

- [Krieghoff et al., 2005] Krieghoff, E., Behrens, J., and Mayr, B. (2005). Nucleo-cytoplasmic distribution of beta-catenin is regulated by retention. *Journal of Cell Science*, 119:1453–1463.
- [Krieghoff, 2006] Krieghoff, E. I. (2006). *Analyzing the Regulation of the Subcellular Localization of beta-catenin by Fluorescence Recovery After Photobleaching*. PhD thesis, Fakultäten der Friedrich-Alexander-Universität Erlangen-Nürnberg.
- [Krivine et al., 2009] Krivine, J., Danos, V., and Benecke, A. (2009). Modelling epigenetic information maintenance: A kappa tutorial. In *Proceedings of the 21st International Conference on Computer Aided Verification, CAV '09*, pages 17–32, Berlin, Heidelberg. Springer-Verlag.
- [Krueger and Heinrich, 2004] Krueger, R. and Heinrich, R. (2004). Model reduction and analysis of robustness for the Wnt/beta-catenin signal transduction pathway. *Genome Informatics*, 15(1):138–148.
- [Kunke et al., 2009] Kunke, D., Bryja, V., and Ernest Arenas, L. M., and Krauss, S. (2009). Inhibition of canonical wnt signaling promotes gliogenesis in P0-NSCs. *Biochemical and Biophysical Research Communications*, 386:628–633.
- [Kuttler and Niehren, 2006] Kuttler, C. and Niehren, J. (2006). Gene Regulation in the Pi Calculus: Simulating Cooperativity at the Lambda Switch. *TCSB*, 4230/2006:24–55.
- [Lange et al., 2011] Lange, C., Mix, E., Frhm, J., Glass, A., Müller, J., Schmitt, O., Schmöle, A.-C., Klemm, K., Ortinau, S., Hübner, R., Frech, M. J., Wree, A., and Rolfs, A. (2011). Small molecule GSK-3 inhibitors increase neurogenesis of human neural progenitor cells. *Neuroscience Letters*, 488(1):36–40.
- [Lange et al., 2006] Lange, C., Mix, E., Rateitschak, K., and Rolfs, A. (2006). Wnt signal pathways and neural stem cell differentiation. *Neurodegenerative Diseases*, 3(1-2):76–86.
- [Lee et al., 2003] Lee, E., Salic, A., Krüger, R., Heinrich, R., and Kirschner, M. W. (2003). The roles of APC and Axin derived from experimental and theoretical analysis of the Wnt pathway. *PLoS Biol*, 1(1):116–132.
- [Lee et al., 2008] Lee, Y.-N., Gao, Y., and yu Wang, H. (2008). Differential mediation of the wnt canonical pathway by mammalian Dishevelleds-1, -2, and -3. *Cellular Signalling*, 20:443–452.

- [Leung et al., 2002] Leung, J. Y., Kolligs, F. T., Wu, R., zhai, Y., Kuick, R., Hanash, S., Cho, K. R., and Fearon, E. R. (2002). Activation of AXIN2 Expression by beta-catenin-T Cell Factor. *The Journal of Biological Chemistry*, 277(24):21657–21665.
- [Lindvall and Bjoerklund, 2004] Lindvall, O. and Bjoerklund, A. (2004). Cell replacement therapy: Helping the brain to repair itself. *NeuroR: The Journal of the American Society for Experimental NeuroTherapeutics*, 1:379–381.
- [Liu et al., 2003] Liu, G., Bafico, A., Harris, V. K., and Aaronson, S. A. (2003). A novel mechanism for Wnt activation of canonical signaling through the LRP6 receptor. *Molecular and Cellular Biology*, 23(16):5825–5835.
- [Lorenowicz and Korswagen, 2009] Lorenowicz, M. J. and Korswagen, H. C. (2009). Sailing with the wnt: Charting the wnt processing and secretion route. *Experimental Cell Research*, 315:2683–2689.
- [Lu et al., 2010] Lu, W., Liu, C.-C., Thottassery, J. V., Bu, G., and Liang, Y. (2010). Mesd is a universal inhibitor of Wnt coreceptors LRP5 and LRP6 and block Wnt/beta-catenin signaling in cancer cells. *Biochemistry*, 49(22):4635–4643.
- [MacDonald et al., 2009] MacDonald, B. T., Tamai, K., and He, X. (2009). Wnt/ β -catenin signaling: components, mechanisms, and diseases. *Developmental cell*, 17(1):9–26.
- [Mazemondet et al., 2011] Mazemondet, O., Hübner, R., Frahm, J., Koszan, D., Bader, B. M., Weiss, D. G., Uhrmacher, A. M., Frech, M., Rolfs, A., and Luo, J. (2011). Quantitative and kinetic profile of Wnt/ β -catenin signaling components during human neural progenitor cell differentiation. *Cellular and Molecular Biology Letters*, 16(4):515–538.
- [Mazemondet et al., 2009] Mazemondet, O., John, M., Maus, C., Uhrmacher, A. M., and Rolfs, A. (2009). Integrating diverse reaction types into stochastic models - a signaling pathway case study in the imperative pi-calculus. In M. D. Rossetti, R. R. Hill, B. J. A. D. and R. G. Ingalls, e., editors, *Proceedings of the 2009 Winter Simulation Conference*, pages 932–943.
- [Meijer et al., 2004] Meijer, L., Flajolet, M., and Greengard, P. (2004). Pharmacological inhibitors of glycogen synthase kinase 3. *TRENDS in Pharmacological Sciences*, 25(9):471–478.

- [Michaelidis and Lie, 2008] Michaelidis, T. M. and Lie, D. C. (2008). Wnt signaling and neural stem cells: caught in the Wnt web. *Cell Tissue Research*, 331:193–210.
- [Mikels and Nusse, 2006] Mikels, A. J. and Nusse, R. (2006). Purified Wnt5a protein activates or inhibits beta-catenin-TCF signaling depending on receptor context. *PLOS Biology*, 4(4):570–582.
- [Mirams et al., 2010] Mirams, G. R., Byrne, H. M., and King, J. R. (2010). A multiple timescale analysis of a mathematical model of the Wnt/beta-catenin signalling pathway. *Journal Mathematical Biology*, 60:131–160.
- [Morgan et al., 2009] Morgan, P. J., Ortinau, S., Frahm, J., Krueger, N., Rolfs, A., and Frech, M. J. (2009). Protection of neurons derived from human neural progenitor cells by veratridine. *Neuroreport*, 20:1225–1229.
- [Morishita, 2004] Morishita, Y. (2004). Noise-reduction through interaction in gene expression and biochemical reaction processes. *Journal of Theoretical Biology*, 228(3):315–325.
- [Muroyama et al., 2004] Muroyama, Y., Kondoh, H., and Takada, S. (2004). Wnt proteins promote neuronal differentiation in neural stem cell culture. *Biochemical and Biophysical Research Communications*, 313:915–921.
- [Nurse, 2000] Nurse, P. (2000). A long twentieth century of the cell cycle and beyond. *Cell*, 100(1):71–78.
- [Olivier and Snoep, 2004] Olivier, B. G. and Snoep, J. J. (2004). Web-based kinetic modelling using JWS online. *Bioinformatics*, 20:2143–2144.
- [Orrell et al., 2006] Orrell, D., Ramsey, S., Marelli, M., Smith, J., Petersen, T., Atauri, P., Aitchison, J., and Bolouri, H. (2006). Feedback control of stochastic noise in the yeast galactose utilization pathway. *Physica D: Nonlinear Phenomena*, 217(1):64–76.
- [Pan et al., 2008] Pan, W., Choi, S.-C., Wang, H., Qin, Y., Volpicelli-Daley, L., Swan, L., Lucast, L., Khoo, C., Zhang, X., Li, L., Abrams, C. S., Sokol, S. Y., and Wu, D. (2008). Wnt3a-mediated formation of phosphatidylinositol 4,5-bisphosphate regulates LRP6 phosphorylation. *Science*, 321:1350–1353.
- [Papkoff and Aikawa, 1998] Papkoff, J. and Aikawa, M. (1998). WNT-1 and HGF regulate GSK3 β activity and β -Catenin signaling in mammary epithelial cells. *Biochemical and Biophysical Research Communications*, 247:851–858.

- [Priami, 1995] Priami, C. (1995). Stochastic pi-calculus. *Computer Journal*, 38(7):578–589.
- [Priami et al., 2001] Priami, C., Regev, A., Shapiro, E. Y., and Silverman, W. (2001). Application of a stochastic name-passing calculus to representation and simulation of molecular processes. *Inf. Process. Lett.*, 80(1):25–31.
- [Roberts et al., 2007] Roberts, D. M., Slep, K. C., and Peifer, M. (2007). It takes more than two to tango: Dishevelled polymerization and Wnt signaling. *Nature Structural and Molecular Biology*, 14:463–465.
- [Sabbagh et al., 2001] Sabbagh, W., Flatauer, L. J., Bardwell, A. J., and Bardwell, L. (2001). Specificity of MAP kinase signaling in yeast differentiation involves transient versus sustained MAPK activation. *Molecular Cell*, 8(3):683–691.
- [Sansom et al., 2007] Sansom, O. J., Meniel, V. S., Muncan, V., Phesse, T. J., Wilkins, J. A., Reed, K. R., Vass, K. J., Athineos, D., Clevers, H., and Clarke, A. R. (2007). Myc deletion rescues apc deficiency in the small intestine. *Nature*, 446:676–679.
- [Schaeffer, 2008] Schaeffer, O. (2008). *On the use of process algebra techniques in computational modelling of cancer initiation and development*. PhD thesis, University of Birmingham.
- [Schilling et al., 2005] Schilling, M., Maiwald, T., Bohl, S., Kollmann, M., Kreutz, C., Timmer, J., and Klingmueller, U. (2005). Computational processing and error reduction strategies for standardized quantitative data in biological networks. *FEBS Journal*, 272:6400–6411.
- [Schlicht and Winkler, 2008] Schlicht, R. and Winkler, G. (2008). A delay stochastic process with applications in molecular biology. *Journal of mathematical biology*, 57(5):613–648.
- [Schmitz et al., 2011] Schmitz, Y., Wolkenhauer, O., and Rateitschak, K. (2011). Nucleocytoplasmic shuttling of apc can maximize β -catenin/TCF concentration. *Journal of Theoretical Biology*, 279(1):132–142.
- [Schmöle et al., 2010] Schmöle, A.-C., Brennführer, A., Karapetyan, G., Jaster, R., Pews-Davtyan, A., Hübner, R., Ortinau, S., Beller, M., Rolfs, A., and Frech, M. J. (2010). Novel indolylmaleimide acts as GSK-3 β inhibitor in human neural progenitor cells. *Bioorganic & Medicinal Chemistry*, 18:6785–6795.

- [Semënov et al., 2001] Semënov, M. V., Tamai, H., Brott, B. K., Kühl, M., Sokol, S., and He, X. (2001). Head inducer Dickkopf-1 is a ligand for Wnt coreceptor LRP6. *Current Biology*, 11(12):951–961.
- [Shimizu et al., 1997] Shimizu, H., Julius, M. A., Giarré, M., Zheng, Z., Brown, A. M. C., and Kitajewski, J. (1997). Transformation by wnt family proteins correlates with regulation of β -catenin. *Cell Growth & Differentiation*, 8:1349–1358.
- [Sidow, 1992] Sidow, A. (1992). Diversification of the Wnt gene family on the ancestral lineage of vertebrates. *Proceedings of the National Academy of Sciences of the United States of America*, 89:5089–5102.
- [Smidt and Burbach, 2007] Smidt, M. P. and Burbach, J. P. H. (2007). How to make a mesodiencephalic dopaminergic neuron. *Nature Reviews Neuroscience*, 8:21–32.
- [Smith and Martin, 1973] Smith, J. and Martin, L. (1973). Do cells cycle ? *Proceedings of National Academy of Sciences of the USA*, 70(4):1263–1267.
- [Strigini and Cohen, 2000] Strigini, M. and Cohen, S. M. (2000). Wingless gradient formation in the Drosophila wing. *Current Biology*, 10:293–300.
- [Takahashi et al., 2006] Takahashi, K., Nanda, S., Arjunana, V., and Tomita, M. (2006). Space in systems biology of signaling pathways - towards intracellular molecular crowding in silico. *FEBS Letters*, 579:1783–1788.
- [Tamai et al., 2004] Tamai, K., Zeng, X., Liu, C., Zhang, X., Harada, Y., Chang, Z., and He, X. (2004). A mechanism for Wnt coreceptor activation. *Molecular Cell*, 13:149–156.
- [Tang et al., 2009] Tang, M., Miyamoto, Y., and Huang, E. J. (2009). Multiple roles of beta-catenin in controlling the neurogenic niche for midbrain dopamine neurons. *Development*, 136:2027–2038.
- [Tarze et al., 2007] Tarze, A., ADeniaud, Bras, M. L., Maillier, E., Molle, D., Larochette, N., Zamzami, N., Jan, G., Kroemer, G., and Brenner, C. (2007). GAPDH, a novel regulator of the pro-apoptotic mitochondrial membrane permeabilization. *Oncogene*, 26:2606–2620.
- [The and Perrimon, 2000] The, I. and Perrimon, N. (2000). Morphogen diffusion: the case of the Wingless protein. *Nature Cell Biology*, 2:E79 – E82.

- [Towbin et al., 1979] Towbin, H., Staehelin, T., and Gordon, J. (1979). Electrophoretic transfer of proteins from polyacrylamide gels to nitrocellulose sheets: Procedure and some applications. *PNAS*, 76(9):4350–4354.
- [Tymchyshyn and Kwiatkowska, 2008] Tymchyshyn, O. and Kwiatkowska, M. (2008). Combining Intra- and Inter-cellular Dynamics to Investigate Intestinal Homeostasis. In Springer, editor, *Formal Methods in Systems Biology: First International Workshop*, pages 63–76. FMSB 2008, Cambridge, UK, June 4-5, 2008, Proceedings.
- [Tyson et al., 2001] Tyson, J. J., Chen, K., and Novak, B. (2001). Network dynamics and cell physiology. *Nature Reviews Molecular Cell Biology*, 2(12):908–916.
- [Uhrmacher et al., 2005] Uhrmacher, A., Degenring, D., Lemcke, J., and Kraehmer, M. (2005). Towards reusing model components in systems biology. In Danos, V. and Schachter, V., editors, *Computational Methods in Systems Biology*, volume 3082 of *Lecture Notes in Computer Science*, pages 192–206. Springer Berlin / Heidelberg.
- [van den Heuvel et al., 1989] van den Heuvel, M., Nusse, R., Johnston, P., and Lawrence, P. A. (1989). Distribution of the wingless gene product in *Drosophila* embryos: a protein involved in cell-cell communication. *Cell*, 59:739–749.
- [van Leeuwen et al., 2007] van Leeuwen, I. M., Byrne, H. M., Jensen, O. E., and King, J. R. (2007). Elucidating the interactions between the adhesive and transcriptional functions of β -catenin in normal and cancerous cells. *Journal of Theoretical Biology*, 247(1):77–102.
- [Wang et al., 2007] Wang, Y. V., Wade, M., Wong, E., Li, Y.-C., Rodewald, L. W., and Wahl, G. M. (2007). Quantitative analyses reveal the importance of regulated hdmx degradation for P53 activation. *PNAS*, 104(30):12365–12370.
- [Wawra et al., 2007] Wawra, C., Kuehl, M., and Kestler, H. A. (2007). Extended analyses of the Wnt/beta-catenin pathway: Robustness and oscillatory behaviour. *FEBS Letters*, 581:4043–4048.
- [Wexler et al., 2009] Wexler, E. M., Paucer, A., Kornblum, H. I., Palmer, T. D., and Geschwind, D. H. (2009). Endogenous Wnt signaling maintains neural progenitor cell potency. *Stem Cells*, 27:1130–1141.
- [Wilkinson, 2009] Wilkinson, D. J. (2009). Stochastic modelling for quantitative description of heterogeneous biological systems. *Nature reviews Genetics*, 10:122–133.

- [Wolf et al., 2008] Wolf, J., Palmby, T. R., Gavard, J., Williams, B. O., and Gutkind, J. S. (2008). Multiple PPPS/TP motifs act in a combinatorial fashion to transduce Wnt signaling through LRP6. *FEBS Letters*, 582:255–261.
- [Xiong and Ferrell, 2003] Xiong, W. and Ferrell, J. E. (2003). A positive-feedback-based bistable ‘memory module’ that governs a cell fate decision. *Nature*, 426:460–465.
- [Yamamoto et al., 2006] Yamamoto, H., Komemado, H., and Kikuchi, A. (2006). Caveolin is necessary for Wnt-3a-dependent internalization of LRP6 and accumulation of β -catenin. *Developmental Cell*, 11:213–223.
- [Yokoyama et al., 2007] Yokoyama, N., Yin, D., and Malbon, C. C. (2007). Abundance, complexation, and trafficking of Wnt/ β -catenin signaling elements in response to Wnt3a. *Journal of Molecular Signaling*, 2:12.
- [Zecca et al., 1996] Zecca, M., Basler, K., and Struhl, G. (1996). Direct and long-range action of a Wntless morphogen gradient. *Cell*, 87:833–844.
- [Zechner et al., 2003] Zechner, D., Fujita, Y., Huelsken, J., Mueller, T., Walther, I., Taketo, M. M., Crenshaw, E. B., Birchmeier, W., and Birchmeier, C. (2003). Beta-catenin signals regulate cell growth and the balance between progenitor cell expansion and differentiation in the nervous system. *Developmental Biology*, 258:406–418.

Erklärung

Ich, Oriane Mazemondet, erkläre, dass ich die vorgelegte Dissertationsschrift mit dem Thema: Spatio-temporal Dynamics of the Wnt/ β -catenin Signaling Pathway: A Computational Systems Biology Approach selbst verfasst und keine anderen als die angegebenen Quellen und Hilfsmittel benutzt, ohne die (unzulässige) Hilfe Dritter verfasst und auch in Teilen keine Kopien anderer Arbeiten dargestellt habe.

Datum

Unterschrift

December 20, 2011

Thesis Statements

1. Understanding the mechanisms of human neural progenitor cells (hNPCs) differentiation into neurons is fundamental to develop replacement therapies in the context of neurodegenerative diseases, e.g. Parkinson's disease.
2. ReNcell VM cells are stable hNPCs that can be cultured *in vitro* and allow experimental investigation of the molecular mechanisms involved in neuron differentiation. However, like stem and progenitor cells, they are too sensitive for certain experiments, e.g. synchronization.
3. The Wnt/ β -catenin signaling pathway plays an important role in the differentiation of hNPCs. Its activation is characterized by spatio-temporal changes of signaling proteins, especially accumulation of β -catenin in subcellular compartments.
4. Western-blot experiments on ReNcell VM cells reveal biphasic kinetics of signaling proteins in general and of β -catenin in particular.
5. Computational systems biology integrates wet- and dry-lab techniques and experiments to explore complex and dynamic biological systems in an integrative manner. Thus, such approach is suitable to explore the possible sources of the biphasic kinetics observed in ReNcell VM cells.
6. Dynamic and stochastic models are suitable to investigate signaling pathways. Their development requires information collection about the pathway structure and kinetic parameters. Those can be retrieved from literature and wet-lab data. However, integrating these diverse types of information in stochastic models deserves particular attention.
7. Model development is followed by its evaluation, i.e. the simulation data are compared to a reference model data or to experimental data, in order to assure that a model can reproduce expected behavior patterns. The influence of parameters onto the model behavior is inquired with sensitivity analysis. This revealed the high influence of the species (Axin) in the model of Wnt/ β -catenin in ReNcell VM cells.

8. Applying different approaches for model analysis reveal that stochastic simulation is central to exhibit problems that occur when adopting parameter values issued from deterministic models. For the Wnt/ β -catenin model in ReNcell VM cells these problems might lie in the model structure or might be due to the low amount of one component (Axin). Increasing the latter seems suitable in the context of ReNcell VM cells.
9. The heterogeneity of ReNcell VM cell populations has to be taken into account when analyzing Wnt/ β -catenin model. Integrating the cell asynchrony necessitates adaptation of model parameters in order to fit the simulation to the wet-lab data. However, the cell asynchrony does not affect significantly the general pattern of β -catenin dynamics and is not the source of the second phase observed in the kinetic analyses.
10. A self-induced Wnt signal within ReNcell VM cell population can reproduce the second increase of β -catenin dynamics. In order to confirm whether this signal is subsequent to continuous Wnt secretion, wet-lab experiments in presence of Wnt/ β -catenin pathway inhibitor, e.g. Dickkopf 1 or Porcupin, should be performed.